FZR
FORSCHUNGSZENTRUM ROSSENDORF

Institute for Safety Research

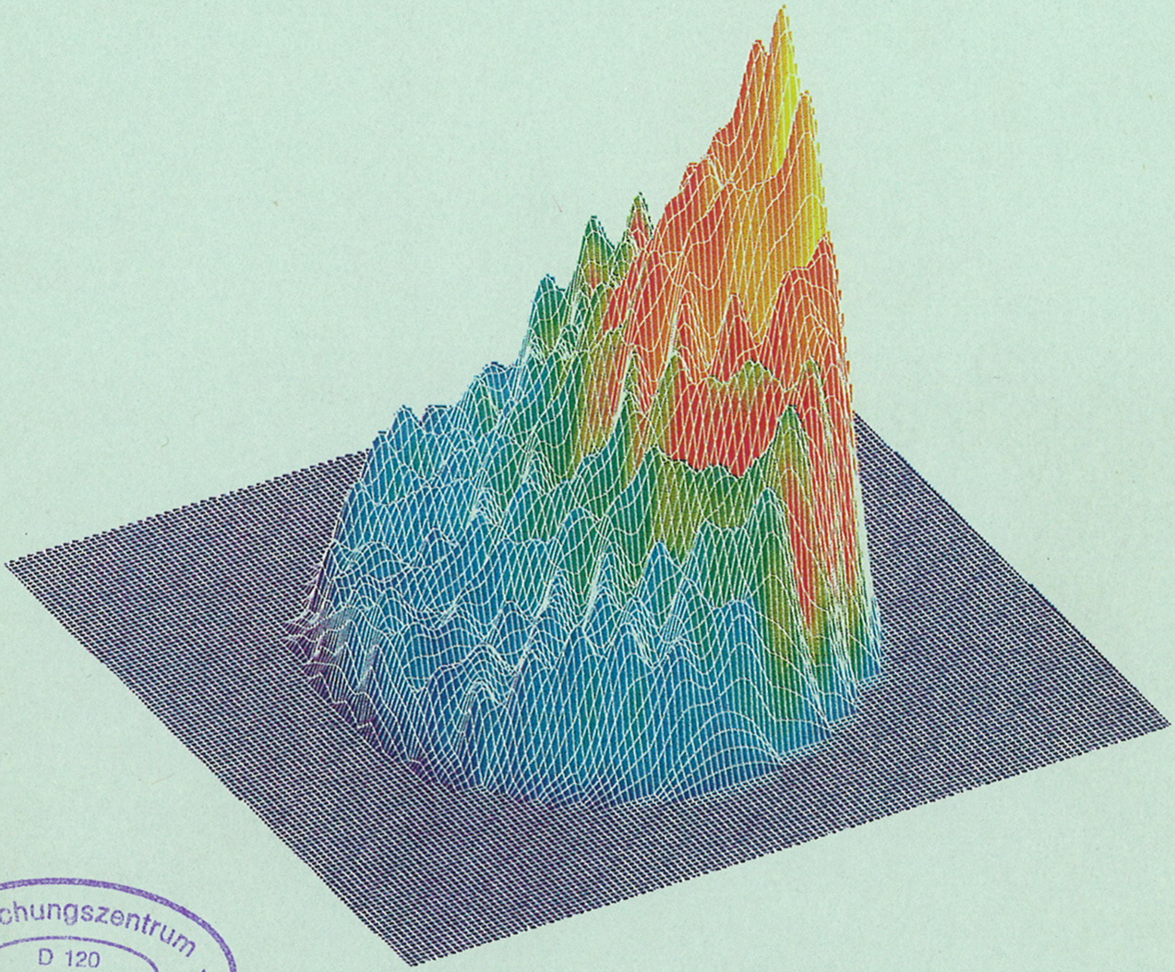

Annual Report 1993

Postfach 511019
D-01314 Dresden, Germany
Tel.: +49-351-591-3480
Fax: +49-351-591-3440

Forschungszentrum Rossendorf e.V.
Institut für Sicherheitsforschung

Annual Report 1993

Editors:
F.-P. Weiß, U. Rindelhardt

FZR-68
Juni 1994

For further information on the research projects described in the present annual report, please address the director or one of the authors at the institute.

Postal address:

Postfach 51 01 19
D-01314 Dresden
Germany

Telecommunication:

Tel.: +49 351 591 3480
Fax: +49 351 591 3440
E-mail weissf-p
@fz-rossen(

Contents

Preface

Generals:

The Institute for Safety Research (IFS) is one of the five scientific institutes of the Research Center Rossendorf that has been founded in the beginning of 1992 as a so called "Blaue Liste" institute which is funded by the Free State of Saxony and by the German federal goverment with 50% each.
The work of the Research Center is mainly directed to the modification and analysis of materials on the one hand and to biomedicine and bioanorganic chemistry on the other hand.
Traditionally being involved in nuclear safety research for the Soviet-type VVER pressurized water reactors, the IFS is going to widen its scientific focus and to contribute to the mentioned main directions with its special scientific expertise.
In its new understanding the research of the institute aims at the assessment and improvement of the safety of technical infrastructures in general.
Striving for that goal IFS is engaged in the following scientific branches:

- thermohydraulics (and neutron kinetics)* of accident sequences
- measuring methods and equipment for two-phase flows
- analysis and characterization of the mechanical behaviour of materials
- measurements and calculations to determine radiations fields
- diagnostics of processes and plants
- application of decision analytical methods to harzard ranking and choice of remediation measures for non-nuclear waste deposits.

Based on the development program since spring 1993 a frame exists which, besides the safety research for nuclear reactors, plans non-nuclear activities to an increasing extent. So, decision analysis is successfully applied to hazard ranking of waste deposits. Other topics are prepared, as e.g. the utilization of modern pattern recognition methods to the early detection of dangerous operating conditions in chemical plants. Nevertheless it can be stated, that the scientific contacts with Eastern European partners kept stable and still improved what consolidates the position of IFS in reactor safety.

Most important results:

To analyse such possible accident sequences at the Soviet-type VVER-reactors which are as well determined by the thermohydraulics in the primary and secondary coolant circuit as by neutron kineties, the 3-dimensional neutron kinetics code DYN3D/M2 that was developed in Rossendorf is coupled to the thermohydraulics program ATHLET of Gesellschaft für Reaktorsicherheit (GRS). One of two possible coupling versions, namely the external coupling where the core thermohydraulics is also described by DYN3D, could be finished. First plausibility calculations were performed and compared with pure point kinetic ATHLET calculations. The obtained agreement is extraordinarily convincing.

*) as for as reactor safety is concerned

In the frame of the IAEA Technical Cooperation Project: "Safety Assessment of WWER-440/213" an international users community of DYN3D has emerged which considerably promotes the further verification of DYN3D.

To open access to data from large scaled thermohydraulic experiments for code validation, the IFS is also concerned in the development of measuring equipment for extreme two-phase flows. A feasibility study has proved an altra-sound transmission method to be well suited to determine not only the flow regime but even the flow rates of the two phases separately. This means a decisive precondition for the introduction of a further non-intrusive measuring technique instead of the well known conductivity probes.

The characterization of the mechanical behaviour of irradiated reactor pressure vessel steel is more and more impeded by the missing operation license for a radioactive testing laboratory.
The analysis of responsible mechanisms of neutron embrittlement has been accelerated by Small Angle X-Ray Scattering (SAXS) analyses performed at HASYLAB, Hamburg. Results obtained up to now, suggest that above all fine spread irradiation induced Vanadium carbides might be responsible for the embrittlement. This is a new result which has not been expected in that kind.

In process and plant diagnostics the existing and new methods are envisaged to be applied to western nuclear reactors and to chemical plants. So for vibration diagnostics a fluid-structure-elemtent has been developed for the description of flow induced vibrations. This element is based on an approximated coupled solution of the fluid equations and the equations of motions of the rigid structural components. It has been verified by dedicated experiments and can now be implemented into finite element vibration models. The field of application ranges beyond modelling the vibrations of VVER-reactor internals.

In the frame of the externally funded (BMU Bundesministerium für Umwelt und Reaktorsicherheit and SMWK Sächsisches Staatsministerium für Wissenschaft und Kunst) project "Remote Monitoring of Eastern European Nuclear Power Plants" a technical concept has been finished for a pilot project in Ukraine. This common project with TÜV (Technischer Überwachungsverein) Rheinland is to enable the Ukraine nuclear authority effectively to meet its surveillance tasks. The concept comprises a backfitting of one unit of the nuclear power plant Saporoshye with the capability to down-load about 100 technological data and about 45 radiological data from the operating instrumentation. It further comprises basic features of remote data transmission and of the monitoring center of the authority in Kiev. The project will be continued in 1994.

A new approach was found in safety research with the assessment of risks connected with conventional and natural radioactive wastes. In 1993 the expert system XUMA (KfK Karlsruhe) for risk assessment was connected to a hydrogeological data bank and has been complemented with decision analytical modules and with a propagation model for radioactive substances. Shortly IFS will be represented in an overall German expert group being responsible for the application of the Baden-Württemberg system of hazard ranking.

A 1993 scientific highlight was marked by organizing the 24. Informal Meeting on Reactor Noise (IMORN 24) together with HTWS Zittau/Görlitz. The meeting was held at Oybin/Zittau and was attended by about 70 experts from all through the world. Among them was a great number of Eastern European participants what hints at the integrating role Rossendorf may play in the scientific east-west dialogue. Moreover, in that context two "Working Group Meetings on Neutronic Analysis" should be mentioned, which were organized by IFS and were initiated and sponsored by the IAEA Vienna. Further, about 30 eastern scientists worked at IFS in 1993.

More information about the work of the Institute for Safety Research can be drawn from the following chapters.

Selected Reports

COMPUTER CODES FOR THE ANALYSIS OF ACCIDENT SCENARIOS AT THE RUSSIAN VVER-TYPE REACTORS

U. Grundmann, D. Lucas, U. Rohde

1. Introduction

Best estimate reactor physical codes become more and more important for the safety assessment of nuclear reactors. To simulate hypothetical accident scenarios for the estimation of safety margins or for the recommendation of backfitting measures a consistent theoretical model of the whole system must be available. That leads to new requirements for the reactor physical codes. They should not only model a part of the relevant phenomena like the thermohydraulics of the cooling system or pure neutron kinetics, or local parts of the reactor system like the core. Best estimate codes aim at the consideration of the whole system. One way to get such codes is to couple codes available for single phenomena or special parts of the reactor. The Institute for Safety Research of the Research Centre Rossendorf (RCR) is developing such best estimate codes especially to provide adapted tools for the accident analysis of the Russian VVER-type reactors.

2. VVER core modelling using DYN3D

The three-dimensional reactor core model DYN3D /1/ has been developed in the RCR to improve the simulation of reactivity initiated accidents (RIA), where space-dependent effects in the reactor core are relevant. In most of the VVER operating countries only point models for neutron kinetics were available in the past.

The neutron flux distribution is calculated in DYN3D using a nodal expansion method for hexagonal geometry. The hexagonal structure of the fuel rod lattice is a specific feature of the VVER-type reactors. The neutron diffusion equations are solved for two energy groups. Steady state and transient behaviour can be calculated.

The code comprises a model of the thermohydraulics of the core, a fuel rod model describing the thermo-mechanical behaviour of fuel and cladding and a heat transfer regime map ranging from one-phase liquid flow to superheated steam. A special model for the mixing of coolant from different primary circuit loops in the lower plenum of VVER-440 type reactors is also included. The code allows the estimation of safety relevant parameters like critical heat flux ratio, maximum temperatures or cladding oxide layer thickness due to metal-water reaction in the high temperature region.

In the frame of the IAEA Technical Cooperation Project "Safety Assessment of VVER Reactors", the code DYN3D was distributed to interested organizations like utilities, research institutes and regulatory boards in Czech, Slovakia, Bulgaria and the Ukraine, where it is used for safety analysis calculations.

In the RCR, DYN3D has extensively been validated and is used to simulate RIA's like:

- uncontrolled withdrawal of control rod groups,
- ejections of control rods or absorber clusters, for instance, the ejection of the most effective control rod with a reactivity worth of about 2 $ from a VVER-440 at hot zero power,
- a loss-of-coolant accident at zero reactor power with positive moderator density feedback leading to a reactivity insertion,
- an accident caused by the entering of a plug of water with reduced boron concentration into the core due to incorrect coolant loop startup procedure at a VVER-440 reactor.

Considering a RIA at PWRs, for a great deal attention is focussed on the simulation of neutron absorbers soluted in the coolant, because just this type of RIA may be connected with considerable reactivity insertion. In VVER-440 reactors, boron dilution or the entering of cold water into the core can be caused by very different mechanisms. Due to the existence of main isolating valves in the cold and hot legs of the primary coolant loops, an incorrect startup procedure for an isolated loop containing a plug of cold water and/or diluted boron acid can become the initiating event for a RIA. Normally, before starting an isolated loop after refilling, first of all the hot leg isolating valve is opened for settling of parameters in the isolated loop to those in the rest of the primary circuit. For the simulation of such an event with DYN3D it is assumed that the loop is put into operation by first starting the main coolant pump and then opening the cold leg isolating valve. After a time delay, due to transport, the plug enters the core. The reactivity insertion is expected to be asymmetric over the core cross section depending on the mixing of the water from the disturbed loop and the other loops in the downcomer and in the lower plenum. At the start of the transient, the reactor is assumed to be operating at 88 % power (1210 MW_{th}). The critical boron acid concentration for this state is 5.345 g H_3BO_3/kg coolant (934 ppm boron concentration) at the beginning of the fuel cycle.

A plug of water with reduced boron concentration of 494 ppm was assumed to be in the hot leg of the isolated loop due to incorrect work of the boron supply system. The postulated accident starts when the plug arrives at the core bottom.
A ramp-like boron concentration decrease with a transition time of 0,1 s is supposed. The plug will have a passing time through the core of 3 s. Further, the reactor protection system is assumed to fail (Anticipated Transient Without Scram, ATWS), so that reactivity insertion is reduced by feedback only.

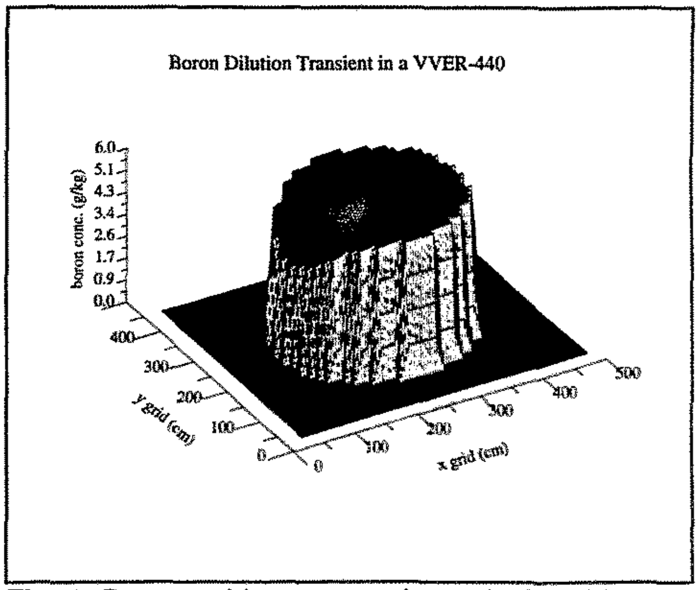

Fig. 1: Boron acid concentration calculated by DYN3D with mixing model (t = 0.35s)

The significance of space-dependent effects is demonstrated in Fig. 1 and 2. The shapes of the boron acid distribution at core bottom and of the axially integrated power density distribution are shown at t = 0.35 s, when the reactor power achieves its maximum.

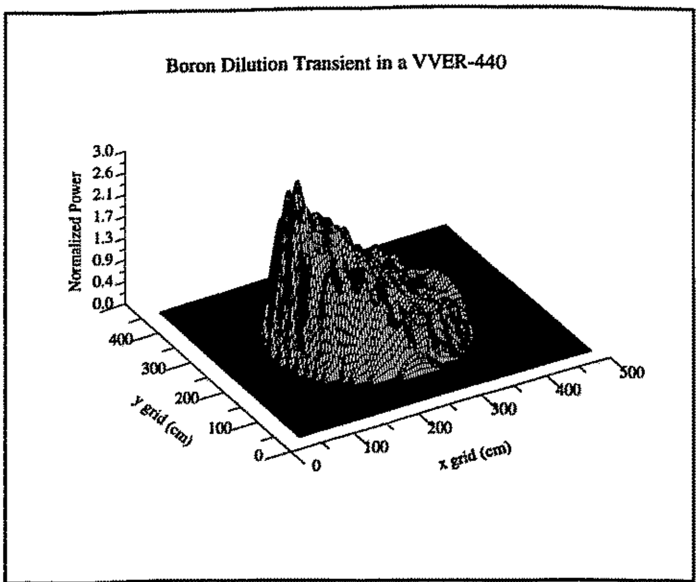

Fig.2: Radial power distibution calculated by DYN3D with mixing model (t = 0.35s)

To compare the capabilities of the mixing model used in DYN3D with other model options, the following simplified descriptions of mixing were considered:

- ideal mixing, leading to a homogeneous distribution of coolant inlet temperatures and boron concentration over the core cross section,
- no mixing, that means, in each of the core sectors the parameters correspond to those in the related primary circuit loop.

The comparison revealed, that the suppression of coolant mixing leads to the largest reactivity insertion and to the highest power peak /2/. The neutron flux shape becomes strongly asymmetric with the maximum in the disturbed sector, so that the reactivity weight of the perturbation is higher than for a more homogeneous perturbation. These results demonstrate that a realistic model for coolant mixing in the downcomer and in the lower plenum is very important for investigations of the considered type of accident. Though DYN3D performs a 3-dimensional analysis of the core it is not capable of considering the thermohydraulic feedback resulting from coolant loops and steam generators.

3. Coupling of DYN3D and ATHLET

Therefore, in the frame of a project supported by the Federal Ministry of Research and Technology (BMFT), DYN3D has been coupled with the advanced thermohydraulic code ATHLET /3/, developed by Gesellschaft für Anlagen- und Reaktorsicherheit (GRS). It can be applied to the whole spectrum of operational and abnormal transients, to small and intermediate leaks and even to large breaks of coolant loops at PWRs and BWRs. ATHLET comprises differently detailed models as options within a common code structure. The code includes basic modules for thermohydraulics, heat transfer and heat conduction, neutron kinetics (point kinetics and 1D neutron kinetics) and reactor control simulation. Within the General Control and Simulation Module (GCSM) a general interface is available, that allows to couple other independent modules to ATHLET without structural changes.

There are two basic ways of coupling ATHLET and DYN3D. The first uses only the neutron kinetic part of DYN3D and integrates it into the heat transfer and heat conduction model of ATHLET. This is a very close coupling along the core (internal coupling). That means the data have to be exchanged between all core nodes of the single models. That's why a great number of data have to be transferred. This version demands extensive additional programming, but it is clearly the way of coupling preferred by all groups working in the field of coupling ATHLET with 3-dimensional neutron kinetics.

In the second way of coupling the whole core is cut out of the ATHLET plant model (external coupling). The core is completely modelled by DYN3D. This is a coupling within the thermohydraulics of the reactor model. The thermohydraulics is split into two parts: one part describes the thermohydraulics of the core, the other part models the coolant system. As a consequence of this local cut it is very easy to define the interfaces. They are located at the bottom and at the top of the core. The pressures, mass flow rates, enthalpies and concentrations of boron acid at these interfaces have to be transferred. So the external coupling needs only a few parameters to be exchanged between the codes and is therefore easy to be realized. It is effectivly supported by the GCSM of the ATHLET code. That's why almost no changes of the single programs are necessary. It is possible to realize the coupling by the interconnection through an interface routine.

For the coupling of ATHLET and DYN3D both ways are realized because both ways have advantages and disadvantages. Only in the case of the external coupling all the models included in DYN3D - for instance a more detailed fuel rod model - can be used. It also enables a 1:1 assignment of coolant channels to fuel assemblies. The input data sets are much simpler than in the case of internal coupling. The interface is very clear and it is easy for the user to keep track of the coupling parameters. On the other hand, there are some restrictions of the thermohydraulic model of DYN3D in comparison with ATHLET. E.g. it is not possible to model the reversal of coolant flow direction in the whole core. The most important disadvantage of the external coupling is the splitting of the thermohydraulics. There is no possibility for a closed implicit solution of the whole system of thermohydraulic equations. The coupling of the two thermohydraulic parts is explicit and very small time steps are necessary for stable calculations. Typical time constants for the fluid flow depend on the sound velocity. This produces rather small time constants. Test calculations showed that the calculations are numerically stable for a maximum time step of about 0.01 s. That means a very long calculation time. But it is possible to get stable calculations even for time steps of about 1 s by smoothing the pressure drop over the core, which is provided to DYN3D as a time-dependent boundary condition, with a first order low pass filter. The low pass filter has practically no influence on the transients that are to be calculated. There are even no distortions for fast and strong transients, what was demonstrated by some test calculations.

For first operating tests of the coupled code and tests of the influence of the low pass filter, 3 exemplary calculations with a simplified VVER-440 data set were compared with pure ATHLET calculations using point kinetics. Two of them concerned RIA transients and one is a loss of coolant accident (LOCA) through a large break. The LOCA calculation clearly demonstrates that the low pass filter has no relevant influence upon the calculated results.

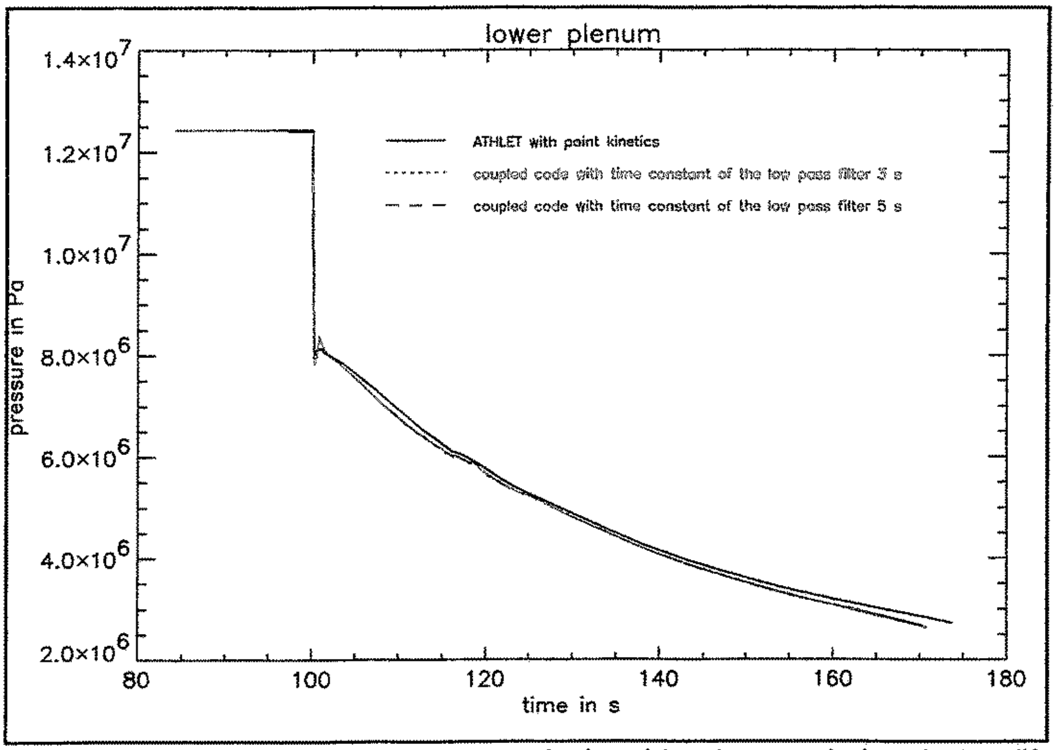

Fig.3: Pressure in the lower plenum calculated by the coupled code for different time constants of the low pass filter in comparison with the pure ATHLET calculation

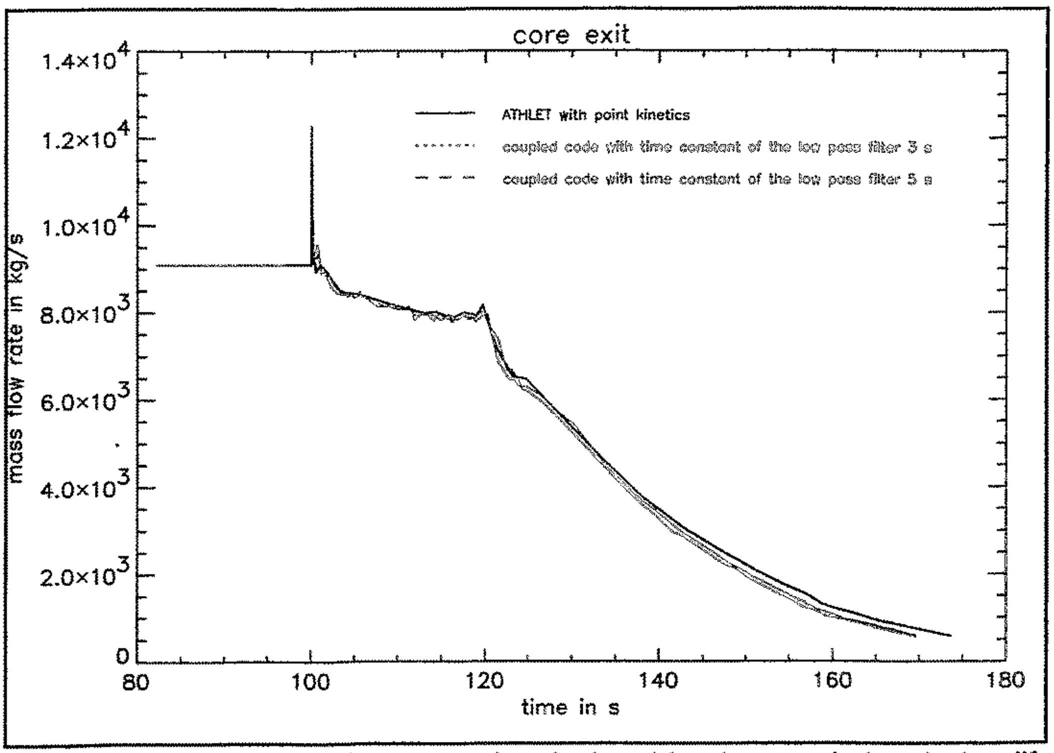

Fig.4: Mass flow rate at the core exit calculated by the coupled code for different time constants of the low pass filter in comparison with the pure ATHLET calculation

A steady state calculation was carried out from 0 s to 100 s. Then a break with a diameter of about 25 cm was suddenly opened in the hot leg . As shown in Fig. 3 there is a very fast and strong change of the system pressure. This causes also rapid changes of the pressure drop over the core. The parameter that responds most sensitively to the filtering procedure is the mass flow rate through the core. Fig. 4 shows that in spite of this sensitivity there is no significant change of this parameter for different time constants of the low pass filter. Moreover, all the mass flow rate curves calculated with DYN3D/ATHLET in the external coupling version agree very well with the mass flow rate *obtained from a pure ATHLET calculation with point kinetics.*

4. Conclusions

The advanced thermohydraulic code ATHLET was coupled with the three-dimensional reactor core model DYN3D. The coupling was accomplished realizing two different coupling strategies. Operating tests of the coupled code system were performed.

During the next working steps plausibility and numerical tests will be performed by comparative calculations between the two coupling versions. After that the coupled code will be validated. This validation aims at the qualification of the code system ATHLET-DYN3D as a best-estimate tool which is applicable to a wide range of possible accident scenarios at VVERs, where as well thermohydraulics of the coolant system as neutron kinetics are necessary for simulation. Typical scenarios of this type are steam line ruptures at one of the steam generators or boron acid dilution in one of the loops.

References

/1/ U.Grundmann, U.Rohde: DYN3D/M2 - a Code for Calculation of Reactivity Transients in Cores with Hexagonal Geometry, IAEA Technical Committee Meeting on Reactivity Initiated Accidents, Vienna, 1989 and Report FZR 93-01, Rossendorf, 1993

/2/ U.Grundmann, U.Rohde: Investigations of a Boron Dilution Accident for a VVER-440 Type Reactor by the Help of the Code DYN3D, ANS 1994 Topical Meeting on Advances in Reactor Physics, April 11-15, 1994, Knoxville

/3/ M.J.Burwell, G.Lerchl, J.Miro, V.Teschendorff, K.Wolfert: The Thermalhydraulic Code ATHLET for Analysis of PWR and BWR Systems, NURETH-4, Proceedings Fourth International Topical Meeting n Nuclear Reactor Thermal-Hydraulics, Volume 2, Karlsruhe, 1989, p. 1234

The project this report is partially based on is funded by the BMFT (Bundesministerium für Forschung und Technologie) and is registered with number No. 150 0925. The authors are responsible for the scientific content of the report.

VERIFICATION OF THE THERMOHYDRAULIC CODE ATHLET FOR THE APPLICATION TO VVERS

E. Krepper

1. Introduction

From the thermohydraulic point of view the main safety related differences of VVER-type pressurized water reactors (PWR) compared to typical western PWR constructions are

- lower geodetic height differences in the primary circuit and
- existence of loop seals (VVER-440: hot and cold legs, VVER-1000: cold legs).
  Loop seals are lowered sections of the primary loops between reactor and steam generator (see Figure 1 for the PACTEL integral test facility).

Both these differences influence the core cooling under natural circulation conditions. Cooling through natural circulation is the most important heat transport mechanism during accident situations.

To investigate the influence of the loop seals in VVER-440 reactors, Finnish experts from VTT Lappeenranta and from the Lappeenranta Technical University conducted a large scale thermohydraulic experiment at the PACTEL facility.

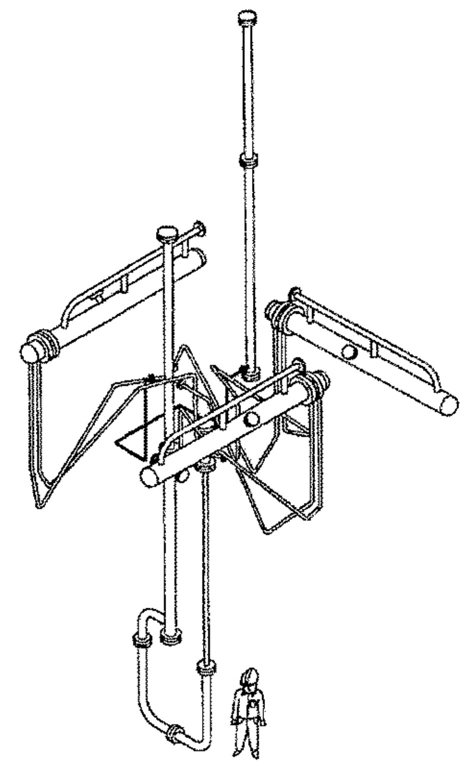

Figure 1
The PACTEL facility

This experiment was integrated into the OECD/NEA/CSNI activities for the verification of large thermohydraulic computer codes as the International Standard Problem No. 33 (ISP-33).

As a contribution to the verification of the thermohydraulic code ATHLET for VVER applications the Institute for Safety Research performed pre- and posttest calculations for ISP-33 [1]. The code ATHLET was developed by Gesellschaft für Reaktor- und Anlagensicherheit Garching [2].

2. The international standard problem NO. 33

The ISP-33 was a natural circulation experiment with stepwise reduced primary coolant inventory. The experiment was conducted at the PACTEL facility located at the Technical Research Centre of Finland in Lappeenranta. It is a full-height thermohydraulic simulator of the Russian VVER-440 type pressurized water reactor with 1 MW maximum heating power of the fuel rod simulators [3]. The volumetric scale is 1:305. The reactor vessel is simulated by an U-tube construction including downcomer, lower plenum, core and upper plenum. Three coolant loops, with double capacity steam generators, are used to model the six loops of the reference power plant. The fuel rod simulators in the core are divided into three parallel channels. Between these channels and the outer core wall, unheated slots are located which were modelled in the ATHLET calculation as a bypass parallel to the core.

During the experiment, the primary coolant which in total amounts to about 650 kg, was reduced stepwise by repeated draining of 60 kg of coolant at intervals of 900 sec. The experiment was continued until the fuel element cladding temperatures exceeded 350 °C.

The stepwise reduction of the coolant inventory does not refer to a realistic accident scenario, but concerning the behaviour of the primary circuit under natural circulation conditions this test is very valuable for the code validation because the formation of the natural circulation is not overlapped by the leak flow itself.

3. Calculated and experimental results

Just after the **first** draining step (t = 1200 to 1380 sec) the pressurizer was fully depleted. At the end of this phase, a vapour bubble occurs in the upper plenum. This bubble grows rapidly after the **second** drain step (2100 to 2160 sec). When the bubble reaches the entrance into the hot legs, the mass flow through the loops stagnates. Simultaneously, the primary pressure increases (Fig. 2 and 3) and as a consequence the pressurizer is partly refilled (see Fig. 2 and 3). The stop of the natural circulation lasted till one loop seal is cleared when the water in the seal is shifted into the steam generator during the next drain.

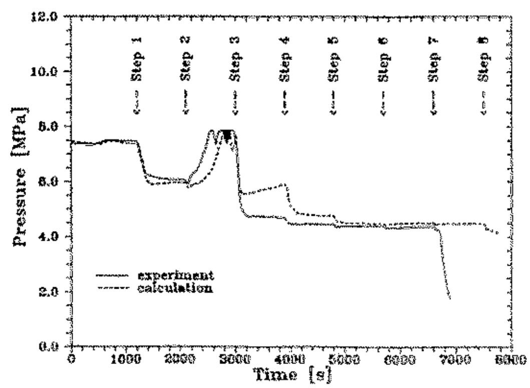

Figure 2
Pressurizer pressure

The flow stagnation and the pressure increase after the second drain step depends strongly on the core outlet temperature at the beginning of the experiment. To describe this in an adequate way the modelling of the steam generator is a key issue. In the ATHLET calculations the secondary side of the steam generator was nodalized linearly, i.e. with the feedwater at the bottom and steam outlet at the upper side. In reality the feedwater inlet is located above the stationary water level. Moreover the strong circulation in the secondary fluid results in a good mixing and thereby in a complete different temperature profile as the theory is capable of describing. Due to that inadequate model the theory overestimates the heat removal from the lower parts of the U-tubes in the steam generator. To compensate these insufficiencies of the model the feedwater temperature was set to 200 °C like at steady state conditions. In the experiment the feedwater temperature was 32 °C.

As already mentioned the **third** drain step (3000 - 3060 sec) reestablishes the natural circulation. In the following periods the mass flow through the three loops became unequal. These unequal coolant flow distributions could, at least qualitatively, be described by the ATHLET calculation (Fig. 3). In the time range 3000 - 3900 sec almost the whole core power is removed over the third loop. After the **fourth** drainage the mass flow is almost equally distributed between the first and the second loop.

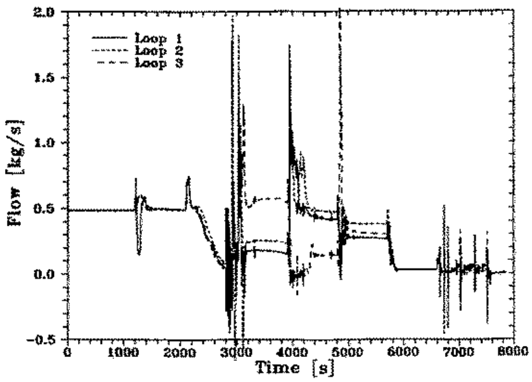

Figure 3
Mass flow in the loops
(Posttest calculation)

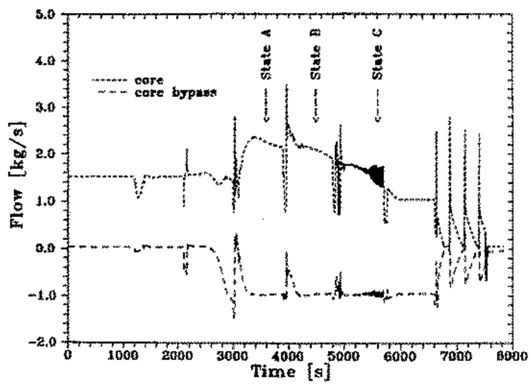

Figure 4
Mass flow in the core
(Pretest calculation)

During the flow stagnation, a flow direction reversal in the core bypass was obtained. In the further experiment, the main stream natural circulation flow was superimposed by a local recirculation flow through the core bypass (see Fig. 4).

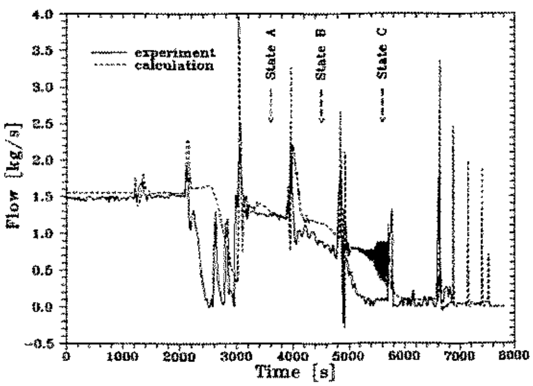

Figure 5
Mass flow in the downcomer
(Pretest calculation)

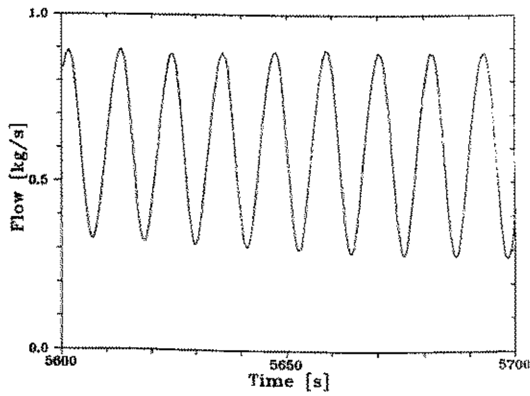

Figure 6
Mass flow in the downcomer
(detail of Fig. 5)

After the drainage of about 50% of the primary inventory, in some calculations cyclic oscillations of the mass flow and the void fractions were observed. This occured after the 5th drain step in the interval t = 5200 - 5600 sec of process time (see Fig. 5 for the mass flow in the downcomer). These oscillations were also observed in the core and bypass mass flow rates (see Fig. 4). A detailed analysis of the calculated results shows, that the oscillations have a rather regular character with a stable period of about 11,5 sec (see Fig. 6).

The mass flow oscillations in the downcomer could not be found in the experimental data set distributed for the posttest calculations. But this was exclusively caused by the low pass filtering of the original time signals and by the sampling interval of 30 sec. An analysis of the experimental data with enhanced time resolution of 2 sec exhibited that the calculated flow rate oscillations could also be seen in the experiment with the same period (Fig. 7 and 8).

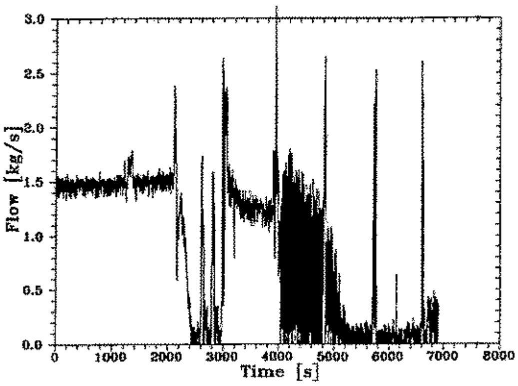

Figure 7
Mass flow in the downcomer
(Experiment, sampling interval 2 sec)

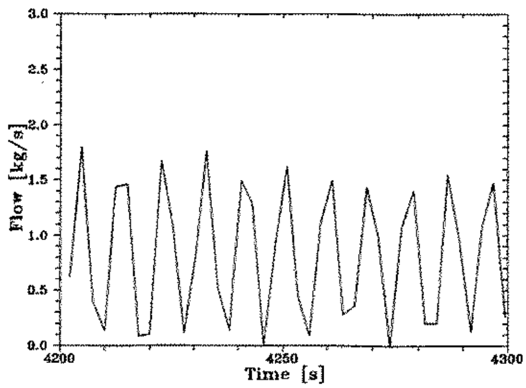

Figure 8
Mass flow in the downcomer
(detail of Fig. 7)

This fact indicates that the oscillations are of physical nature. To verify this assumption and to distinguish oscillations caused physically from oscillations caused numerically, an analytical model was developed by U. Rohde [4]. According to that model the observed oscillations could be interpreted as a density wave instability in the local circulation circuit core/core bypass. Even the oscillation frequency could be reproduced by the model and it confirmed that the whole thermohydraulic system is in a stable condition during states A and B whereas it is unstable during state C (Fig. 5).

While the experiment provides increasing fuel cladding temperatures after the **7th** drain step, in the ATHLET calculation the temperature rise did not occur before the **8th** drain step. This corresponds with the fact, that the calculated collapsed level in the pressure vessel is always higher than measured in the experiment (Fig. 9). This phenomenon is explained by a water accumulation in the primary steam generator tubes due to adhesive forces which are not considered in the theory.

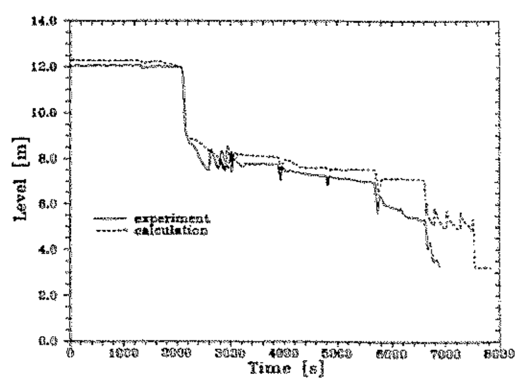

Figure 9
Level in the pressure vessel

4. Conclusions

The experimental results have affirmed that in the primary circuit of a VVER-440 reactor a natural circulation can be established both in the one-phase and in the two-phase flow mode. A temporary stagnation of the circulation before the clearing of the hot leg loop seal does not lead to fuel rod overheating. Moreover, in a certain range of the coolant inventory the system tends to flow instabilities.

The calculations have proved the ATHLET code to be suited for the calculation of natural circulation phenomena in VVER reactors. The agreement between experiment and calculation is comparable to the results of other thermohydraulic codes like RELAP or CATHARE. The detailed analysis of the flow rate oscillations is a special result of the Rossendorf contribution to the standard problem. The fact that ATHLET predicted these oscillations rather good, demonstrates the quality of the code. The water accumulation in the steam generator tubes was neither considered in the calculations with ATHLET nor with the other codes. This hints to a need of further development of the steam generator model.

References

[1] E. Krepper
ISP-33 Pre- and Posttest Calculations in the FZ Rossendorf
ISP-33 Second Workshop, Lappeenranta May 1993

[2] M.J. Burwell, G. Lerchl, J. Miro, V. Teschendorff, K. Wolfert
The Thermalhydraulic Code ATHLET for Analysis of PWR and BWR Systems, NURETH-4, Proceedings Fourth International Topical Meeting on Nuclear Reactor Thermal-Hydraulics, Volume 2, Karlsruhe 1989, p. 1234

[3] H. Purhonen, J. Miettinen
PACTEL - General Description for ISP
ISP-33 First Workshop, Lappeenranta February 1992

[4] E. Krepper, U. Rohde
Natural Circulation Instabilities during a LOCA of VVER-Type reactors
New Trends in Nuclear System Thermohydraulics, Pisa 1994

The project this report is partially funded by the SMWK (Sächsisches Ministerium für Wissenschaft und Kunst) and is registered with No. 4-7541.82-FZR/301. The autor is responsible for the scientific content of the report.

CHARACTERIZATION OF IRRADIATION-INDUCED DEFECT STRUCTURES IN VVER-TYPE PRESSURE VESSEL STEEL 15Cr2MoV BY SMALL ANGLE X-RAY SCATTERING

J. Böhmert, M. Grosse

1. Introduction

In addition to thermal aging and fatigue, the material state of the reactor pressure vessel (RPV) is changed as a consequence of the neutron irradiation.
Due to the neutron loading the ferritic RPV steel provides an increased strength and a reduced toughness what causes a rise of the ductile-to-brittle transition temperature. This safety relevant phenomenon is known as neutron embrittlement. The safety assessment aims at proving that a catastrophic failure of the RPV can be excluded under all conditions occuring during regular operation or during design based accidents.
Neutron embrittlement is a special safety issue at the Soviet-type VVER-reactors, in particular at the older VVER-440/230 reactors. Moreover, after long operation time neutron embrittlement may become a general problem independent on the reactor type, and has carefully to be considered when life-time extension is intended.
Fig. 1 schematically shows the parameters (outer circle) and mechanisms in the material (inner circle) which influence the process of neutron embrittlement.
In view of the complexity of embrittlement, it became usual to characterize the degree of embrittlement in a merely empirical way by mechanical testing of specimens that were irradiated with high neutron flux in special channels near the core (surveillance programme). Due to this high flux the embrittlement of the specimes advances faster than that of the RPV. Thus, the deterioration of the mechanical properties of the RPV can be predicted.

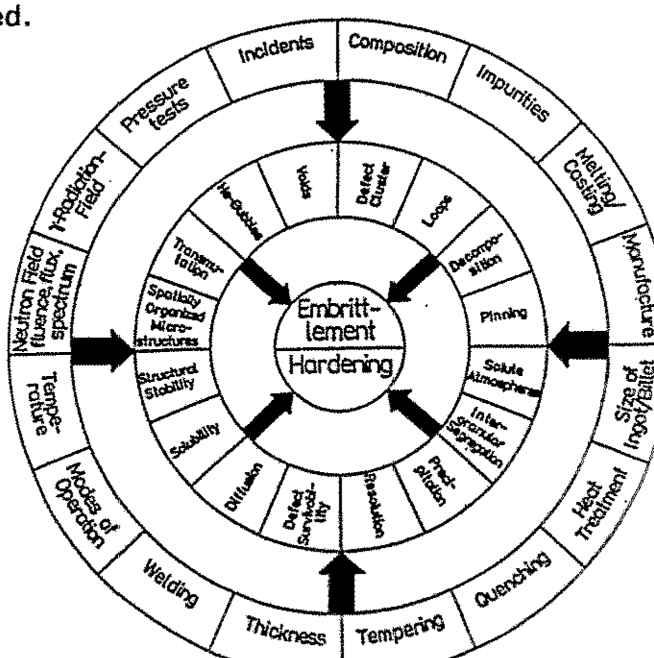

Fig. 1
Factors of influence and fundamental mechanisms of neutron embrittlement

Nevertheless, a physical understanding of the irradiation-induced structural modifications and of the resulting changes of mechanical properties is required to assess reliably the current state of the RPV.
The understanding must be based on an embrittlement model which considers:

- the nature of the irradiation-induced microstructural changes,
- the influence of irradiation and metallurgical parameter variations on the microstructure,
- the micromechanical modelling of the fracture process, and
- the correlation of the micromechanical process with the macroscopic strength and toughness parameters.

Just to provide contributions to the development of such a comprehensive model, the microstructure of irradiated VVER RPV steel was investigated and the results were compared with the measured mechanical properties of that material.

2. Microstructural features induced by irradiation

According to Pavinich et al. [1], neutron embrittlement has been attributed to the following mechanisms:

- lattice defect production caused by neutron displacement cascades
- formation of ultrafine, Cu-rich precipitates
- ultrafine phosphide formation
- ultrafine carbide formation
- temper embrittlement caused by P segregation.

There is experimental evidence for the occurrence of all processes in RPV steels [2]. Their significance is depending on irradiation temperature, flux, fluence, and the composition or heat treatment of the steel. But it has been common opinion that the second mechanism is the predominating one [3,4]. The solubility of Cu in Fe is very low (0,002 % at 300 °C). The neutron irradiation provokes an enhanced diffusion and thereby an accelerated precipitation of Cu (irradiation-enhanced precipitation). Typically the precipitates have a diameter of 2 nm, a length of 10 nm and a mean composition of 12 at % Copper [5].
Fisher and Buswell [6] assume, as a second important mechanism, the formation of damage clusters or loops. Such clusters might be microvoids stabilized by impurities or minor alloying elements, for instance Cu (Cu-coated microvoids).
Currently the formation of P segregation at the grain boundaries is discussed [7]. The formation of ultrafine carbides or carbonitrides is noticed [5], but evaluated as not significant.
These findings are related to ASTM steels. The behaviour of the VVER-440-type RPV steel 15Cr2MoV(A) differs from that, mainly owing to the fact that it does not contain Ni but V.
Investigations of irradition defects in this steel were rarely published only.
Kocik et al. [8,9] carried out TEM-analyses (Transmission Electron Microscopy) of Czech steel and found, besides dislocation loops and a refinement of vanadium carbide particles, black dots of more than 8 nm in size. The structure and composition of these dots could not be identified. Brauer et al. [10-13] used positron annihilation and Mößbauer spectroscopy for a comprehensive study. By these methods they provided

indirect results which suggest the generation of irradiation-induced carbides to be the major defect mechanism. SANS experiments (small angle neutron scattering) [14] *show precipitates with a mean diameter of 1...5 nm and a total volume fraction of* 0,1...0,36 %, depending on Cu content and neutron fluence. The A-ratio determined from the scattering intensities of magnetic and nuclear scattering ranges between 1.6 to 5.3 and increases with the Cu content. A = 11.0 corresponds to pure fcc Cu, A = 1.4 to voids.
Recently atom probe field ion microscopy was even applied [15]. The analysis revealed grain boundary segregation.

3. The method of anomalous small angle X-ray scattering (ASAXS)

Inhomogenities of the electron densities with a size of 0,5...500 nm cause an elastic scattering of an even X-ray wave towards small angles. The intensity of this small angle scattering I(Q) is given by

$$I(Q) = a \cdot |n_p \cdot f_p - n_M \cdot f_M|^2 \, \frac{1}{n_M} \, c_p \cdot V_p \cdot S_1(Q) \tag{1}$$

with:

Q	*scattering vector*
a	calibration factor
$f_{P,M}$	mean scattering length (atomic scattering factor) of the particle or matrix respectively
$n_{P,M}$	mean number density in the particle or matrix, respectively
c_P	volume fraction of the particles
V_P	volume of the particle
$S_1(Q)$	specific structure factor; Guinier - approximation (spherical particles): $S_1(Q) = e^{-\frac{Q^2 R_G^2}{3}}$
R_G	radius of gyration

The atomic scattering factor f at small angles is given by

$$f(E, Q \rightarrow 0) = Z + f'(E) + if''(E) \tag{2}$$

with Z being the number of electrons surrounding the atom and the complex expression f'(E) + if"(E) which describes the contribution of anomalous scattering. This contribution is only significant and only strongly depends on the energy near the absorption edges of an element. As an example, Fig. 2 shows the energy dependence of the atomic scattering factor of vanadium and iron. Thus, the contrast variation of the small angle scattering (SAXS) intensity at different energies provides information on the chemical composition. The presence of a certain element can be concluded from the energy level at which a strong change of the intensity occurs. Furthermore the precise measurement of the energy of the edge reveals the binding state (chemical shift).

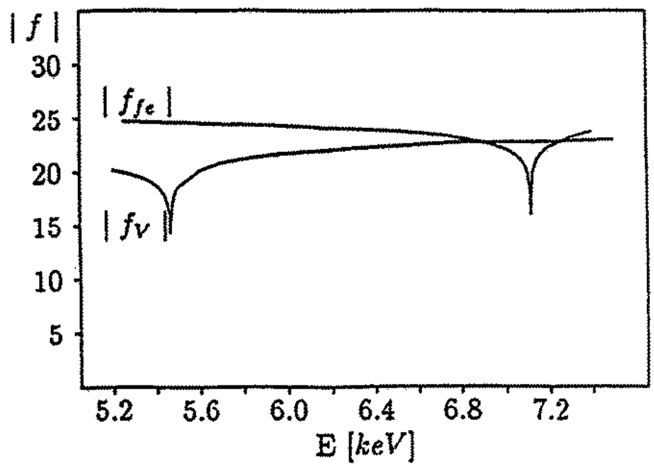

Fig. 2
Energy dependence of the atomic scattering factors of iron and vanadium

4. Recent Results

Specimens were prepared from VVER-type 15Cr2MoV RPV steel (Russian code 15Kh2MFA) manufactured by SKODA/Czechoslavakia. Its chemical composition is given in Tab. 1, material UJV. The steel is of low Cu content. The material was irradiated in the research reactor of the Czech Nuclear Research Institute Rez up to a fluence of 2.1 x 10^{23} m^{-2} (E > 1.0 MeV) at 306 °C.

Table 1
Chemical composition of the materials

Material	C	Si	Mn	Ni	Cr [wt. %]	Mo	V	S	P	Cu
UJV	0.16	0.19	0.42	0.09	2.84	0.63	0.34	0.014	0.013	0.10
GG	0.15	0.23	0.55	0.25	2.59	0.59	0.27	0.01	0.01	0.24
GH	0.16	0.29	0.54	0.07	2.70	0.68	0.28	0.02	0.01	0.09
C	0.15	0.12	0.28	0.07	2.35	0.70	0.23	0.03	0.02	0.14
D	0.18	0.14	0.29	0.07	2.61	0.68	0.35	0.03	0.05	0.14
E	0.15	0.18	0.36	0.07	2.60	0.67	0.30	0.03	0.02	0.34
F	0.15	0.25	0.42	0.07	2.65	0.68	0.29	0.03	0.04	0.32
HH	0.04	0.64	1.25	0.06	1.34	0.50	0.21	0.01	0.01	0.08

The small angle scattering of the RPV steel foils was measured at the JUSIFA facility of the Hamburg synchrotron laboratory HASYLAB. Fig. 3 shows the SAXS patterns of irradiated and unirradiated material. The difference $\Delta I(Q)$ between these two patterns is caused by the irradiation induced defects.

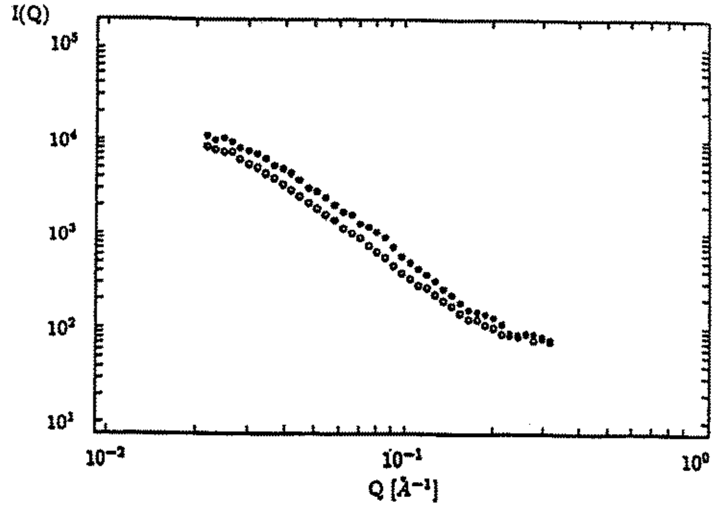

Fig. 3
Small angle X-ray scattering patterns of irradiated (.) and unirradiated (o) material

In order to investigate the effect of contrast variation the SAXS intensity at the scattering vector $Q=0$ was calculated by extrapolation of the linear part of the curve log (I(Q) vs. Q^2 (Guinier-Plot). Fig. 4 depicts the energy dependence of $I(Q=0)$. Near the K_α absorption edge of vanadium a significant contrast variation is obtained, what confirms the vanadium contents of the precipitates.
The energy of the absorption edge corresponds to a vanadium valence smaller than four. So the precipitate will probably be V_3C_4.

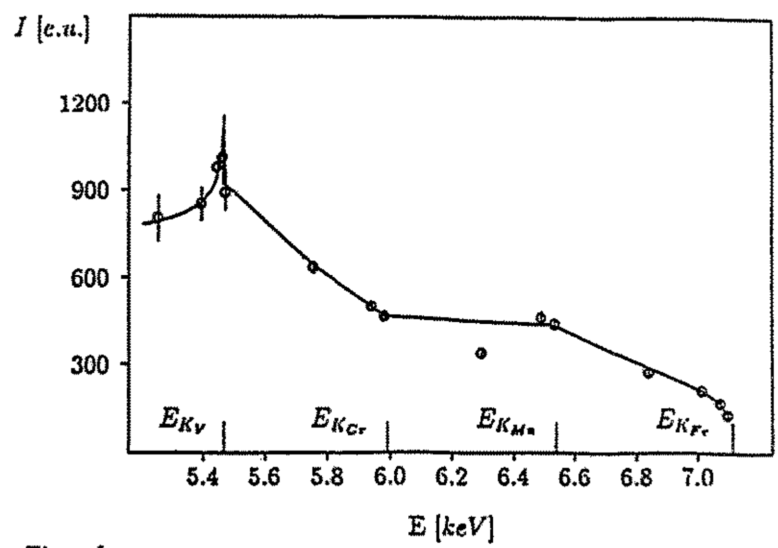

Fig. 4
Energy dependence of the SAXS intensity $I(Q=0)$

Additional information can be obtained by magnetic contrast variation from the ratio of nuclear and magnetic scattering (A-ratio) in the SANS experiments [14]. For steel of similar composition and fabrication (specimens of the surveillance programme of the Hungarian Nuclear Power Plant Paks, material HH and GH in Table 1) an A-ratio of 1.8...1.9 was found. Table 2 compares the A-ratios of different kinds of clusters or precipitates. The assumption of vanadium-rich carbides V_3C_4 provides the best agreement with the experimental data. Both results support the hypothesis, derived from positron annihilation experiments [10], that the irradiation-induced precipitates in the VVER-type RPV steels might be carbides, at least in those VVER steels with low Cu content.

Table 2
Comparison of the measured A-ratio with calculated A-ratio of some possible kinds of clusters

Kind of cluster	A-ratio
measured value	1.8...1.9
fcc-copper	11.0
bcc-cooper	7.0
voids	1.4
metallic vanadium	1.4
VC (NaCl structure	2.4
$V_{0.86}Cr_{0.09}Mo_{0.04}Fe_{0.01}C$	2.7
V_4C_3 (NaCl structure)	1.9

The correlation between the mechanical properties and the volume fraction of irradiation-induced precipitates also substantiates the existence of a specific kind of irradiation-induced precipitates in VVER-type RPV steel. In Table 1 (material GG...HH) the chemical composition of different heats of 15Cr2MoV steel is given. There are heats of original RPV base and weld metal manufactured in Russia and Czech, respectively, and there are heats of special laboratory melts.
Strength and toughness values of heats GH and HH are published in [16].

Fig. 5 presents the correlation between the volume fraction f of the irradiation-induced precipitates, determined by SANS, and the shift of the ductile-brittle transition temperature ΔT_{41}. ΔT_{41} is proportional to $\sqrt{f}$. The slope of the curve depends on the amount of Cu. The embrittlement of steels with high Cu content (Cu > 0.2 %) is less influenced by the irradiation-induced precipitates than the embrittlement of steels with lower Cu-content (C < 0.15 %).

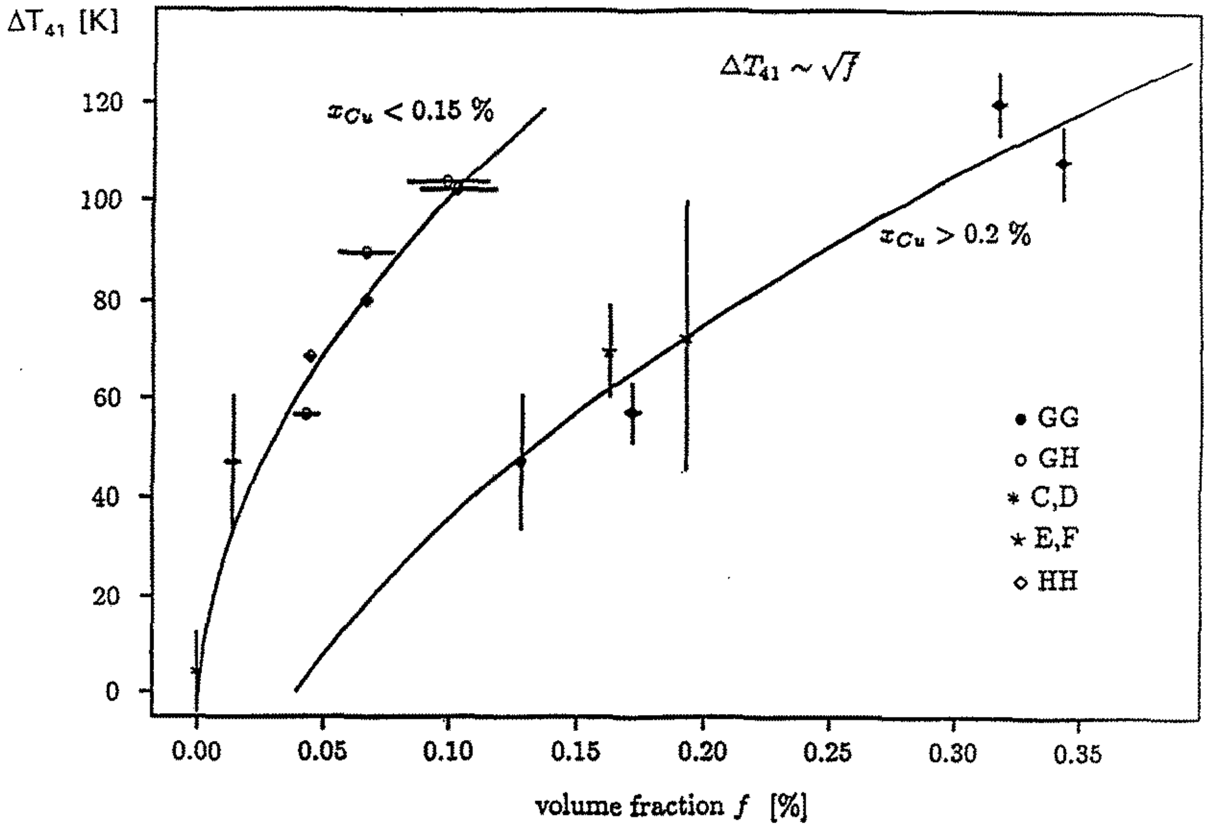

Fig. 5
Correlation between volume fraction of radiation-induced precipitates f and shift of the ductile - brittle transition temperature ΔT_{41} for 15Kh2MFA steel of different chemical composition

The explanation might be as follows:
As known, the ductile-brittle transition temperature is considered the temperature for which the maximum tensile stress exceeds the microscopic fracture strength within a characteristic distance in front of the notch tip (e.g. [17]). The maximum tensile stress depends on the yield strength and on the strain hardening properties. The yield strength increases with the irradiation (irradiation hardening). The theory [18] just predicts a dependence of the hardening on the volume fraction of irradiation-induced precipitates that corresponds very well with the curve shapes in Fig. 5.
The change of the strain hardening may be a consequence of the various strength and size of the precipitates. When the particles are small and coherent the precipitates are cut by dislocation. By shearing particles the effective particle size decreases in the slip plane and, thus, the resistance against further dislocation motion as well. Therefore the deformation is inhomogeneously concentrated and the strain hardening is low. On the other hand bigger and semi- or incoherent particles and glide dislocation interact by the Orowan mechanism. In this case dislocation loops are created around the precipitates which impede the further dislocation motion in the slip plane and so cause a homogeneous deformation with higher strain hardening.

From this point of view it can be assumed that the different slopes of the curves in Fig. 5 are caused by different types of the predominating precipitates and the related changes in the interaction mechanism between particles and dislocations. In Cu-poor 15CrMoV steel, small coherent irradiation-induced vanadium carbides are predominant. As a result, increasing content of these precipitates leads to inhomogeneous deformation, early crack initiation and large shift of the transition temperature. Cu-rich precipitates are produced by irradiation of RPV steels with higher Cu content. These precipitates are not cut by glide dislocation and their effect on the increase of the transition temperature is weaker.

5. Conclusion

There is a remarkable evidence that vanadium rich carbide precipitates are induced by irradiation of Cu poor VVER-type RPV steel. This result reveals a new aspect in the understanding of the mechanism of neutron embrittlement. Up to now vanadium has been regarded by the Russian experts as to be stabilizing against irradiation effects [19]. In further experiments the presented finding will have to be substantiated. Especially the influence of the Cu and the effect of thermal annealing requires further investigation.

References

[1] W.A. Pavinich, T.J. Griesbach, W.L. Server
"An Overview of Radiation Embrittlement Modeling for Reactor Vessel Steels", Radiation Embrittlement of Nuclear Reactor Pressure Vessel Steels: An International Review (Fourth Volume), ASTM STP 1170, L.E. Steele, Ed., American Society for Testing and Materials, Philadelphia, 1993, pp. 99-117

[2] G.R. Odette, G.E. Lucas
Irradiation Embrittlement of Reactor Pressure Vessel Steels: Mechanisms, Models and Data Correlations; in L.E. Steele (ed.): Radiation Embrittlement of Nuclear Reactor Pressure Vessel Steels (Second Volume), ASTM STP 909, Philadelphia, 1986, p. 206-241

[3] G.R. Odette
Steels, Scripta Met. 17 (1983) 1183

[4] G.E. Lucas, G.R. Odette, P.M. Lombrozo, J.W. Sheckhard: Effects of Composition, Microstructure and Temperature on Irradiation Hardening of Pressure Vessel Steels, in F.A. Garner, J.S. Perrin (eds.): Effects of Radiation on Materials, 12th Intern. Symposium, June 1984, Williamsburg, VA, ASTM-STP 870, Vol. II, pp. 900-930, ASTM Publ., Philadelphia, 1985

[5] R.G. Lott, S.S. Brenner, M.K. Miller, A. Wolfenden
Trans. ANS 1993 (67), 303-304

[6] S.B. Fisher, J.T. Buswell, Int. J. Pressure Vessel and Piping 27 (1987) 91

[7] C.J. Bolton, R.B. Jones, J.T. Buswell, R.H. Priest, R. Moskovic
Application of Modelling of Copper Precipitation and Grain Boundery *Segregation of Phosphoros*, IG-RDM IV, *Meeting 1992*, *Fontainbleau*, *Nov. 92*

[8] J. Kocik, E. Keilova
Nucl. Mat. 176 (1990), 126

[9] J. Kocik, E. Keilova
Materials Science Forum, 97-99 (1992) 837

[10] G. Brauer, L. Liszkay, B. Molnar, R. Krause
Nucl. Eng. Design 127 (1991), 47-68

[11] G. Brauer, L. Liszkay, B. Molnar
Position Annihilation Studies of Neutron Irradiated Reactor Pressure Vessel Steels, Rep. ZfK-637(Aug. 1988)

[12] G. Brauer, M. Sob, J. Kocik
Positron Annihilation Study of Radiation Damage in Neutron Irradiated Reactor Pressure Vessel Steels, Rep. ZfK-703 (April 1990)

[13] G. Brauer, W. Matz, L. Liszkay, B. Molnar, R. Krause
Positron Annihilation and Moessbauer Studies of Neutron Irradiated Reactor Pressure Vessel Steels, Material Science Forum 97-99 (1992), 379-385

[14] G. Brauer, F. Eichhorn, F. Frisius, R. Kampmann
Investigation of Neutron Irradiated Soviet Type Reactor Pressure Vessel Steels by Small Angle Neutron Scattering, Effects of Radiation on Materials: 16th. Internat. Symp., ASTM STP 1175, S.K. Kumar, D.S. Gelles, R.K. Nanstad, E.A. Little (Ed.), Philadelphia, 1994 (in press)

[15] M.K. Miller, R. Jayaram, P.J. Othen, G. Brauer
Preliminary APFIM Characterizations of VVER Steels, IGRDM-IV, Fontainebleau, Nov. 1992

[16] F. Oszvald, P. Trampus, F. Gillemot
preprint "Summary of the Surveillance Results at NPP Paks" EWGRD & WGRD-VVER Workshop "Pressure Vessel Surveillance Programmes and Their Application"; Řež (1993)

[17] R.O. Ritchie, J.F. Knott, J.R. Rice
J. Mech. Phys. Solids 1973 (21) 395-410

[18] R.W. Cahn, P. Haasen (eds)
Physical Metallurgy, third edition, Elsevier, Amsterdam 1983, Vol. II

[19] A. Kryukov, Russian Research Center "Kurchatov Institute", Reactor Technologies and Material Institute, private communication

NEUTRON FLUENCE CALCULATIONS AND SPECTRUM ADJUSTMENT FOR THE RHEINSBERG PRESSURE VESSEL STEEL IRRADIATION PROGRAM

H.-U. Barz, B. Böhmer, J. Konheiser, I. Stephan

1. Introduction

The starting point of these investigations is the irradiation program performed in the Rheinsberg reactor for three different reactor periods during 1984 to 1988. In this program more than a thousand steel specimens were irradiated at different positions. Additionally a considerable number of activation monitors were installed. For the planned mechanical testing of these specimens information of the irradiation condition of all specimens is needed. Therefore, the neutron fluences at the different irradiation points have to be determined for all relevant reactor periods. With the limited number of activation monitors, located not exactly on the needed positions and not covering exactly the needed energy range, this can be done only by detailed neutron transport calculations. The activation monitoring results can be used to proof the calculations. Spectrum adjustment allows to combine in an optimal way the results of transport calculations and measurements.

2. Monte Carlo calculation of fluences for different reactor periods

As the fission sources in the reactor core are known by standard burn up calculations the engagement was focussed on the determination of the neutron distribution outside the core at special irradiation positions, provided the time integrated fission sources for each considered reactor period are given. This problem is a typical neutron transport problem where the neutron transport equation can be applied.

The justification of this approach comes from the fact that the cross sections in the core region for the interesting energy range greater than 20 keV are only very little influenced by the burn up. Therefore, instead of different flux calculations for the given time steps it is sufficient to superimpose the fission sources.

Fig. 1 shows a 90° sector of a cross section through the Rheinsberg reactor. The target channels (T) and the other irradiation channels (S) where the irradiations for three different reactor periods are carried out are specially marked.

The results represented in the following were obtained with the Monte Carlo code TRAMO[1] that was developed in Rossendorf. The Monte Carlo method has very many advantages in comparison with other methods, because the real technical system with all

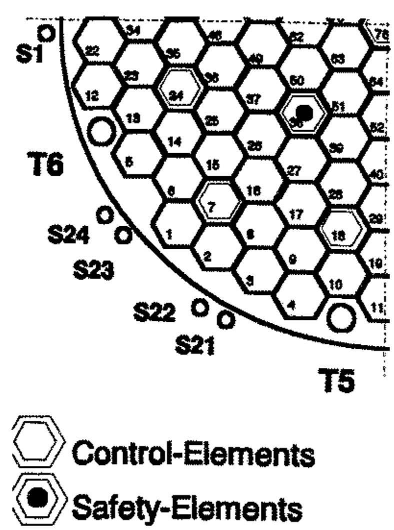

Fig. 1: Sector of the Rheinsberg reactor

known geometrical details can be taken into account and some mechanisms of neutron behaviour can be described more accurately than by means of deterministic codes.

So e.g. the correlation between the scattering angle and the energy loss of the neutrons was treated more exactly than usually by considering the scattering especially for hydrogen using the collision laws in the cm-(center of mass) system.

The main problems of Monte Carlo calculations are connected with the statistical errors. To diminish these errors the "weight window" method has been applied in a generalized manner/2/. Shortly spoken the method consists in the introduction of forced weights for each region and each energy group. Each particle on its geometrical and energetical way has the order to come near to these weights. If the forced weight is greater than the weight of the entering particle it is killed with a given probability and if the particle is not killed, it gets the higher forced weight. The killing probability is chosen in that way, that the mean weight is equal to the weight of the original particle (Russian Roulette). If the forced weight is smaller the incoming particle is splitted, that means the total weight is distributed on more particles. The weights themselves are dependent on the region and energy range, where an especially low statistical error should be obtained (detector area). The rule was used that the weights have to be inverse proportional to the mean contribution to this detector area of a particle started in the given region and energy group (importance function). The efficiency of this rule is transparent but until now only proved for very simple cases. Particles with high importance are statistically treated more accurate then particles with a low one. For the sources the same procedure is used. Many particles are started in regions and with energies of high importance to the results while only a few are treated if they are assumed to have a low influence.

The weights are also determined by Monte Carlo calculations using the own code TRAWEI. This technique decreases the statistical errors even for sources, which are optical far from the detector region. One advantage of this method is its generality. It can also be used for very complicated geometrical systems. By these measures very accurate results in a rather detailed structure were obtained.

If there is sufficient information about the source distribution and the details of the system (compositions, nuclear densities, geometrical data) the only remaining source of errors is connected with the used group data.

3. Used group data and correlation between slowing down and scattering angle

Two different cross section group data were used for the calculation. One set is the ABBN-78 set that was improved in the following manner. The anisotropy of the elastic scattering was considered by a calculated angle dependent scattering function for each isotope and each energy group in the cm-system. These functions were determined for a grid of 20 angle intervals.

By means of these functions and the given collision laws in the cm-system the Monte Carlo simulation is capable of calculating the exact energy loss.

Another set of 123 group data, that was applied in the relevant energy range beyond 21.5 keV, is based on the JEF-1 data. These group data were provided by the University of Stuttgart with scattering matrices up to the P_L-order of five in the laboratory system.

This representation of scattering anisotropy permits to take into account the mixtu-

re of isotopes and all kinds of scattering, but provides an unsatisfying description of scattering within the given group, because the Legendre expansion approximates large forward peaks rather badly. Therefore, hydrogen scattering was treated in a different way. As the scattering of hydrogen is really isotropic in the centre of mass system, hydrogen is considered as stated before with a constant angle function.
For comparison also the influence of the different fission spectra based on ABBN-78 and JEF-1 data was studied. Moreover for one typical case the code MCNP has been used to have a comparison not only for the used data but also for the calculation code. In Table I some results for these different calculations are given.

Table I: Examples of Calculations for different data and codes (reactor period 1984/1985 target channel T6, layer 111.0-190.0 cm, five specimens, fluences in n/cm^2)

	ABBN78	JEF-1	MCNP(ENDF/B4)
1. E>.5MeV			
I	1.013+20 (.3%)	1.028+20 (.35%)	1.01+20 (1.94%)
II	5.994+19 (.27%)	6.008+19 (.30%)	6.108+19 (2.5%)
III	5.306+19 (.26%)	5.335+19 (.28%)	5.288+19 (2.7%)
IV	8.526+19 (.30%)	8.570+19 (.32%)	8.504+19 (1.8%)
V	1.208+20 (.28%)	1.210+20 (.29%)	1.208+20 (1.8%)
2. E>1.0MeV			
I	7.323+19 (.36%)	7.402+19 (.40%)	7.186+19 (2.2%)
II	4.350+19 (.33%)	4.333+19 (.35%)	4.362+19 (2.9%)
III	3.834+19 (.33%)	3.840+19 (.33%)	3.763+19 (3.1%)
IV	6.170+19 (.36%)	6.184+19 (.38%)	6.010+19 (2.5%)
V	8.742+19 (.34%)	8.736+19 (.35%)	8.580+19 (2.1%)

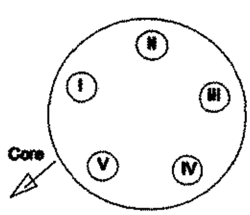

It is indeed very surprising that the results for both group sets are in a very good agreement. This agreement also exists for the group spectra if the 123-group results are condensed to ABBN-group structure. Agreement can be stated for the target channels and for the other irradiation channels too, but not for positions outside the pressure vessel.

4. Some comments of the calculations for Rheinsberg experiments

The calculations are not yet finished and the representation of the results will be published later. Here only a few comments are given.
Neutron spectra, cumulative fluxes for E>1.0MeV and E>0.5MeV together with dpa-values were calculated for a great number of specimens and positions of monitors. As the flux distributions in the target channels have large gradients in radial direction in general the specimens had to be subdivided into different parts. A great number of calculations had to be performed to reveal the vertical dependence of the fluences.
In spite of the needed detailed structure of results and the great number of different calculations it was possible to obtain mean statistical errors in the order of one percent or less (see Table I) showing the success of the used variance reducing methods.

5. Activation Measurements

In 1993 Russian neutron monitors with three activation probes and five usable detector reactions in each, that were irradiated *1984/85 in target channel 1, were* extracted from phantom bodies and analysed with a gamma-spectrometer for the reactions described in Tab.II.
Since the Russian niobium used in the monitors was not resistant to irradiation and the channel temperatures, it could be extracted only partly as a powder. This caused a relatively high weight error of up to 10%. Activation rates were obtained for five axial and up to three radial positions for 16 detector sets. Further detector sets for other Rheinsberg irradiation positions were prepared for spectroscopic analysis.

Table II: Detector reactions

detector reaction	threshold (MeV)	half-life	γ-energies (keV)	fluence range
$^{93}Nb(n,\gamma)^{94}Nb$	thermal	2.03+4a	703/871.1	$>10^{18}$
$^{93}Nb(n,n')^{93m}Nb$	0.1	16.13a	16.6/18.6	$>10^{18}$
$^{54}Fe(n,p)^{54}Mn$	3.0	322.2d	835	$10^{16}...10^{22}$
$^{63}Cu(n,\alpha)^{60}Co$	6.8	5.271a	1173/1332	$10^{18}...10^{22}$

6. Spectrum Adjustment for optimal use of experimental and calculation results

A generalized least squares adjustment procedure, based on an improved version of the program system COSA2 /3/, is used for simultaneous evaluation of transport calculations and activation measurements. It allows to combine information from both sources, calculations and measurements, in an optimal way.
Besides the new measurements for target channel 1 (84/85) old measurements for target channel 6 (84/85) /4/ have been evaluated. In contrast to former evaluations based on rather coarse removal-P1 spectrum calculations, due to the high precision of the Monte Carlo spectrum calculation no input normalization was necessary now, as it is usually applied before adjustment. Different cross section libraries used for calculating the detector response function yielded little differences in the results. As an example results of a reevaluation of activation measurements in target channel 6 are shown in Fig.2. A rather close agreement can be stated for all three curves in the energy range above 100 keV which is important for material embrittlement.
The results are much more influenced by the change from the formerly used Gaussian shaped spectrum covariance matrices to more realistic ones, as was shown by test calculations with different approximations for the spectrum covariance matrices. Further developments in spectrum adjustment methodology should therefore be directed especially to more precise evaluations of spectrum covariances.
The experiment-theory comparison, performed during the adjustment procedure, gave higher then expected differences between calculated and measured reaction rates, but in general good agreement between calculated and adjusted values of

the mainly interesting fluence integrals.

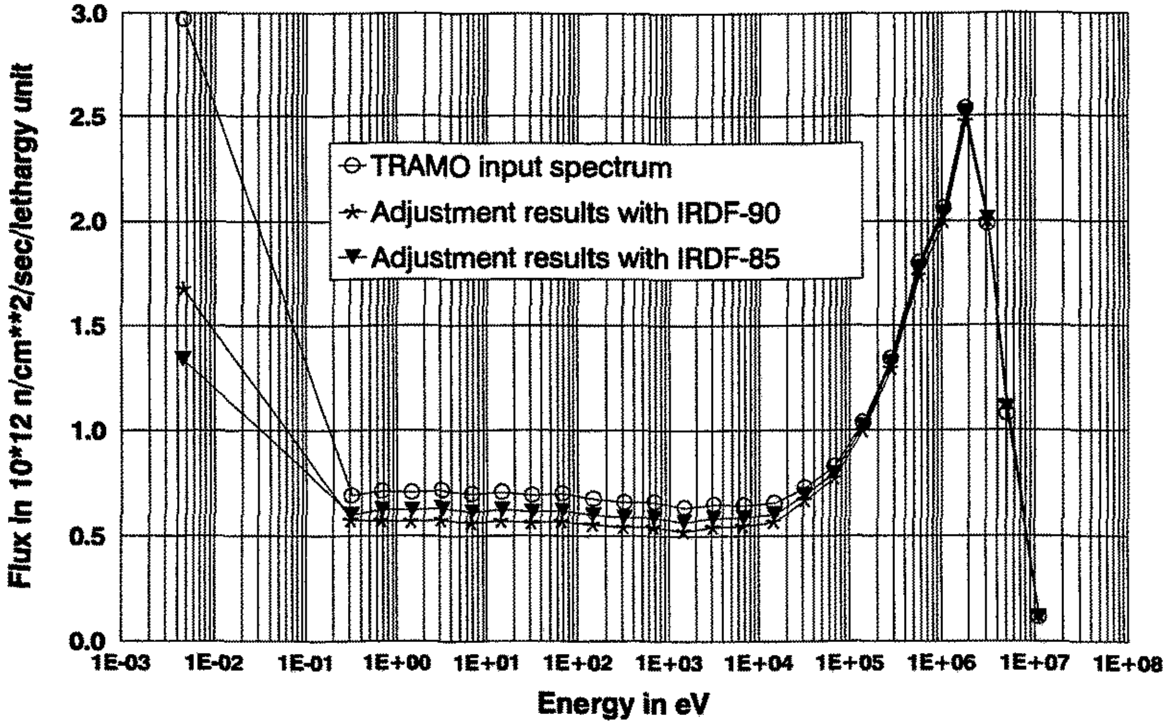

Fig.2: Adjustment results with different detector cross sections for target channel 6, position E4A, reactor period 1984/85 Rheinsberg (corrected thermal cross sections)

7. Summary

Monte Carlo neutron transport calculations are well suited to determine the neutron fluence in reactor pressure vessel material. The sensitivity against applied group data sets is only low at least for regions not so far from the core. Some disadvantages of the Monte Carlo method can be considerably decreased by weight window techniques and exact treatment of scattering angle-energy loss correlation. The accuracy and reliability of the fluence spectrum calculations have been proved by evaluation of activation measurements using a spectrum adjustment method.

8. REFERENCES

[1] H.-U. Barz, TRAMO - a Flexible Multigroup Neutron Transport Code on the Basis of the Monte Carlo Method for Flux Calculations, ZfK-705, Rossendorf 1990

[2] H.-U. Barz, Problems of Weight Determination for the Multigroup Monte Carlo code TRAMO for Neutron Flux Calculation, Progress in Nuclear Energy, Vol. 24, pp. 69-75, 1990

[3] B. Böhmer, COSA2 - Ein Spektrumsjustierungsprogramm zur Auswertung von Aktivierungsmessungen auf der Basis der verallgemeinerten Methode der kleinsten Quadrate, ZfK-735, Rossendorf 1991

[4] H.-C. Mehner, B. Böhmer, U. Hagemann, K. Popp, H.-P. Schützler, I. Stephan, Neutronendosimetrische Überwachung der Bestrahlung von Reaktordruckbehälterstrahlproben, Kernenergie 32 (1989) S.149-154

ACOUSTIC LEAK DETECTION AT COMPLICATED TOPOLOGIES USING NEURAL NETWORKS

G. Hessel, W. Schmitt, and F.-P. Weiß

1. Introduction

Methods of acoustic leak monitoring are of practical interest for a variety of pressurized systems confining toxic, explosive or combustible fluids. An advanced leak monitoring system must be capable of detecting a leak promptly, localizing it and eventually, if possible, estimating the leak rate. In recent years acoustic leak monitoring systems have been developed to localize leaks at simple geometrical structures as pipe lines and pressure vessels with a smooth surface and only a small number of connection branches, respectively. Existing methods using the attenuation (Jax and Ruthrof, 1989) or the propagation time differences (Fuchs and Riehle, 1991) of the airborne or structure-borne sound are not applicable to complicated structures especially when the thickness of the pressure confining walls is not great enough to allow the full development of a surface wave or when a great number of branches provoke sound reflections. Multiple propagation paths with and without reflection and the different sound modes generate a great number of maxima in the cross correlation function. There is no clear maximum that could be used for leak localization. A similar confusing constellation is found when the attenuation method is used, because it can only be successfully applied if one sound mode is clearly predominating. In case of the soviet-type VVER-440 pressurized water reactors even conventional leak monitoring methods, such as measuring the released radioactivity or moisture, fail because there is an air circulation of 80000 m^3/h under the protective cover (Fig. 1). Considering the shortcomings of all the existing leak detecting principles, a new method again based on the measurement of the leak induced sound but also applying pattern recognition is being developed. The capability of neural networks (Loos, 1993) to localize leaks at the reactor pressure vessel (RPV) head of VVER-440 reactors is discussed in the following.

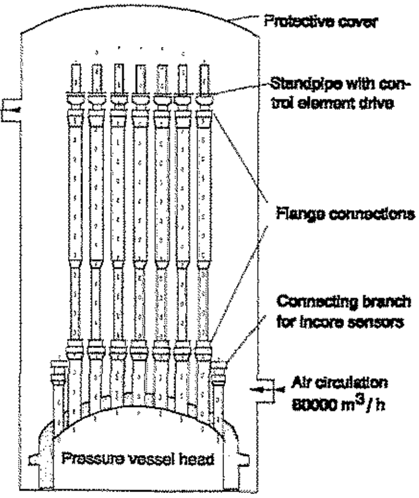

Fig. 1 Scheme of the pressure vessel head of a VVER-440

2. Aspects of leak monitoring

Though the results of the current research work are also applicable to chemical plants, it was especially initiated by leaks that occurred at VVERs operated at Central and Eastern Europe. The problem was addressed in basic safety reports (GRS, 1991; IAEA, 1991) which consequently recommended the installation of leak detecting and localizing systems at the VVER pressure vessel head. The sketch in Fig.1 indicates the structure of a VVER-440 RPV head. The vessel head construction consists of the upper calotte, 37 standpipes containing the control element drives, and 18 connecting branches for incore sensors at the periphery. Totally there are about 100 flanges in different heights. All these elements are endangered by leaks. The leaks in this region of the primary circuit do not only result in a loss of coolant but might also lead to a standpipe tear off followed by control element ejection and consequently to a reactivity initiated accident.

3. Working principle

It is the idea of the new method to use sophisticated pattern classification systems for leak localization at three-dimensional topologies. In the training phase, the pattern classifier is trained using a mobile source of sound simulating the leak at all positions, endangered by leaks. The sound is measured by a multisensor array mounted at the structure. RMS-values, components of power spectra or coherence functions are used to extract the feature vectors. After having trained the classifier for all positions, unknown leaks can be localized in the classification phase. Since this approach does not need an analytical model of the sound propagation, an adaptation of the method to different types of plants can be easily achieved. Therefore, the pattern-recognition-based approach can be transferred to different plants with complex topologies.

4. Leak experiments

Twelve acoustic emission (AE) sensors directly mounted at the structure and three high frequency microphones installed at the inner wall of the protection vessel were used to measure the leak induced sound (see Figs. 1, 2). All the AE-sensors could also be operated in the transmitting mode what is necessary for the calibration of the AE-sensor array and for the simulation of leak noise as well. The sound signals from the AE-sensors were simultaneously measured up to 500 kHz. The microphone signals were acquired up to 70 kHz. The positions of AE-sensors, microphones and simulated leak positions are shown in Fig. 2. A sound source based on a compressed air jet was used. The air jet direction is indicated by arrows. The leaks denoted by LRn and Lrn, respectively, were located on the top and in the middle of a standpipe being 7 m long. The other leaks in Fig. 2 were placed at the bottom flanges of the standpipes and at the connecting branches for incore sensors.

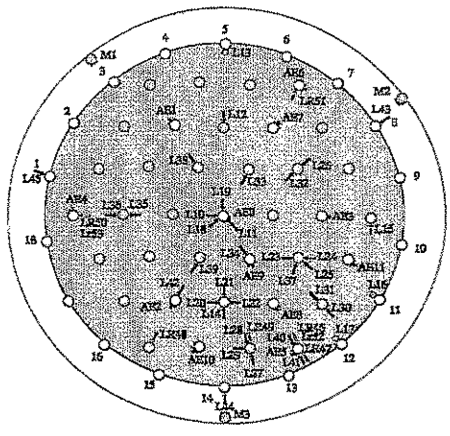

Fig. 2 Positions of AE-sensors (AEn), microphones (Mn) and leaks (Lm) at the pressure vessel head

5. Neural network approach

Without going into mathematical details, only a few basic principles of neural network topology and the most important differences between the used network types are briefly to be explained. Figure 3 shows a typical multilayer network consisting of an input layer, a hidden layer and an output layer. The number of neurons in the input layer is identical with the number of features X_i while the number of output neurons corresponds to the number K of classes to be recognized. Obviously in this application the different classes represent different leak positions L1...LK. During the training phase the network is confronted with pairs of input $\underline{X}$ and output patterns $\underline{O}$ to adjust the weights between the neurons in different layers. This procedure is called supervised learning. A trained network can assign the offered input vectors to the leak positions.

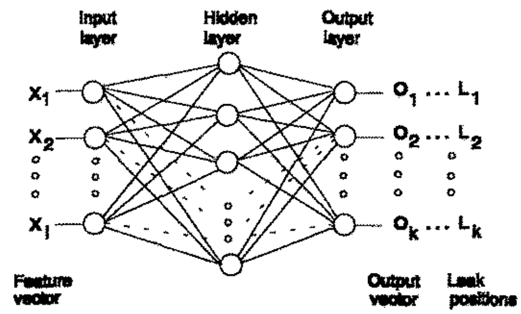

Fig. 3 Multilayer neural network

5.1 Perceptron networks P1 and P2

While P2 is a network with three layers (see Fig. 3), P1 contains no hidden layer. Therefore, P1 can only successfully be applied when the classes are linearly separable in the feature space. Both the P1 and P2 networks use the error-backpropagation algorithm to achieve minimum error of the obtained outputs with regard to the desired outputs by adjusting the weights (Rumelhart, Hinton and Williams, 1986). It is a disadvantage of the error-backpropagation procedure that it might only find a local minimum of the squared error in dependence on the weights. For networks with a large number of nodes this technique is very slow especially if many neurons are needed in the hidden layer. On the other hand, the training cannot be speeded up significantly by increasing the so called learning parameter because the convergence of the classification error might be lost. Though P2 networks require long computation time for learning, they are often used since they dispose of an advantageous generalization capability.

5.2 Reduced nearest neighbour network RNNN

Though having the same topology as P2 (Fig. 3), the RNNN realizes a rather different algorithm. Instead of the weights the hidden neurons are characterized by prototype vectors and by a vector $\underline{r}$ describing the receptive field around the tip of the prototype vector $\underline{W}_j$ belonging to node j. The so called *City distance measure* d_j *defined by*

$$d_j = \sum_i d_{ji} \quad \text{with} \quad d_{ji} = \max(0, |W_{ji} - X_i| - r_i) \qquad (1)$$

between $\underline{W}_j$ and the topical feature vector $\underline{X}$ is used as input of the hidden layer neuron j. So if $\underline{X}$ is in the receptive field of the neuron, d_{ji} will be set zero, otherwise it is the real distance reduced by r_i. The outputs of the hidden layer neuron O_j and of the output neuron O_k, respectively, are given by

$$O_j = 2e^{-d_j/2} - 1 \quad \text{and} \quad O_k = \max_j [V_{kj} O_j] \qquad (2)$$

where the weights V_{kj} between the output neuron k and the hidden layer neuron j can only assume the values 0 or 1.

5.3 Kohonen network KN

This is a counterpropagation net modified for classification tasks (Loos, 1993). As hidden layer, a two-dimensional self-organizing Kohonen map is used to arrange hidden neurons representing input patterns with similar properties closely together (Kohonen, 1984). Instead of applying the City distance measure (1), the well-known Euclidean distance between $\underline{X}$ and the prototype vectors $\underline{W}_i$ is used. The transfer functions of hidden neurons and of output neurons are the same as for RNNN (2).

6. Leak localization using airborne sound

It was found that the coherence functions between the two high frequency microphones provide suitable feature vectors characterizing the source location of the airborne sound. Certainly, the reason for this is that each leak position results in a typical fictive nonlinear sound propagation from the one to the other microphone. And this special nonlinear transfer determines the coherence function. Moreover, using the coherence, the spectral changes of the leak noise over the time do not influence the classification. Therefore, 200 points of the coherence function up to 70 kHz were taken as features. The networks were trained with the same data and also the classification was tested for identical data sets not included in training. For example, the set of training data comprises 221 coherence functions, 17 for each of 13 leak positions. The investigation proved that P1 (200/13) (number of nodes in different layers) and RNNN (200/87/13) provided 100% correct classification even after only 5 minutes of training time. In contrast to that it took about 10 hours of training the P2 net (200/100/13) also to achieve 100% correct classifications of the same data. This long training resulted from 100 hidden neurons needed for minimum error convergence. Also, the long training time of 8 hours for the KN network was impracticable.

To differ between leaks at different heights of the standpipe, an extended feature vector with 600 elements was used. In addition to the coherence function, further features were extracted from the autopower spectral densities (APS) of both microphone signals. The distinction between the height levels becomes possible due to the steeper descent of the APS with increasing frequency for the upper leak positions. Here it must be remarked that the RNNN and KN could not be applied to vectors with 600 features due to insufficient convergence. For more than 15 trained leak positions, all the investigated networks exhibited lacking convergence when 600 features were used. Therefore, the number of features has significantly to be reduced if 50 or even more leak positions are to be recognized.

7. Leak localization using structure-borne sound

The learning and recall capabilities of neural networks were compared in scenarios where only a few features (12) are available to identify a large number of classes (44). The feature vectors were formed from 12 RMS-values of AE-sensor signals. Training and reclassification were performed with 1540 input vectors; 35 for each of the 44 classes (leaks). The data set used to test the classification capability comprised more than 450 feature vectors (about 10 for each class). The results listed in Table 1 show that the RNNN do not only learn considerably faster than the other classifiers, they also provide 100% correct reclassification and a high classification accuracy of 100%. The high rate of misclassification (39%) indicates that the P1 network cannot linearly separate the 44 classes using only 12 features. However, the P2 network is capable of correctly classifying when the appropriate number of hidden nodes could be found for the special classification problem. In this case, correct classifications were achieved with 25 hidden nodes.

Table 1 Training and classification capability

Network	P1	P2	KN	RNNN
Parameter	12/44	12/25/44	12/132/44	12/106/44
Training time	7h	20h	3h	12min
Reclassification	65%	100%	92%	100%
Classification	61%	100%	91%	100%

It should further be mentioned that RNNN and KN dispose of a lower separability between the different classes than the P2 network. P2 assigns the feature vectors to the correct classes with an output activity (or membership) of almost 1.00 in all cases, while the activities of all other output neurons keep below 0.05. The classification rate of 91% does not permit the conclusion that Kohonen networks are not suited for leak detection at complicated structures. A more detailed inquiry proves L10 and L18 not to be separable by KN because they are located at the central standpipe with an angle shift of only 45° (see Fig. 2). They are assigned to one and the same class, because those neurons of the Kohonen map which are not unambiguously connected to a single class are eliminated in the second phase of the training. Nevertheless, for practical purposes the recognition of the leaking standpipe is sufficient.

The property of the Kohonen map to maintain the topology can be utilized to determine the necessary number of sensors and their best suited positions. Table 2 gives the classification rates of the RNNN and KN for some selected sensor configurations. Though the separability decreases with decreasing number of sensors, the RNNN assigns correctly even if only three sensors are available. The deterioration of the separability of the RNNN results in smaller differences between the output activities of the different output neurons. So for three sensors, e.g. the activity of the right output neuron was still 1.00 but the activities of the other neurons came very near to that value (0.98).

Table 2 Classification rate versus sensor configuration

Sensor Number Configuration	12 0-11	9 0-8	8 1-8	7* 0-6	6 1-6	3 4-6
RNNN	100%	100%	100%	100%	100%	100%
KN	92.2%	97.8%	97.8%	100%	96.4%	90.1%

* Arrangement of the 7 sensors:

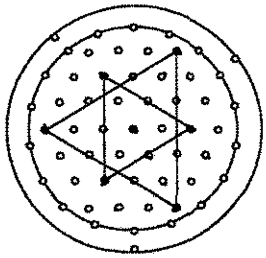

The KN network achieves the best classification with 7 acoustic emission sensors. It is supposed that the decrease of the correct classification rate in spite of the increasing number of sensors is caused by the Euclidean distance measure. The additional five sensors do not contribute to the separability but they provoke a background noise in the distance which eventually leads to degraded classification.

8. Investigation of the generalization capability

The ability of a classifier even to handle patterns of untrained classes consistently is of practical interest because in some applications the patterns of all the possible classes are not available during the learning phase. To investigate the generalization of a net for patterns of not trained classes, all the used neural networks were trained with the same set of measuring data comprising patterns of 27 different leak positions. The feature vectors contained 7 RMS-values of the optimum AE-sensor configuration.

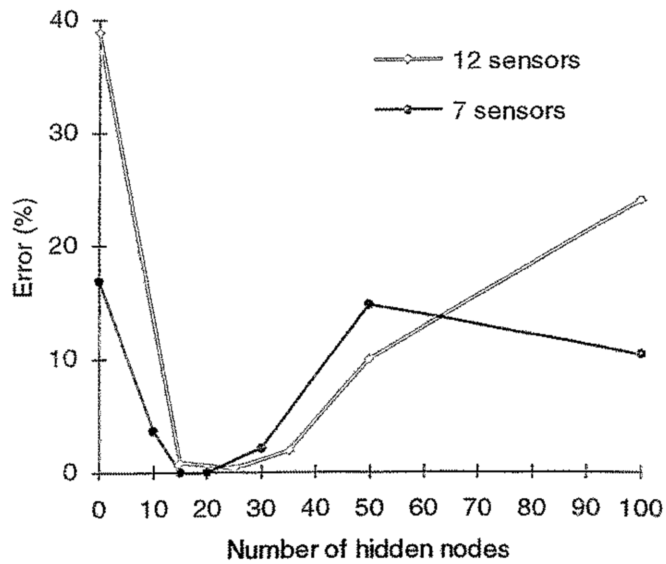

Fig. 4 Classification error of the perceptron net, P2, for two sensor arrangements as a function of the number of hidden neurons

Before making any generalization test, the neural networks were optimized with regard to the number of hidden nodes. Figure 4 shows how the number of hidden nodes influences the classification of perceptron nets. As indicated by the minimum of the classification error, the best results of classification are attained with 15 up to 20 nodes in the hidden layer. When using the 12 sensors configuration the minimum occurs with 25 hidden neurons. The minima in Fig. 4 demonstrate that the decision boundaries which are formed by the nonlinear transfer through the sigmoid functions of the optimized number of hidden neurons match the complexity of the real arrangement of the classes in the feature space.

Eight leak positions excluded from training were presented to the different classifiers to determine their ability to perform useful generalization. This generalization test proved the P2 network with 15 hidden neurons to possess the best developed generalization capability. The bar charts in Fig. 5 display the generalization capability of P2 in dependence on the number of hidden neurons by means of the activity of the assignment of the eight untrained leak positions to trained leaks. In all cases, the untrained patterns are unambiguously assigned to the same standpipe, e.g. LR50/Lr53 and L41/L40, or to a neighbouring position, such as L39/L42, L22/L28, and L16/L17 (see Fig. 2). Moreover, it must be remarked that the assignment to other classes is very small, less than 0.05.

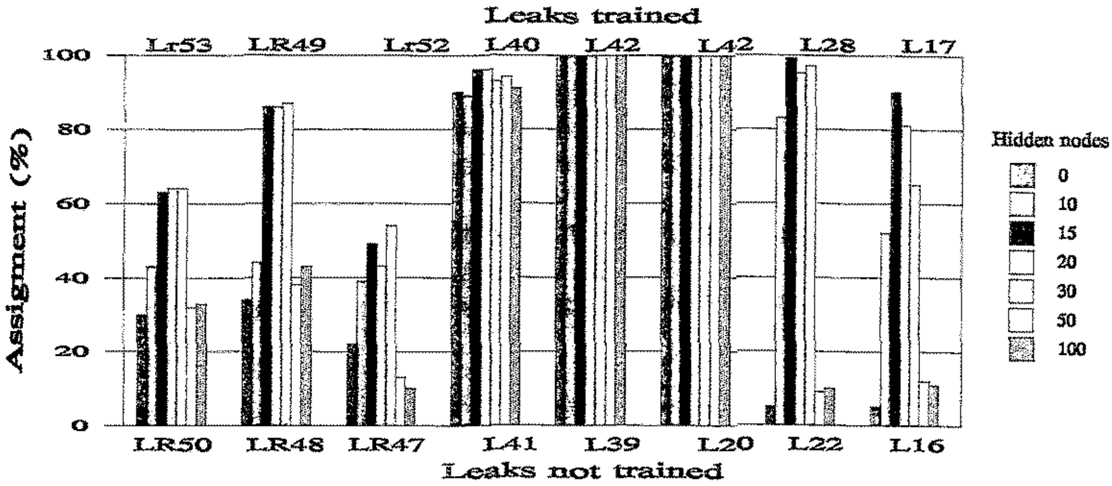

Fig. 5 Assigment of untrained leaks as a function of the number of hidden nodes (P2)

On the other hand, the bar charts of L39/L42 and L20/L42, for example, indicate that the assignment could be made fully independent on the number of hidden neurons for all untrained leaks if both the net and the sensor configuration were optimized.

It should be noticed that the P1 is not able to separate the pairs of neighbouring leaks referred to in Fig. 5. The application of RNNN and KN to untrained leaks leads to ambiguous results because they produce similar assignments to several classes.

9. Conclusion

The efficiency of neural-network-based classification for leak localization at complicated 3-dimensional topologies could be proved experimentally. Appropriate features for detection and localization are RMS-values of structure-borne sound signals measured by AE-sensors. Up to 50 different leak locations can be identified by RNNN, KN and P2 networks. Through fitting the sensor configuration to the topology, the number of necessary sensors could be reduced from 12 down to 7. The leak detection by airborne sound is a complementary method and is especially needed if the structural components where leaks might occur are located at different geodetic height levels. In cases where a large number of features (a few hundreds) are required, only the P2 perceptron network provides 100% of correct classifications. However, due to convergency problems the number of trainable leak locations had to be restricted to 10. Consequently, future emphasis must be put on the extraction of a minimized set of features. Though the optimized perceptron network (P2) disposes of a useful generalization capability, further investigation is necessary to improve the classification accuracy of pattern classes which are not represented by the training data.

References

Jax, P. and K. Ruthrof (1989). Acoustic Emission Inspections of Nuclear Components Considering Recent Research Programmes. Nuclear Engineering and Design , 113, 71-79.

Fuchs, H.V. and R. Riehle (1991). Ten Years of Experience with Leak Detection by Acoustic Signal Analysis. Applied Acoustic, 33,1-19.

Loos, M. (1993). Bedienhandbuch NEUROPRO, MEDAV Schrift Nr. 394, Uttenreuth.

Gesellschaft für Reaktorsicherheit (GRS) GmbH (1991). Sicherheitsbeurteilungen des Kernkraftwerkes Greifswald, Block 5 (WWER-440/W-213) GRS-83 , S. 58

IAEA-Report (1991). The Safety of Nuclear Power Plants in Central and Eastern Europe. IAEA-Rosen.cha / 91, p. 13

Rumelhart, D., G. Hinton and R. Williams (1986). Learning representations by back propagating errors. Nature, 323, pp. 533 - 536.

Kohonen, T. (1984). Self-Organization and Associative Memory, Springer Verlag, Berlin

The project this report is based on is partially funded by the SMWK (Sächsisches Staatsministerium für Wissenschaft und Kunst) and is registered with No. 7541.83-FZR/2. The authors are responsible for the scientific content of the report.

COMPONENT VIBRATION OF VVER-REACTORS
- DIAGNOSTICS AND MODELLING -

E. Altstadt, M. Scheffler and F.-P. Weiss

1. Introduction

The reason why a theoretical vibration model is urgently needed for VVER-reactors lies in the occurrence of flow induced vibrations of RPV internals. Control element and core barrel (CB) vibrations are known to have occurred in the former East German power plant Greifswald (Grunwald and Hennig, 1984; Altstadt and Weiß, 1993) and also in other East European installations. In some cases these vibrations were accompanied by serious and safety relevant damages. To avoid the mature formation of such damages in the future, noise diagnostics monitoring procedures were applied (Grabner *et al.*, 1977; Liewers *et al.*, 1987; Hessel *et al.*,1988; Meyer, 1989).

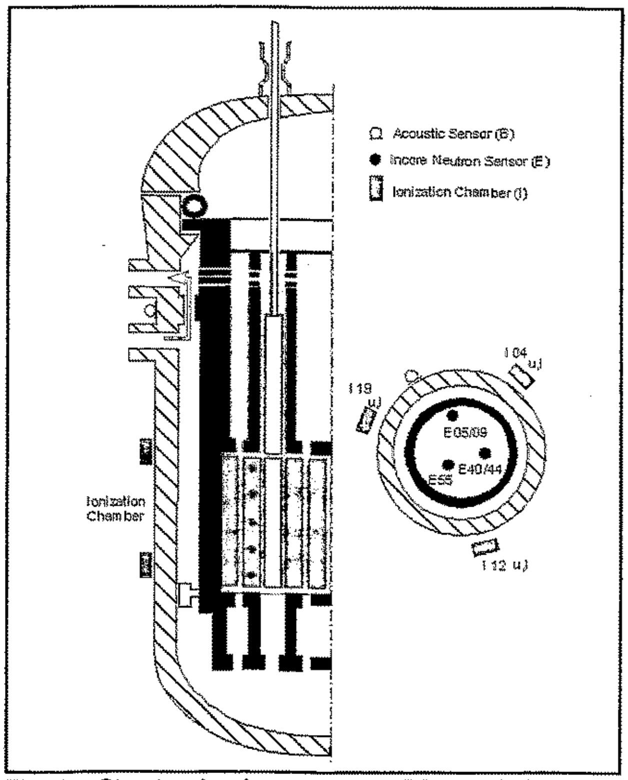

Fig. 1 Structural scheme of the RPV with internals and sensor positions for the detection of CB motion

During CB motion at the former Greifswald power station relative amplitudes of up to 5 mm between CB and RPV were estimated (Liewers *et al.*, 1987; Meyer, 1989). These high amplitudes were a consequence of the plastic deformation of the so called spring pipe segments which are to transmit the clamping force of the reactor vessel top upon the upper flange of the CB (see Fig. 1). The unsufficient fixing of the CB resulted among others in damaged guide lugs. Figure 2 gives a view of one of the 8 guide lugs welded with the RPV. Due to the fact that CB vibration was accompanied by a quasi-static axial shift of the CB inside the vessel a considerable part of the guide lug was eroded. Up to 18 mm of material were worn off. Especially the quasistatic axial shift is a safety relevant incident.

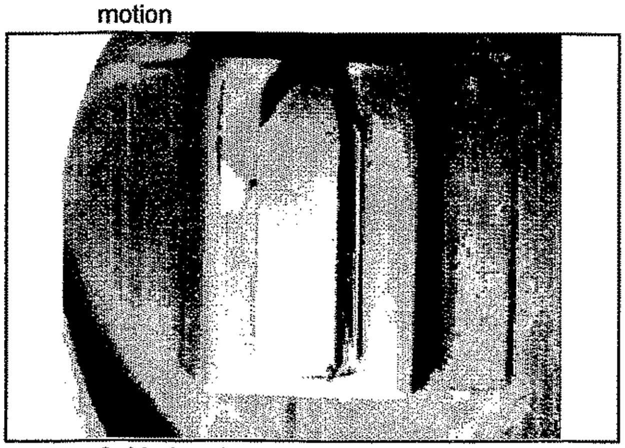

Fig. 2 Guide lug damaged by abnormal CB motion

To achieve early fault detection capabilities a theoretical vibration model of the whole primary circuit is necessary. Such a model must permit

- the description of the normal vibrations of the components, especially to assign the measured vibration frequencies in neutron noise, pressure fluctuations or mechanical displacements to vibration modes of the whole coupled mechanical system
- the determination of physical limits for frequency shifts and amplitude changes as alarm thresholds for on-line vibration monitoring
- the assessment of mechanical loads connected with the failure of a certain component. This option is important for damage propagation investigations.

2. A Finite-Element-Model for the primary circuit

The model comprises the whole primary circuit, including steam generators, loops, coolant pumps, main isolating valves and certainly the reactor pressure vessel and its internals. It was developed using the finite-element-code ANSYS® on a Hewlett-Packard workstation platform. The model has a modular structure, so that various operational and assembling states can easily be considered.

Reactor Pressure Vessel and Internals

The experimental experience exhibited the frequency range 0-30 Hz to be mainly interesting for the mechanical integrity of the whole system. Thus it is sufficient to assemble the model from 1D pipe elements. Figure 3 shows a topology scheme of the finite-element-model

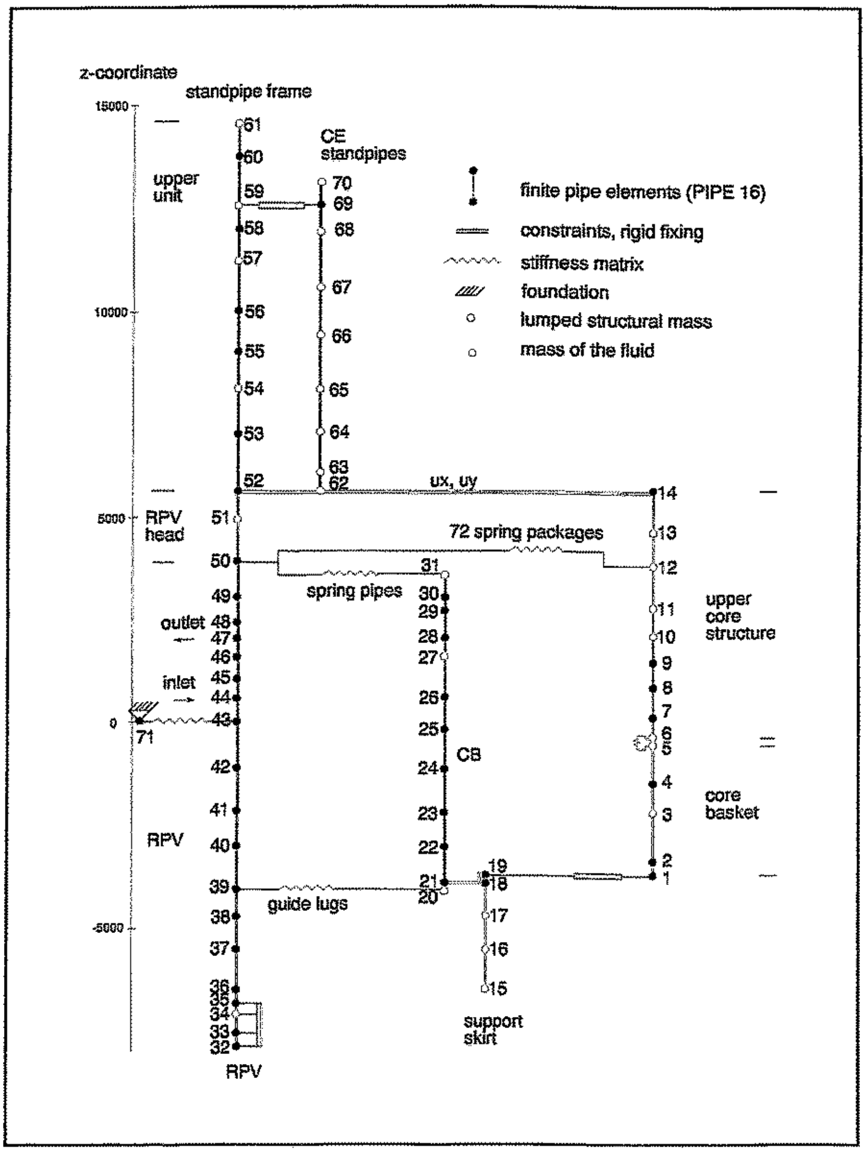

Fig.3 Topology of the finite-element-model for the reactor pressure vessel and its internals

for the RPV and all the internals: CB, CB support skirt, core basket, upper core structure. The model of the RPV head considers the upper callotte, the control-element standpipe frame and the standpipes themselfes. Each of the 71 nodes connecting two elastic pipe elements has 6 degrees of freedom. Different reactor components are mutually connected by stiffness matrices (12 by 12) which e.g. represent the CB guide lugs (nodes 20 and 39), or the ring foundation (nodes 43 and 71), or the spring pipe segments between the upper flange of the CB and the RPV head (nodes 31 and 50). The parameters of those stiffness matrices were estimated in separate calculations. Extreme stiff connections are modelled by constraints. Such forced conditions were introduced for the mutual coupling of the CB, the CB support skirt and the core basket in the region of the core support grid. Another place is the upper RPV callotte which stiffly connects the upper core support structure, the bottom point of the standpipes and the bottom point of the standpipe frame.

Up to now the influence of the coolant has been taken into account by lumped masses, though there is a finite fluid-structure-element under development which explicitely describes the additional inertia and attenuation connected with the presence of the fluid (Grunwald and Altstadt, 1994).

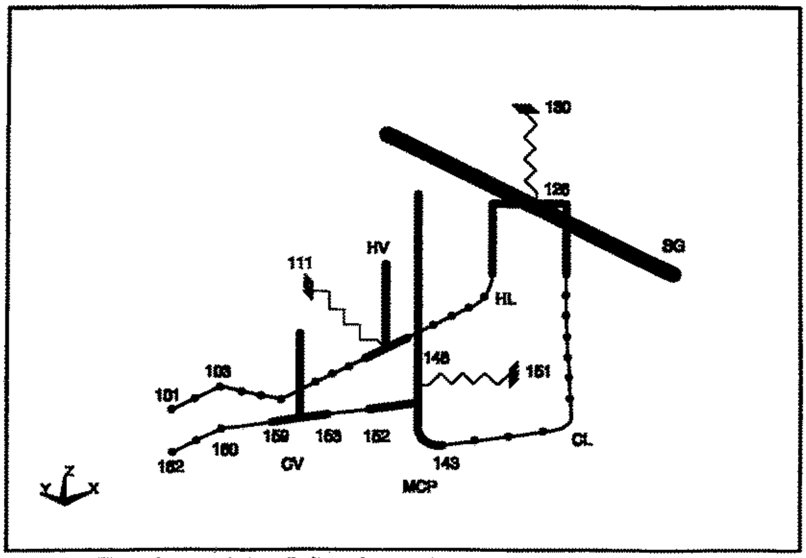

Fig. 4 Topology of the finite-element-model for the coolant loop

Coolant Loops

In analogy to the RPV with internals, the loop model consists of pipe elements, pipe tee and pipe elbow elements, structural mass elements (which are formulated as 6 by 6 inertia matrices), stiffness matrices and constraints (see Fig. 4 for the topology). The loop model includes the steam generator (SG), the hot leg (HL), the cold leg (CL), the main coolant pump (MCP), the hot isolating valve (HV) and the cold isolating valve (CV). Special attention was put on the SG support and on the connection of the SG with the secondary circuit, both modelled by a separately calculated stiffness matrix between the SG center node and the ground. Neglecting these couplings, one would drastically underestimate especially the first eigenfrequency of the loop. Also the bearings for the MCP and the HV are represented by stiffness matrices. The parameters of the loop model could be adjusted using results from modal analysis experiments performed at coolant loops in the Greifswald NPP and in the Dukovany NPP, Czech, as well.

Coupled Model

The vibration behaviour of the RPV and the six coolant loops cannot strictly be separated. Neither the RPV is a fix clamping for the loops nor is the loop inertia neglectable for RPV motions. The total mass of the RPV with all internals is about

600 t and that of one loop is about 290 t. So in general it is to be expected that the mode shapes will be coupled. Fig. 5 shows the whole primary circuit. The connection of RPV and coolant loops is realized by rigid area constraint equations between RPV (node 47, Fig. 3) and the first (hot) nodes of all six loops and between RPV (node 44) and the last (cold) nodes of all six loops respectivly.

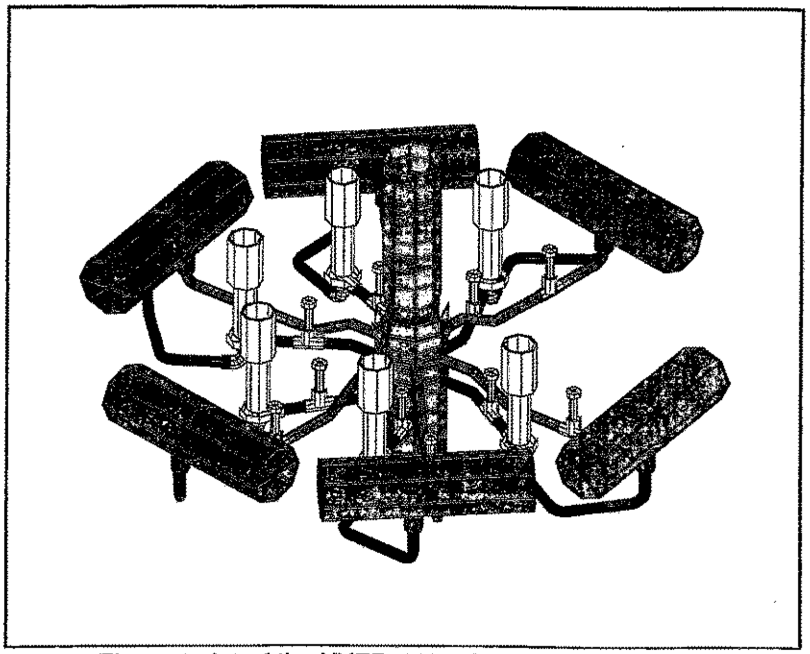

Fig. 5 Element plot of the VVER-440 primary circuit

3. Results

Modes of the Reactor Pressure Vessel and its Internals

In the first stage the loops and the reactor pressure vessel were modelled separately. The influence of the loops was taken into account by selecting a non-homogeneous stiffness of the ring foundation over the circumference. The frequencies of the east-west displacements were lowered since in this direction the masses of the loop components must additionally be moved. A short description of the eigenmodes for eigenfrequencies up to 36 Hz is given in table 1. The longitutional modes (z-direction) excepted, generally each mode shape occurs twice according to the different stiffnesses of the ring foundation in x and y direction. The eigenmodes 7, 8 and 9 (Fig. 6) are particularly important for the detection of possible degradations of the internal clamping elements like the guide lugs and the spring pipe segments.

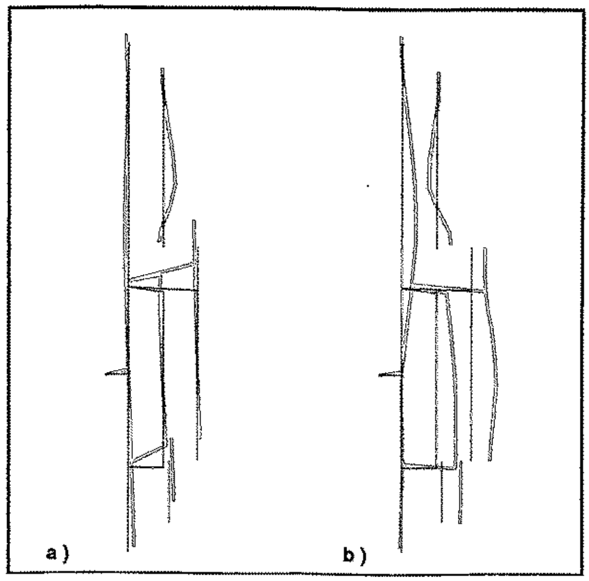

Fig. 6 a) Mode 7 (18Hz)
b) Modes 8 and 9 (26.3 / 26.9 Hz)

Mode 7 at 18 Hz is above all a z-vibration of all the internals while the vessel amplitude itself is rather small. Also the relative displacements connected with the pendulum component of this mode can be neglected. The modes 8 and 9 at 26.3 Hz and at 26.9 Hz are related to anti-phase motions of the RPV with respect to all internal components. Further these modes are characterized by elastic deformations of the internals and by anti-phase beam modes of the standpipes with respect to the standpipe frame.

Tabel 1 Eigenfrequencies and mode shapes of the RPV with internals

No.	f/Hz	verbal description
1. 2.	3.6 4.7	in-phase pendulum motion of RPV, CB and CB-internals; 1. beam mode of the upper unit in-phase (x-z, y-z-plane)
3. 4.	9.0 10.8	in-phase pendulum motion of RPV, CB and CB-internals; 1. beam mode of the upper unit in anti-phase (x-z, y-z-plane)
5. 6.	15.9 16.1	in-phase pendulum motion of RPV, CB and CB-internals; 2. beam mode of the CE standpipes (x-z, y-z-plane)
7.	18.0	z-vibration of all internals, small z-amplitude of the RPV, in-phase pendulum motion of RPV, CB and CB-internals, 2. beam mode of the upper unit
8. 9.	26.3 26.9	anti-phase pendulum motion of the RPV with respect to all RPV-internals, elastic deformation of CB and CB-internals, anti-phase beam modes of standpipe frame and standpipes
11. 12.	36.6 36.6	almost pure beam modes of standpipe frame and standpipes

Modes of the Coolant Loops

The finite-element-model of the loops has already been adjusted with modal analysis experiments performed as well in the former Greifswald power station as in the Dukovany plant in Czech.
In the frequency range up to 30 Hz about 20 eigenfrequencies were found. Figure 7 e.g. depicts 4 mode shapes for an empty loop (without coolant) calculated with the model. The mode shape connected with the lowest eigenfrequency at 1.15 Hz is a pure tangential displacement of the whole loop with respect to the RPV. The mode shape at 2.1 Hz essentially corresponds to a torsional vibration of the steam generator

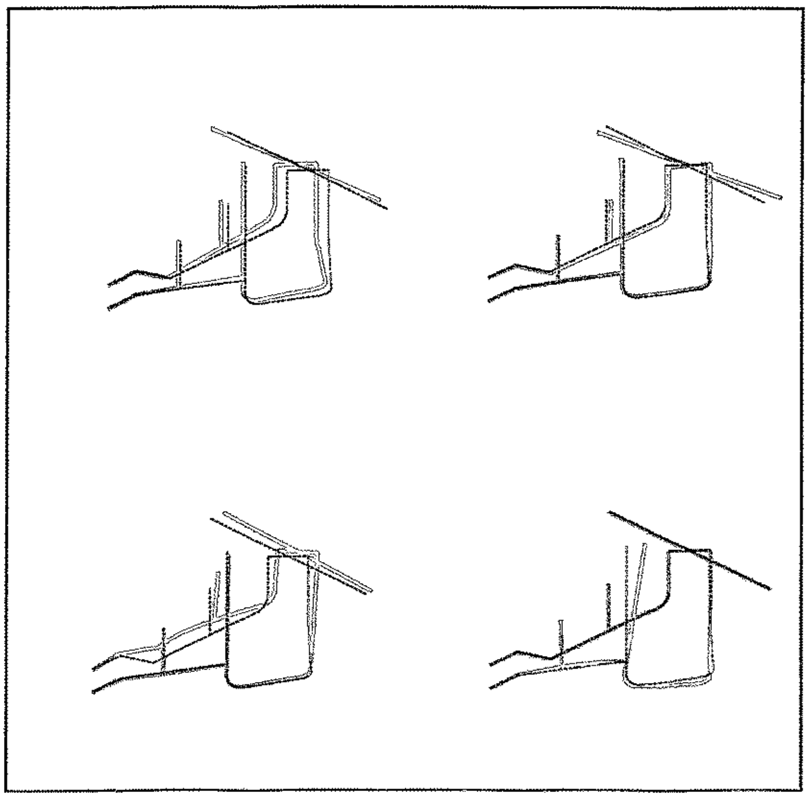

Fig.7 Mode shapes of a VVER-440 coolant loop at 1.15 Hz, 2.1 Hz, 4.2 Hz and 5.4 Hz

around the collector nozzles. At 4.2 Hz the mode shape is a radial steam generator vibration with respect to the RPV. Even the HL and the HV are displaced. Another eigenfrequency is centred at 5.4 Hz and is mainly determined by the beam mode vibration of the whole coolant pump in the CL plane.

Coupled Modes

The coupling of all six coolant loops with the RPV results in a great number of eigenfrequencies of the complex system due to the coupling of different degrees of freedom. The whole model then consists of about 450 finite elements with about 2300 active degrees of freedom. In the frequency range up to 30 Hz more than 100 eigenfrequencies are obtained. Many of them are close together but exhibit different mode shapes. Most of the mode shapes are characterized by various loop displacements in many different phase relations with the RPV being almost in rest position. Some mode shapes only exhibit large displacements of the loops and of the RPV as well. For example Fig. 8 shows the lowest mode shape at 3.6 Hz which has significant displacements of the RPV and of the internals. It confirms that this frequency belongs to a vibration in east-west direction what was assumed when the loop influence was only simulated in the calculations of the RPV vibrations. All six loops and the RPV with the internals are displaced in-phase in the x-z plane.

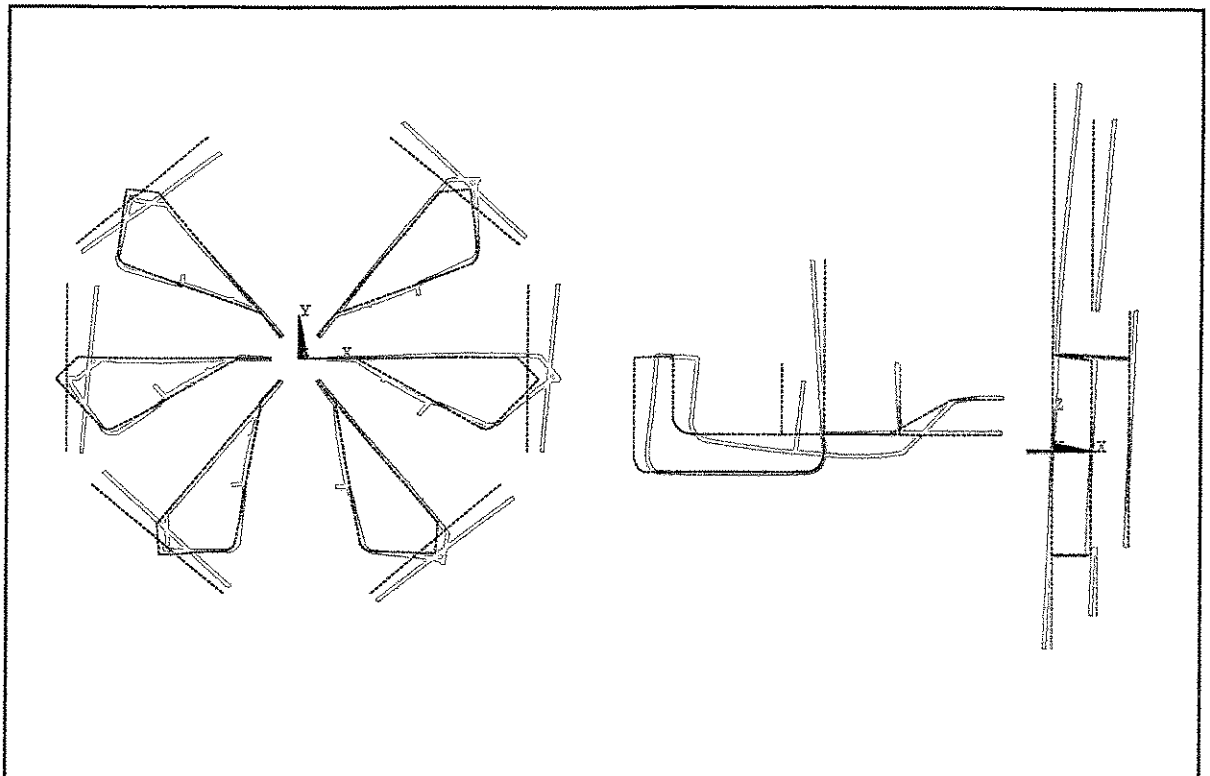

Fig.8 Coupled mode of the primary circuit at 3.6 Hz

Sensitivity Studies and Failure Simulation

To reveal which modes are best suited to detect degradations of the safety relevant internal components, sensitivity studies were performed by varying certain parameters of the finite-element-model. To recognize the basic tendencies in frequency and amplitude shifts when RPV clamping elements degrade, it is sufficient to use the approximate consideration of the loops by a non-homogenious stiffness of the RPV ring foundation.

Figure 9 now indicates how the spectra of the RPV acceleration in x and z direction would change in case of the failure of two spring pipes (in total there are 6 spring pipes).

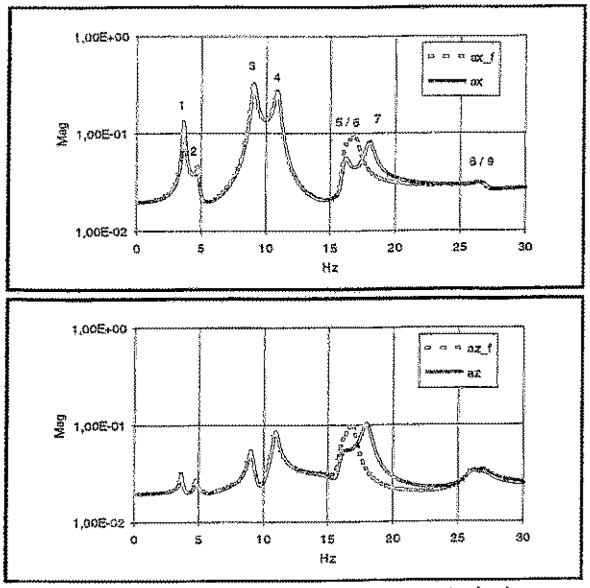

Fig. 9 RPV bottom acceleration spectral change, failure of 2 spring pipes (—— normal, ---- failure)

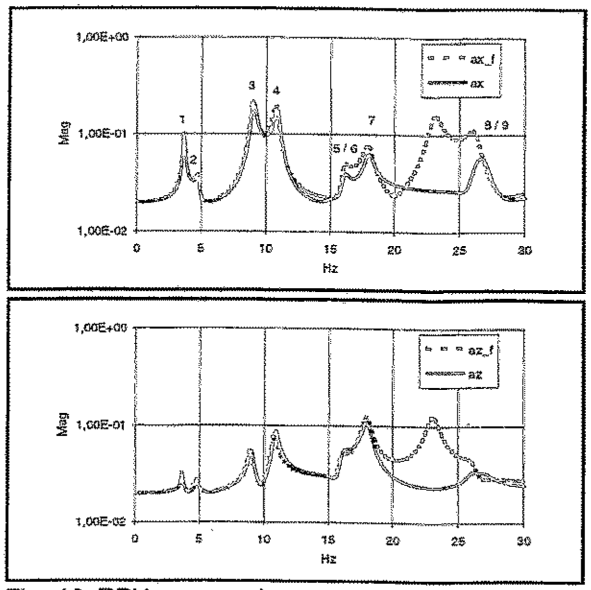

Fig. 10 RPV upper plenum acceleration spectral change, fracture of 2 guide lugs (—— normal, ---- failure)

The measuring position is assumed at the RPV bottom. A significant effect is observed in a down shift of eigenfrequency 7 at about 18 Hz. This effect can be seen in the acceleration for all three directions. For x and z-direction there is also a small amplitude increase at eigenfrequencies 5 and 6 at about 16 Hz. It is really remarkable that all the other mode shapes exhibit neither a frequency shift nor a change in the amplitude.

Another component that needs careful monitoring are the guide lugs. As expected, above all the two eigenfrequencies pertaining to anti-phase pendulum motion do respond to a loss of guide lug stiffness. There is almost no effect in the other eigenfrequencies. Figure 10 shows the response changes between a force exciting the reactor at the RPV bottom and the acceleration that would be measured at the upper plenum. The failure of guide lugs, in this case two, can be recognized in the acceleration spectra of all directions. There is one interesting effect which should be hinted on. Though the guide lugs do not have a stiffness for the z-direction also a clear amplitude change appears in the z-acceleration. Also for that component it is amazing that the effect produced by the failure is restricted to a small frequency range. This restriction to rather limited frequency bands may make the identification of failures easier.

4. Conclusions

The first results obtained with the vibration model for a VVER-440 reactor hint at the opportunity to establish a monitoring procedure that is capable of distinguishing between

guide lug and spring pipe failures, because these two types of failures are mapped in different and separated frequency regions. Moreover it seems that it is possible to detect these failures by performing excore vibration measurements, what is important since incore vibration measurements are difficultly to be implemented over longer time periods. By measuring the displacements for x- and y-direction even the localization of the failed spring pipe or guide lug might become achievable.
The results indicate that the lower eigenfrequencies connected with in-phase pendulum motions of the pressure vessel and of the internals are rather insensitive to these failures.

When monitoring can be restricted to the RPV and the internals, it will in general be sufficient to simulate the influence of the loops by inhomogeneous stiffness of the ring foundation. All modes with significant amplitudes of the RPV and of the internals respectively can satisfyingly be described with that approximation.

Finally, it is absolutely clear that the theoretical model needs further adjustment by vibration and neutron noise measurements from VVERs.

References

Altstadt, E. and F.-P. Weiß (1993). Experimental and Numerical Investigation of Control Element Vibration During Abnormal Core Barrel Motion at a VVER-440 Type Reactor. *Proceedings of the 1993 International Simulators Conference (Simulators X, Arlington, VA)*, 25(4), 48 - 53.

Altstadt, E., P. Liewers, M. Scheffler, P. Schumann and F.-P. Weiß (1994). Komponentenschwingungen an WWER-Reaktoren - Diagnose und Modellierung. *Preprints der Jahrestagung Kerntechnik (Stuttgart)*.

Grabner, A., P.Liewers, P. Schumann and F.-P. Weiß (1977). Decomposition of Noise Signals Composed of Many Similar Components. *Progress in Nuclear Energy (SMORN II, Gatlinburg 1977)*, 1.

Grunwald, G. and K. Hennig (1984). Treatment of Flow-Induced Pendulum Oscillations. *Kernenergie*, 27(7), 286 - 291.

Grunwald, G. and E. Altstadt (1994). Analytical and Experimental Investigations for Modelling the Fluid-Structure-Interaction in Annular Gaps. *Preprints of the IFAC-Symposium on Fault Detection Supervision and Safety for Technical Processes (SAFEPROCESS '94)*, 147-152.

Hessel, G., P. Liewers, P. Schumann, W. Schmitt and F.-P. Weiß (1988). A Noise Diagnostics System for Operator Advice. *Nuclear Safety*, 29(3).

Liewers, P., W. Schmitt, P. Schumann and F.-P. Weiß (1987). Detection of Core Barrel Motion at WWER-440 Type Reactors. *Progress in Nuclear Energy (SMORN V, Munich 1987)*, 21, 89 - 96.

Meyer, K. (1989). Modellierung der Übertragung von Spaltzonenschwingungen eines Druckwasserreaktors WWER-440 auf die Schwankungen der Neutronenflußdichte. *Kernenergie*, 32 (8).

The project this report is based on is funded by the BMFT (Bundesministerium für Forschung und Technologie) and is registered with No. 1500916. The authors are responsible for the scientific content of the report.

SPECIFICATION OF A TECHNICAL SYSTEM TO IMPROVE THE OPERATIONAL MONITORING OF ZAPOROZH'YE NPP BY STATE SUPERVISORY AUTHORITIES OF UKRAINE.

M. Beyer, H. Carl, L. Langer, K. Nowak+, P. Schumann, A. Seidel, P. Tolksdorf+†, J. Zschau

(+Technischer Überwachungs-Verein TÜV Rheinland, Fachbereich Kerntechnik)

The introduction of a modern operator-independent monitoring capability for Central and Eastern European nuclear power plants by the national supervisory bodies responsible for reactor safety and radiation protection can contribute in a relatively quick and inexpensive manner towards improving the safety of Russian-VVER-type nuclear power plants.

Such a continuous monitoring capability is not a substitute for the necessary safety enhancement of Russian reactors by technical backfitting, but rather supplements safety enhancement in accordance with the defense in depth concept.

Such a monitoring system shall be designed so as to not restrict in any way the operator's responsibility and scope of action.

Within the scope of a program sponsored by the German Federal Minister for Environmental Protection and Reactor Safety for the cooperation of the Central and Eastern European states and the CIS in the area of nuclear safety, the Institut für Sicherheitsforschung of Forschungszentrum Rossendorf Inc., in a joint effort with the nuclear technology section of TÜV Rheinland (German state-level independent authority for technical certification), has developed a specification for a technical system designed to improve the operational monitoring accomplished by the Ukrainian State Supervisory Board GosAtomNadsor (GANU). The pilot system shall be installed at the Ukrainian nuclear power plant Zaporozh'ye, unit 5 [1]. The nuclear power plant at Zaporozh'ye with its six Russian nuclear reactors of the type VVER-1000/W-320 is the largest nuclear energy site in the CIS, see Fig. 1.

The specification of the technical system is based on detailed research including:

- State government structures with respect to their influence on nuclear energy use,
- legal foundations, rules and regulations for the utilization of nuclear energy,
- the intentions of the Ukrainian supervisory authority GosAtomNadsor as they relate to NPP monitoring,
- economic conditions and feasibility to procure required measurement and computer equipment,
- special safety features peculiar to the plant and site which were noted during an inventory taken in the NPP Zaporozh'ye, unit 5.

The specified technical system plans the integration of

- 49 different technical parameters of the monitored unit,
- 18 different radiological parameters related to the monitored unit and the site
- and of 6 different meteorological parameters

into the supervision. Some of the measuring channels have to be backfitted.

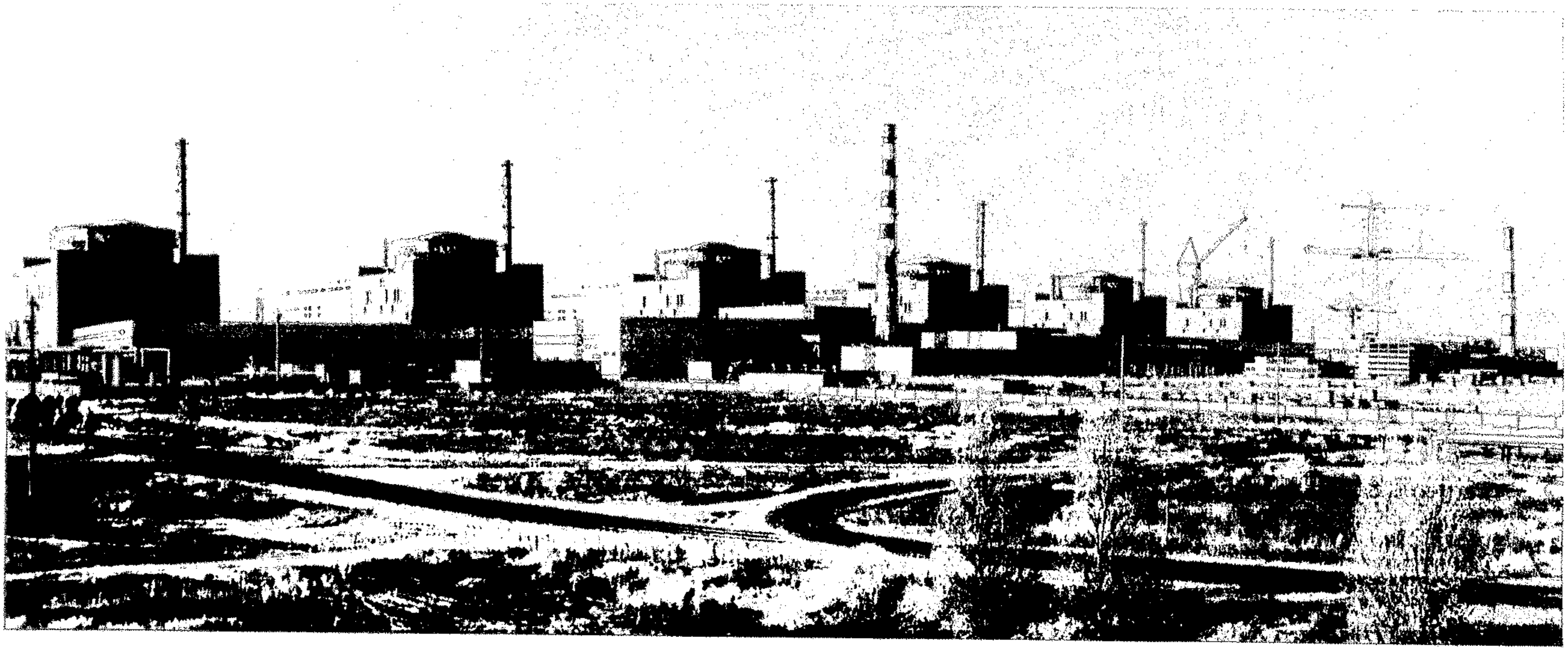

Fig.1 Nuclear power plant at Zaporozhye, Ukraine, with six uniform units of the type WWER-1000/W-320

Photo: Schumann/Langer (FZR)

These parameters were selected on the base of defined protection objectives which in turn are further translated into control tasks. The selection of the parameters took into account the technical concept for the VVER-1000 reactors, the noted safety short-comings, the lower automation degree of the system compared to Western European standards, and the actual technical configuration in the Zaporozh'ye NPP.

Supported by international experience, four protection objectives were established for the pressurized water reactor VVER-1000:

- S1: ensure reactor shut-down,
- S2: ensure core cooling,
- S3: ensure heat removal from the primary circuit and ensure its integrity, and
- S4: the integrity of the containment.

These protection objectives are implemented by nine control tasks which refer to certain parts of the plant, mediums, processes, and plant conditions to be monitored:

- K1: General plant condition
- K2: Barrier effectiveness against the emission of radioactive substances
- K3: Radioactivity inventories
- K4: Release of radioactive substances into the air
- K5: Immission in the environment
- K6: Meteorological conditions
- K7: Release of radioactive substances into water
- K8: Alert upon exceeding limit values
- K9: Plant condition in the event of an incident/accident

While the protection objectives still may be generally valid for different reactor types, the control tasks are specially tailored for Russian-type pressurized water reactors, the plant in Zaporozh'ye and its equipment.

The concept of the protection objectives was derived from German and American experiences related to remote monitoring. Since the designed technical system uses information from different subsystems it may regarded as to be, to some extent, complementary to the utilities' surveillance which is to monitor the compliance of the actual operating conditions with the "*limits and conditions of safe operation*".

As depicted in Figure 2, the technical system is structured hierarchically and characterized by the following features:

- Technological measurement values are decoupled from the process computer system and taken over into Transfer Computer unit 5, radiological unit information and radiological and meteorological site information are passed to Transfer Computer Auxiliary Building.
- All measurement values are deposited in the On-site Computer after credibility check, compressed and transformed into logical data channels,
  assessments are made and alerts developed by comparing the data with limit values at NPP level,
  exceeded limit values are reported to operator and authority,
  and data transfer is controlled.
- Data receipt and administration, *information processing, assessment, documentation* and archiving are accomplished in the Saporog Center of the on-site GANU Inspector and also in the Kiev Center of the supervisory authority GANU.

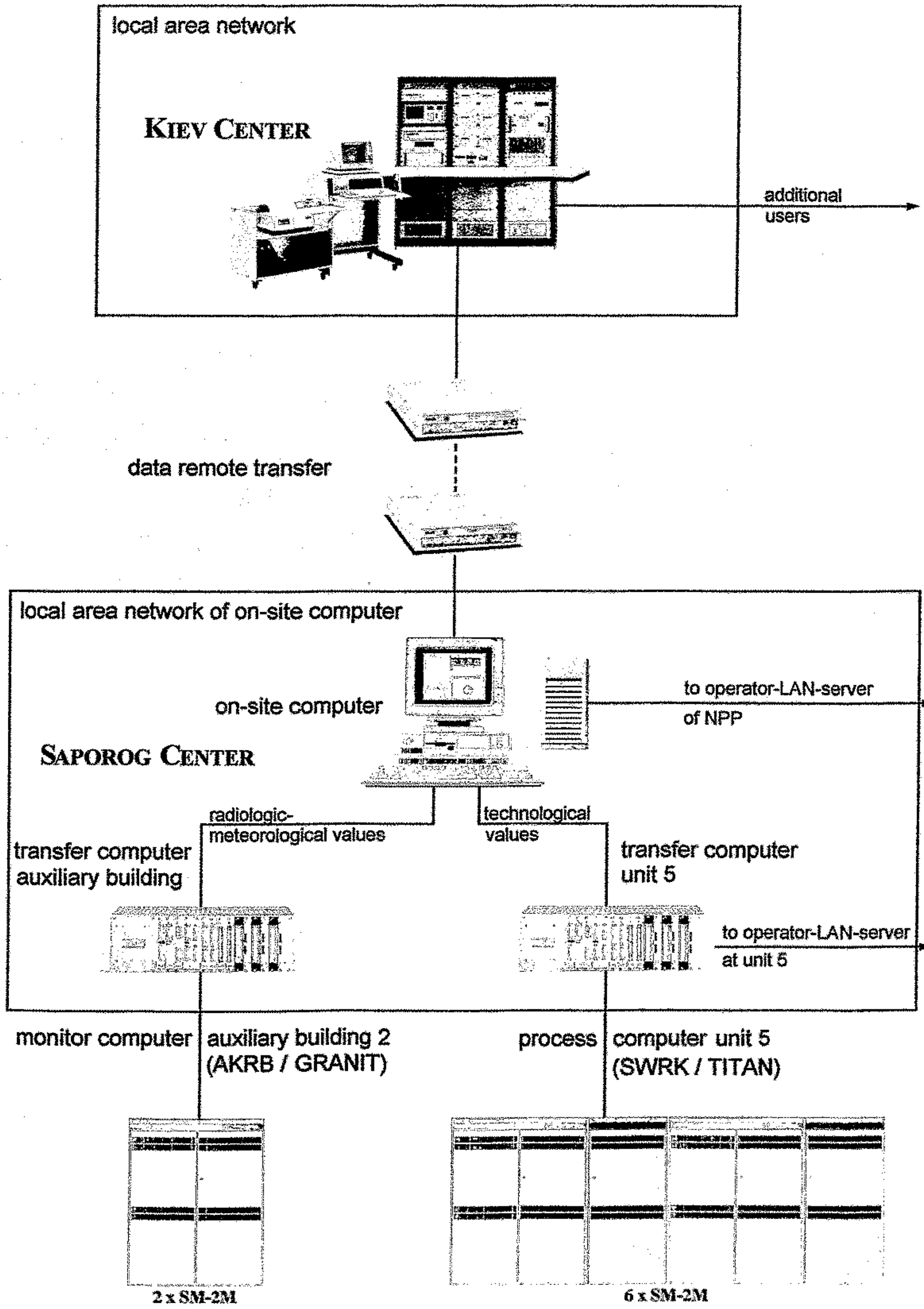

Fig. 2 Structure of the spezified system for monitoring by the regulatory authorities

Important elements in this context are the compression of monitoring-specific data and transformation into logical data channels, the automatic assessment through comparison of individual parameters or parameter combinations with special (monitoring) limit values, and the reporting of deviations in the form of a signalization and a protocol both to the authority and to the operator. A total of 39 possibilities for generating an alert report are planned, including 7 resulting from combination of several different parameters.

Table 1 gives the quantity of data preprocessing at the unit.

For monitoring one unit	
49 technological parameters (that means 49 different physical parameters)	18 radiological und 6 meteorological parameters (that means 24 different physical values)
will be used.	

To do this	
402 individual values	75 individual values
are decoupled from the process computer system SM-2M	
of the unit.	of the auxiliary building.

They are checked and compressed	
by the TRANSFER COMPUTER UNIT 5	by the TRANSFER COMPUTER AUXILIARY BUILDING
and transferred into the ON-SITE COMPUTER.	

Based on these primary values in the ON-SITE COMPUTER	
98 logical data channels	54 logical data channels
are formed by logical combinations and/or by comparison with limit values and are further used for supervision purposes.	

During undisturbed operation of the unit the technological data are transferred every 10 minutes and the radiological/meteorological data every 60 minutes in form of data files with a capacity of 1-2 KBytes. In case of safety-relevant limit value crossings the transfer interval will be reduced to 1 and 10 minutes, respectively, to enable a more exact prognosis by a more detailed observation.

The estimated costs of establishing the technical system in its minimal version, that means a system of the absolutely necessary quantity of supervision tasks (without costs for system installation, meteorological mast, buildings and special software development) are approximately DM 1.3 Million, plus DM 0.65 Million for the most necessary upgrading of measuring devices at one unit.

The hardware costs for the integration of a further reactor unit are about DM 0.2 Million plus costs for necessary measuring devices. Linking of the second auxiliary building for acquisition of radiological data from further three reactor units needs approximately DM 0.11 Million.

The data from various subsystems combined in the technical system and the assessment of that are also available to the utilities and provide them with an overview of the safety condition of the plant which in this form was not available before.

The specified technical system with its modular organization and open structure:

- offers sufficient reserve for including additional monitoring parameters,
- enables the extension from one to six blocks through block related duplication,
- allows for the inclusion of additional NPP sites into the monitoring by the authority,
- may be included into a National Information System for Crisis Situations as contemplated in the Ukraine.

In the configuration described, the technical system does not replace the operational control and monitoring devices, nor does it limit the responsibility of the operator or its scope of action regarding the safe plant operation. Rather, by making available the technical means for the remote transfer of data, the system enables the supervisory authority to monitor and to evaluate the operational state independent of the operator and therefore gives the conditions to influence the plant operation by imposing special requirements. As a result of its technical equipment and monitoring-specific information processing, the system enables early detection and reporting of safety relevant incidents/accidents and possible resulting release of radioactive substances. With this, it constitutes a technical basis for the early warning of the public in hazardous situations as well as for the effective initiation of emergency protective measures.

The authors gratefully thank Messrs. V. V. Artemtschuk, A. O. Lebedew and V. I. Verpeta of Zaporosh'ye NPP for their fruitfull discussions and assistance during the inventory in the NPP and the conceptional work, Messrs. V. N. Glygalo and V. M. Kwasov of the Scientific Centre of the Ukrainian State Commitee on Nuclear and Radiation Safety for supporting the specification from the authorities point of view, and Messrs. V. I. Gavrilyuk and Y. L. Tsoglin of the Institute for Nuclear Research of the Ukrainian Academy of Science for their independent evaluation of the safety state of Russian-VVER-1000 type reactors.

The project is mainly funded by the BMU (Bundesministerium für Umwelt, Naturschutz und Reaktorsicherheit) and registered with No. INT 9210/1,2. The authors are responsible for the scientific content of the paper.

Reference:

[1] Beyer, M., u.a., Aufbau eines technischen Systems zur Verbesserung der betrieblichen Überwachung der KKW durch die staatlichen Aufsichtsbehörden (Saporoshje), Abschlußbericht in 3 Bänden zu den BMU-Projekten INT 9210/1 und INT 9210/2, Forschungszentrum Rossendorf, Institut für Sicherheitsforschung und Technischer Überwachungs-Verein Rheinland, Fachbereich Kerntechnik, Dezember 1993

COMPUTER SIMULATION OF A PLASMA NEUTRON SOURCE

H. Kumpf, St. Krahl, K. Noack, G. Otto, S. Collatz[1]

1. Introduction

The starting point of the activities around a plasma neutron source at Rossendorf has been the observation, that the second important problem in fusion research is the development of radiation proof, low activation materials for future fusion reactors. This task may even gain top priority as soon as the stable confinement of a fusion plasma will have been demonstrated. But progress in the field of fusion material research is seriously impeded by the lack of an adequate neutron source.
An unbiased review of existing proposals for neutron sources serving for material research purposes led to the conclusion, that a solution to the final problem of end-of-life tests of macrosamples can probably be provided only by a plasma machine. This does not exclude the application of accelerator based neutron sources to the intermediate task of calibrating the effects of reactor irradiations on microsamples. The above assessment is largely based on considerations of energy efficiency. Thus roughly 1 MW neutron power is needed for meeting the usual demands in irradiation volume and neutron flux. This implies a conversion efficiency at least in the % range, because it is unrealistic to admit more than tens of megawatts power consumption from the grid. But this is the realm of fusion devices exclusively.
Among the numerous proposals of neutron sources based on plasma devices the Novosibirsk concept of a plasma mirror in the gas dynamic regime [1] seems to be the most realistic one. This is why the related research work in the Research Centre Rossendorf (RCR) runs in close cooperation with the Budker Institute of Nuclear Physics (INP). At present the experimental work in Novosibirsk is based on the Gas Dynamic Trap (GDT) facility. An advanced facility, the Hydrogen Prototype being a 2:1 plasma model of the final neutron source, is now under design and partially even under construction.
In the first step the Rossendorf group contributed to the Novosibirsk project by defining terms for the design of the source imposed by shielding demands [2]. It turned out, that the superconducting coils can well be shielded even in a compact set-up, the key issue being the radiation load of the warm part of the mirror magnet. In this most exposed part organic insulators have to be avoided.

2. Integrated Transport Code System

The scientific collaboration between the Budker Institute and the Institute of Safety Research is mainly directed to the development of an Integrated Transport Code System (ITCS). Fig. 1 shows the scheme of the system. Its goal is the cal-

[1]Visitor to Institute of Safety Research

culation of physical effects connected with the particle fields appearing inside the neutron source device (see Fig. 4), i. e. with
- the target plasma,
- the fast ion population and
- the neutral gas.

The code system is designed to consider the full dependence of the transport phenomena on space, energy and angle variables as well as the interactions between the three particle fields. At present the single modules are under development. The group of the Budker Institute elaborates a one-dimensional (in space) MHD code for the target plasma and a two-dimensional method for the fast ion module being founded on an expansion in appropriate, non-negative basic functions. The efforts in Rossendorf are focussed on the development of mathematical models and transport codes for the fast ion and neutral gas modules. Both modules use particle simulation techniques [3].

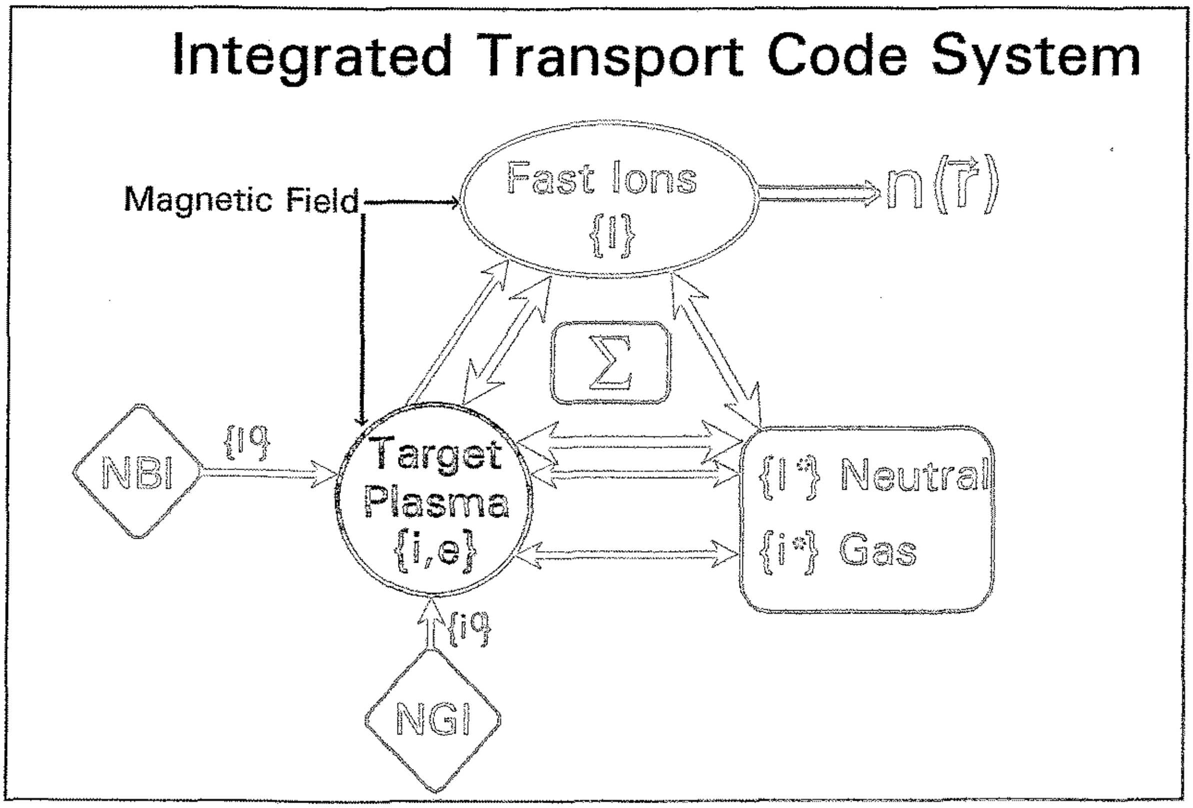

Fig. 1: Scheme of the ITCS

Within the ITCS the fast ion module holds the central part because the field {I} of the fast ions ($I = D^+$, T^+ of 80-100 keV initial energy) determines the neutron source distribution $n(\vec{r})$. A first version of a Fast Ion Transport code (FIT) has been developed. It is based on the so-called background approximation assuming the (r, z)-profiles of densities and temperatures for both the target plasma and the neutral gas to be known and the direction dependences of these fields to be isotropic. The fast ion distribution function $f_I(\vec{r}, v, \vec{\Omega}, t)$ is then the solution of the Landau-Fokker-Planck equation

$$\frac{\partial}{\partial t} f_i + \left[v\vec{\Omega}\frac{\partial}{\partial \vec{r}} + \frac{e}{m}\left(v\vec{\Omega}\times \vec{B}\right) \frac{\partial}{\partial \vec{v}}\right] f_i = \frac{1}{\tau_s * v^2} * \frac{\partial}{\partial v}\left(v^3 + v_c^3\right) f_i +$$
$$D_{ii} * \left[\frac{\partial}{\partial \zeta}\left(1-\zeta^2\right) \frac{\partial}{\partial \zeta} + \frac{1}{\left(1-\zeta^2\right)} * \frac{\partial^2}{\partial \varphi^2}\right] f_i - \langle\sigma v\rangle_{cx} f_i + S. \tag{1}$$

The streaming term on the left-hand side of Eq. (1) describes the motion of the ions under the Lorentz-force in an external magnetic field $\vec{B}$. The first and second term on the right-hand side model the moderation of the velocity v by the target plasma and the diffusion of the flight direction $\vec{\Omega}$ by ion-ion collisions, respectively. The latter contains a nonlinearity caused by collisions between fast ions. The third term represents their loss rate by charge-exchange processes with neutral gas atoms. S is the source distribution of the fast ions which is generated by the Neutral Beam Injection (NBI) into the target plasma. The parameters τ_s, v_c, D_{ii}, and $\langle\sigma v\rangle_{cx}$ are calculated from the information about the target plasma and the neutral gas. The transport code FIT simulates stochastically independent fast ion histories in such a way that the mean of their distribution in phase space is just given by f_i from Eq. (1). For this end the simulation procedures of the diverse processes must be constructed in a well defined manner. The evolution of a history in time is simulated according to the leap-frog method illustrated in Fig. 2. Particle location $\vec{r}$ and kinematic parameters v, $\vec{\Omega}$ with the statistical weight w are alternately calculated at times shifted against each other by half a time-step dt/2. The time-step dt is restricted by the stability criteria for the ion motion in the magnetic field. For this procedure the *BORIS*-algorithm [4] is used. The coefficients $\langle\cdots\rangle$ determining the changes of the velocity and of the flight direction are derived from Eq. (1).

The code FIT is written in FORTRAN 77 with the special demand to maximally utilize the vector capability of the CONVEX C-3820 computer. It has been tested in a series of simplified model calculations. For the next step of the code development it is planned to introduce the time-dependence in the fast ion transport as well as in the target plasma and neutral gas description. This feature will allow to validate the mathematical models by comparing with results measured in experiments at the GDT facility.

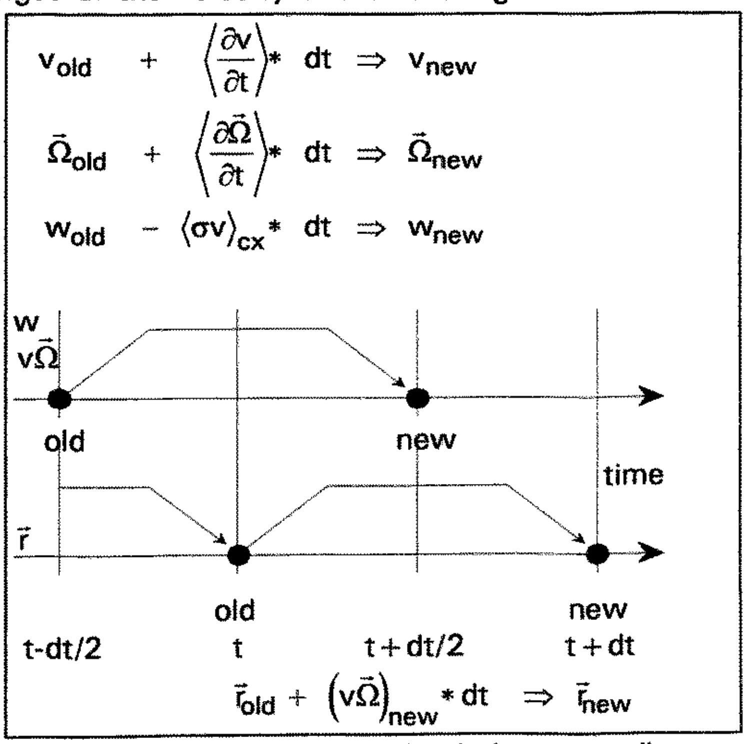

Fig. 2: Particle transport simulation according to the leap-frog method

To get a high efficiency of the neutron generator the losses of fast ions must be minimized. In this respect the question of the adiabaticity of their motion plays a decisive role. The magnetic moment μ of a gyrating ion is only an adiabatic invariant of its motion, i. e. μ does not remain exactly constant but varies to a certain degree. This effect means physically that the angle between the ion flight direction and the axis of the system changes in course of their motion between the mirrors. In magnetic fields with stronger gradients the deflection of the flight direction vector from its initial value may accumulate even up to the point when the direction vector reaches the loss cone. Then the ion flies through the mirror throat out of the system.
This effect was numerically studied for the Hydrogen Prototype with the magnetic field according to the present design. Fig. 3 represents the results. The magnetic field components B_z and B_r/r are the values on axis. The fluctuating curves show the variations $\Delta\mu/\mu_0$ for different ions that have been started with the same initial values in the mid-plane. For the proton and deuteron the μ-variations are enclosed by a well defined envelope whereas the triton does not exhibit this acceptable behaviour but indicates the approach to instability. Detailed investigations have shown that this effect is caused by relatively high values of the second spatial derivatives in the magnetic field. Furthermore, it has been demonstrated that by an appropriate rearranging of the field coils this undesired effect can be suppressed. The results of this study suggest an inspection of the adiabaticity problem in the neutron generator predesign with the help of the same numerical method.

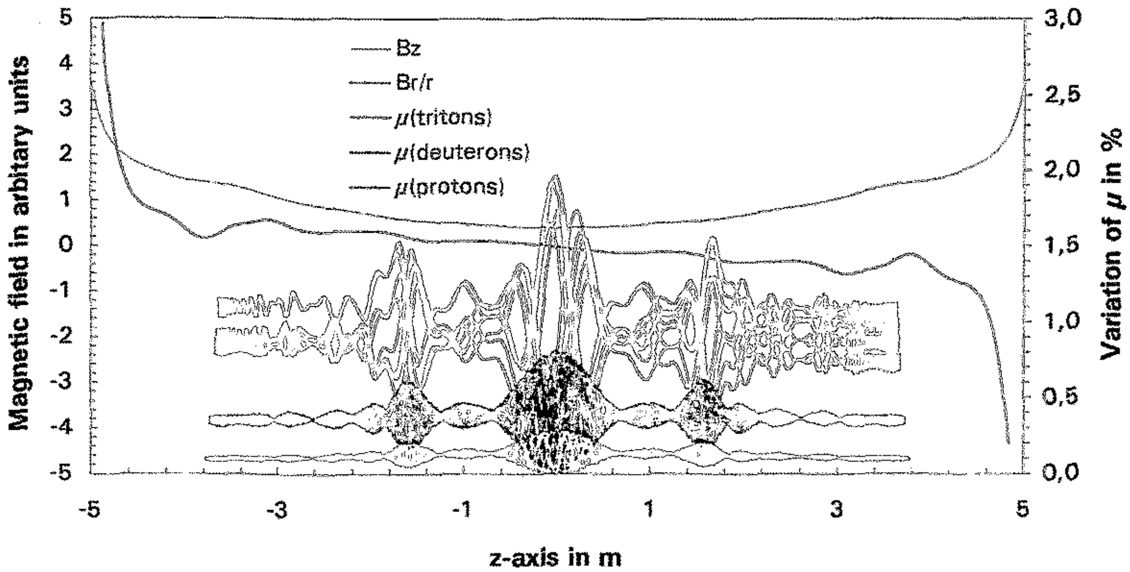

Fig. 3: Variation of the magnetic moment μ in the Hydrogen Prototype

The neutral gas contained in the central cell of the mirror device causes losses of fast ions as well as of plasma ions by charge-exchange processes. This is why the neutral gas transport is included in the ITCS. Notwithstanding this general goal of a neutral gas module the first phase of the code development was directed to the solution of an actual problem in the Hydrogen Prototype design. The target plasma continuously streams out of the central cell into the expanders (see Fig. 4). For maintaining stationary conditions plasma has to be supplied. A possible method is the gas feeding. That means hydrogen gas is injected into and ionized by the plasma itself. Obviously, this method may be used only provided the plasma density is not too low. With the help of the developed code TUBE various versions of such a gas feeding device have been studied.

TUBE simulates the linear neutral gas transport according to the Monte Carlo method. The interactions with plasma and metallic walls are similarly treated as in the EIRENE code that has been developed for solving neutral gas problems in tokamaks [5]. TUBE allows to calculate the ionization source density and leakage currents in a cylindrical grid in dependence on the neutral gas influx as well as on plasma parameters. The wall geometry may be composed as a sequence of cones and cylinders. Up to now TUBE is capable of simulating the time-independent, coupled transport of H atoms and H_2 molecules. Analogously as in the fast ion transport code the plasma is considered as independent background the density and temperature of which must be given by (r,z)-profiles. In the transport simulation this space dependence is taken into consideration by the δ-impact technique [6]. For the proposed parameters the neutral atoms interact with the plasma by two types of ionizing collisions: electron impact with free electrons and charge-exchange with plasma ions. Molecules are dissociated by electrons in various reactions. Neglecting the short transport of the intermediate product H_2^+ they are lumped in one effective process producing hydrogen atoms and ions [7]. The calculations have shown that the transport of molecules must not be neglected.

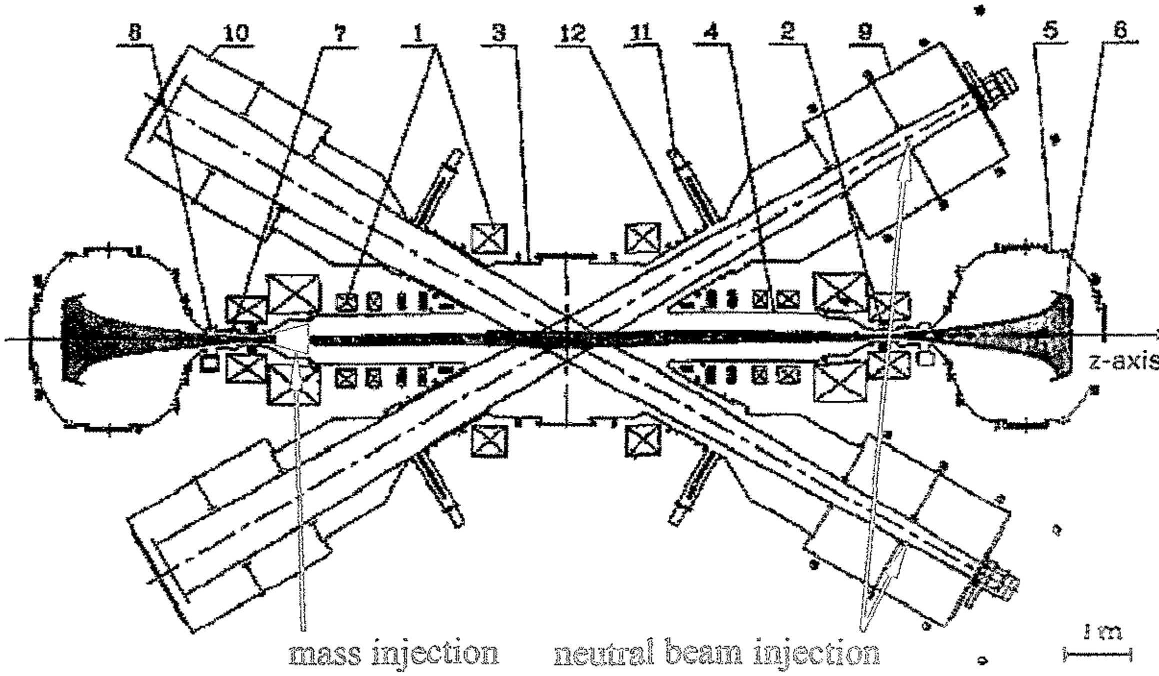

1 ... central cell coils
2 ... mirror coil
3 ... central vacuum chamber
4 ... lateral section
5 ... expander
6 ... plasma dump
7,12 ... bellows
8,11 ... slide valve
9 ... neutral beam injector
10 ... beam dump

Fig. 4: View of the Hydrogen Prototype

The goal of the proposed gas injection is to feed the plasma in the central cell without significantly increasing the density of neutral particles in this region. Therefore the generated ion current in the corresponding direction should be maximized but the nonionized gas current minimized. In the calculations the device was modelled as an open metallic tube of a certain length and diameter enclosing the target plasma and located between the mirror coil and the turning points of the fast ions (see Fig. 4). The hydrogen gas is injected through a ring-shaped gap in the mid-plane of the tube wall. Fig. 5 shows results of calculations for several aperture angles of the tube. They all apply to the same energy spectrum of the hydrogen gas influx and to the same plasma parameters. For the evaluation of the results one additional fact is of importance. The density peak of the fast ions in the region of their turning points generates a peak of the electrostatic ambipolar potential in the central cell. For the standard regime of the prototype the height of this potential is expected to amount to about 1.5 times the plasma temperature T_0. Therefore, the central cell will be fed only by those ions having a kinetic energy of their motion along the z-direction greater than this value. The analysis of all numerical results allows to conclude that

- in case of the Hydrogen Prototype the proposed gas injection technique enables a sufficient plasma feeding in a certain range of plasma parameters and that
- there is an optimal aperture angle but only with a slight gain in efficiency.

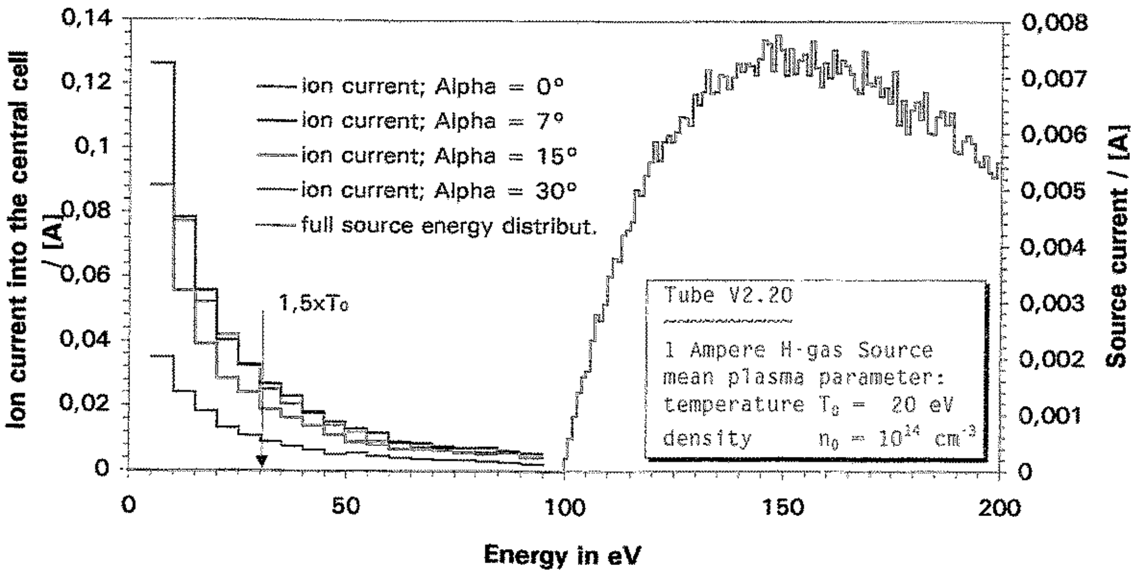

Fig. 5: Ion current into the central cell in dependence on the kinetic energy of their motion along the z-direction

The next step of the code development will be directed to the solution of neutral gas problems at the GDT facility. For that purpose the time dependence of the neutral gas transport simulation and of the plasma description has to be incorporated. The code TUBE is written in FORTRAN 77 and does not require any special soft- or hardware.

3. Conclusions

The fast ion and neutral gas code modules presently under development in Rossendorf have already demonstrated their usefulness in partial applications. The next step in their development will be the validation of physical models by comparing with experimental results from the GDT facility. For this end, the codes have to be modified to meet the GDT conditions. Furthermore, the experience in the code application has shown the need to develop more efficient algorithms without essential loss in accuracy.

References:

[1] A. A. Ivanov and D. D. Ryutov: Nucl. Sci. Eng. 106(1990)235-242

[2] H. Kumpf, K. Noack and V. G. Krasnoperov: "Neutronic Problems of a Compact 14 MeV *Plasma Neutron Source*", *Report FZR 93-11*

[3] R. W. Hockney and J. W. Eastwood: "Computer Simulation using Particles", Adam Hilger, Bristol and New York, 1988

[4] C. K. Birdsall and A. B. Langdon: "Plasma Physics via Computer Simulation", Adam Hilger, Bristol and New York, 1991

[5] D. Reiter: "Randschicht-Konfiguration von Tokamaks: Entwicklung und Anwendung stochastischer Modelle zur Beschreibung des Neutralgastransports", Report Jül-1947, Jülich, 1984

[6] I. Lux, L. Koblinger: "Monte Carlo Particle Transport Methods: Neutron and Photon Calculations", Boca Raton, Ann Abor and Boston, 1991

[7] R. K. Janev, W. D. Langer, K. Evans and D. E. Post: "Elementary Processes in Hydrogen-Helium Plasmas", Springer Series on Atoms an Plasmas Vol. 4, Springer-Verlag, Berlin and Heidelberg, 1987

APPLIED DECISION ANALYSIS AND RISK EVALUATION

W.Ferse, F.Schröder

1. Projects and Goals

The workgroup 'Applied Decision Analysis and Risk Evaluation' was founded in 1992. It's research interests focus on the development of computer aided decision systems. In 1993 it was the main task to complete a knowledge based system used in Saxony (see next section) with decision support modules.

2. The Knowledge Based System XUMA

XUMA (German synonym for expert system on environmental hazards of contaminated sites) is a joint project of the Institute for Applied Information Science of the Karlsruhe Nuclear Research Centre and the State Institute for Environmental Protection of Baden-Württemberg. XUMA is to support the responsible offices in the uniform evaluation of the hazard potential of contaminated sites and to relief the staff in their routine work. It makes available all the specialists knowledge for them and allows to take into account the most new findings with the help of a knowledge acquisition component.

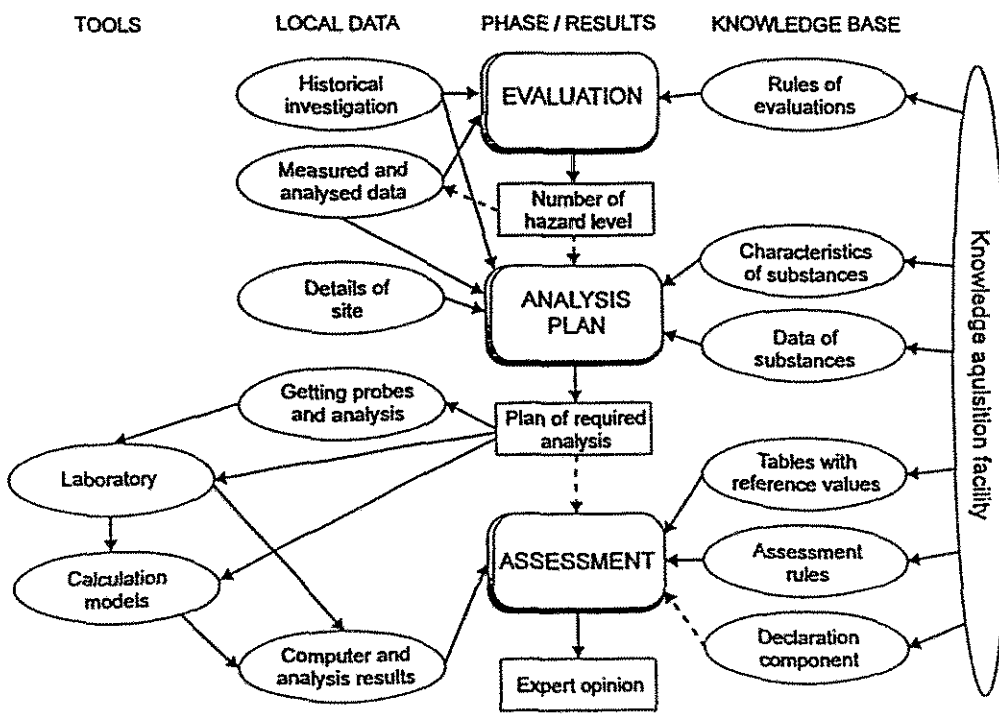

Figure 1: Structure of XUMA

XUMA includes a knowledge base with the principal methods for handling contaminated sites. The main features of XUMA are:

- Evaluation of contaminated sites,
- Creation of analysis plans,
- Assessment of contaminated sites,
- Knowledge acquisition tool,
- Explanation Support.

Fig. 1 illustrates how XUMA works. XUMA runs under the operating system UNIX® on a SPARC workstation. It communicates with a relational database (oracle®) in which the site-specific and the knowledge base data (substances, branches, etc.) are stored. XUMA is designed according to the client-server principle. The server is written in LISP and ART®, a hybrid expert system development environment. The user communicates with XUMA through the client - a Graphical User Interface (GUI), managed by User Interface Management System Open-UI®.

The Research Centre Rossendorf Inc. (FZR - Forschungszentrum Rossendorf) together with Nuclear Analytics and Engineering Rossendorf Inc. (VKTA - Verein für Kernverfahrenstechnik und Analytik Rossendorf) apply the computer program system XUMA as one component of the information-system for environmental protection in Saxony.

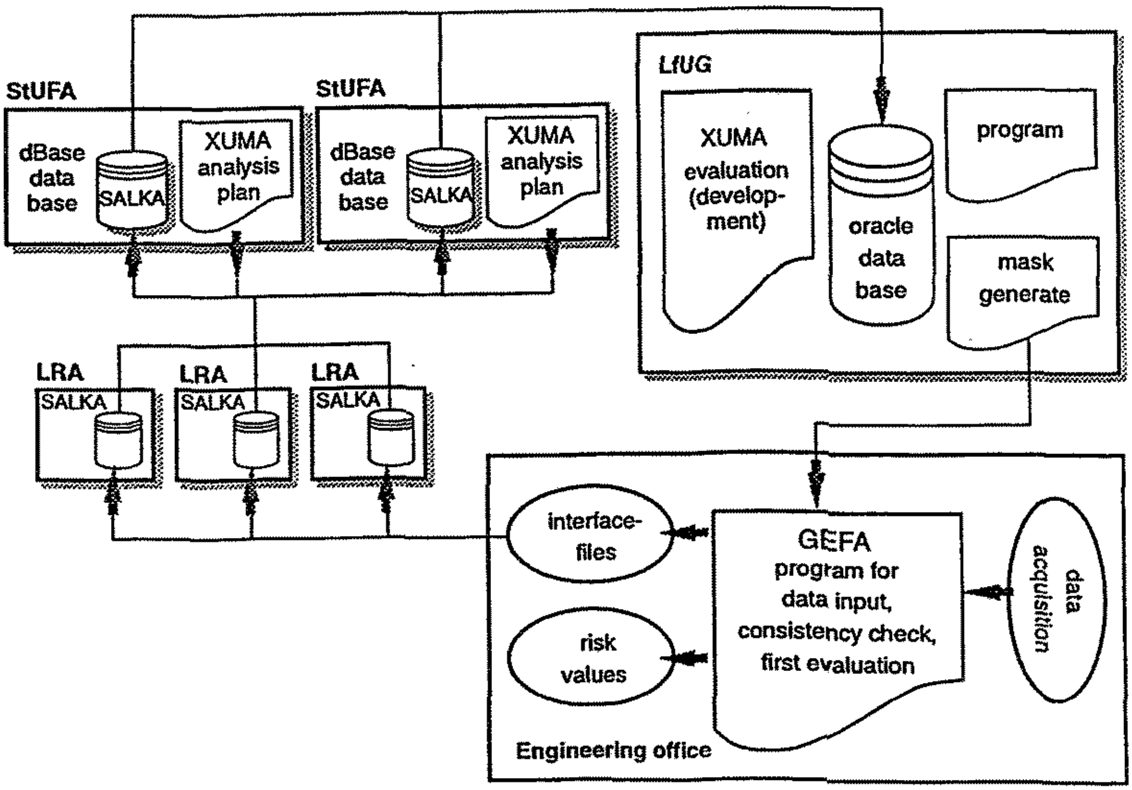

Figure 2: Structure of the registration and evaluation system in Saxony

The model for treating contaminated sites, implemented in XUMA, is based on a method developed at the State Institute for Environmental Protection of Baden-Württemberg. With this method it is possible to determine priorities with respect to the environmental hazard and to derive the necessity of further investigations or remedial actions at the site.

This principal method is used in Saxony too. However, some changes in the system, due to differences in the underlying methods, are necessary to run XUMA in Saxony.

3. Changes Made to XUMA

First of all the XUMA knowledge base for the evaluation function had to be changed completely. This was due to differences of the Saxonian evaluation model, in comparision with the original one XUMA was designed for. It was necessary to enlarge the definition of knowledge representing structures describing the contaminated site, as well as to design new rules, acting on these structures. A method for handling incomplete data was implemented too. Thus XUMA is capable of handling ranges (best/worst case) of possible risk values arising from a contaminated site. In future the following works have to be carried out:

- improving knowledge acquisition tool and handling of uncertain knowledge,
- re-engineering of the client-server architecture and
- development of new evaluation facilities.

4. XUMA's Embedding into Environmental IT-Systems in Saxony

Figure 2 shows the structure of the Environmental IT-Systems in Saxony. The lines between the objects represent the data flow. On-line data connections do not exist. Therefore, the data are transferred as follows:

The data acquisition is performed by the engineering offices. In order to ensure data consistency and data completeness the engineering offices use an interface program (GEFA[1]) which can be generated automatically from the knowledge base of the expert system XUMA.

As a second step, the data are transferred to the offices responsible for the district (LRA - Landratsamt). Each LRA of a governmental district stores the data in a database (SALKA) and transfers a copy to the responsible governmental office (StUFA-Staatliches Umweltfachamt). Besides storing their own data (SALKA) all StUFAs transfer the data to the State Environmental Protection Agency of Saxony (LfUG - Landesamt für Umweltgestaltung und Geologie). At LfUG the complete data of the State of Saxony are available. In order to handle these data different programs are connected to this database. Some of the main functions of these programs are shown in figure 3. The upper part of this figure represents the site-evaluation system which is partly implemented in XUMA, while the lower one describes the decision support system for remedial actions.

---

[1]GEFA: Gefährdungsabschätzung Altlasten

LfUG mainly uses XUMA to aid the further development of the evaluation model. The StUFA offices apply XUMA to establish analysis plans.

5. The Support Program GEFA

GEFA is a support system for data acquisition and evaluation, which works in the same way as the XUMA evaluation function does. The program is a result of the fruitful cooperation between FZR and Technical University Dresden.

GEFA was designed in such a manner, that parts of it can be automatically generated from XUMA's knowledge base. So it is possible to get a new version of GEFA after XUMA's knowledge base has been changed, without any changes made to the source code of GEFA.

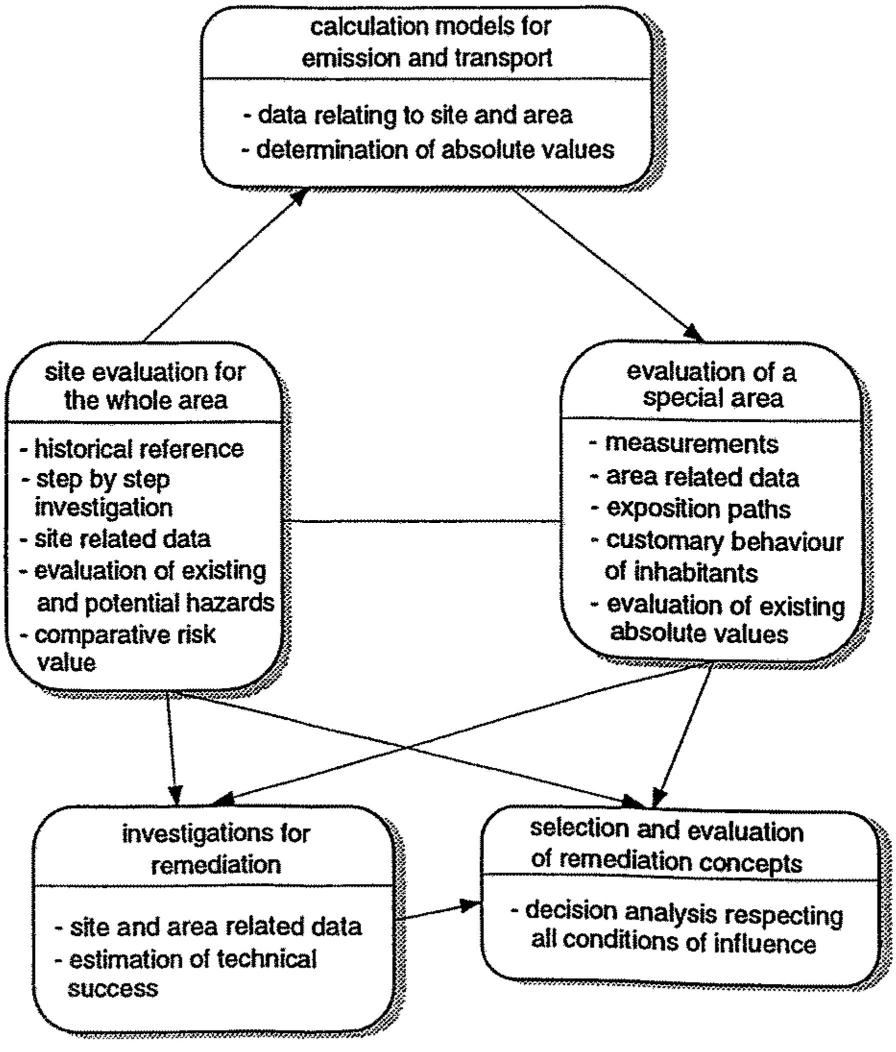

Figure 3: The main components of a site evaluation and remediation system

GEFA was developed for local use in engineering offices and LRAs, because the costs caused by an installation of XUMA at all the concerned institutions would be unacceptably high. GEFA presents a Graphical User Interface similar to that of XUMA. The user can generate a protocol of the session which includes the input data and the evaluation results. Additionally GEFA generates a set of interface files for the data base system SALKA and XUMA's database. These files have a fixed format, designed especially to the requirements of XUMA. A change to a neutral exchange format, based on STEP[2], is planned.

The available version of GEFA fulfils the desired goal only partially. Presently rules cannot be generated from XUMA. Further works will be directed to this capability.

The project described in this report is funded by the SMWK (Sächsisches Staatsministerium für Wissenschaft und Kunst) and is registered with No. 4-7541.83-FZR/313. The authors are responsible for the scientific content of the report.

[2]STEP is an International standard (Standard for the Exchange of Product Data), ISO 10303

INVESTIGATIONS ON RENEWABLE ENERGY SYSTEMS

D. Brünig, W. Hirsch, R. Lischke, F. Naehring
U. Rindelhardt, G. Teichmann

1. Introduction

The activities of the Renewable Energy Group were focussed on three topics in 1993:

- Investigation of energy transformation in grid coupled photovoltaic systems,

- *Start of two regional projects in solar thermal application,*

- Contributions to the Saxonian wind measuring programme.

The main results are summarized in this paper.

2. *Grid coupled photovoltaic systems*

The investigations of grid coupled photvoltaic systems were based on 43 small (e.g. 1 to 5 kW_p installed power P_{in}) photovoltaic plants, which were built in 1992 in the frame of the German 1000-roof-photovoltaic-programm. The totally installed power was 134 kW. Additionally a reference unit was installed in the photovoltaic (PV) test field in Rossendorf.

All the plants were equipped with 3 electricity counters for measuring the solar produced energy (E_{PV}), the energy supplied to the grid (E_+) and the energy delivered from the grid (E_-) to the owner of the system. For measuring the irradiation in the module plane at 12 plants solarimeters with integrator were mounted. The data were monthly collected and analysed in the FZR.

Two main parameters are used for describing the energetic results of the systems. The Final Yield

$$Y_F = \frac{E_{PV}}{P_{in}}$$

is the specific energy output of the systems, scaled by the installed power. In Figure 1 the seasonal variation of Y_F is shown. Besides the monthly mean value from all systems the maximum monthly value is presented. The strong difference between the values obviously shows the different energy losses in the systems. In 1993 the mean specific energy output of the 43 systems was 685 kWh/kW_p, the best result was 912 kWh/kW_p.

A deeper view in the energy transformation of the photovoltaic systems gives the so called Performance Ratio:

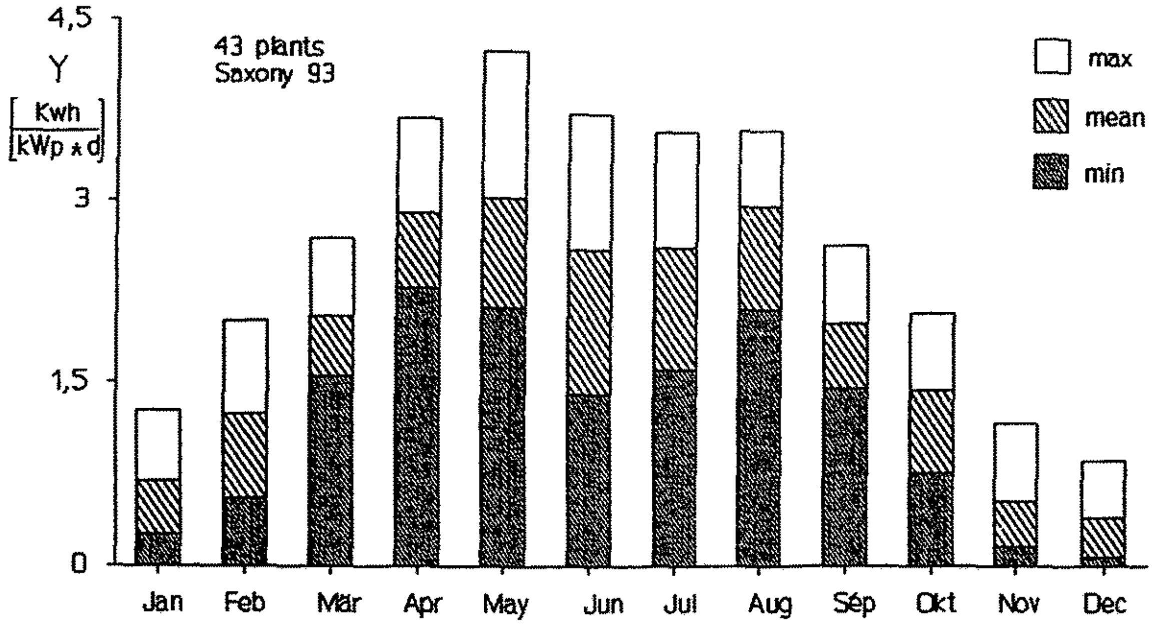

Fig. 1: Monthly variation of the Final Yield

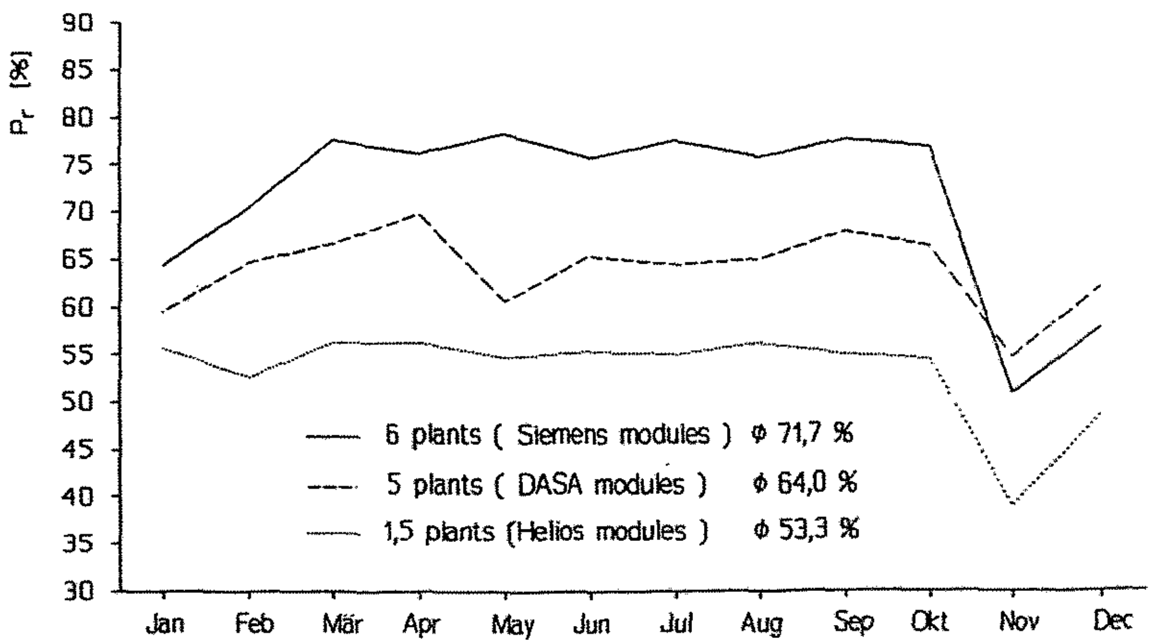

Fig. 2: Monthly Performance Ratios of different PV plants

$$P_R = \frac{E_{PV}}{H\, A_G \eta_G}$$

H: solar insolation
η_G: modul efficiency at STC
A_G: modul area

The Performance Ratio includes all losses in the system caused by

- the deviation of the spectra and incidence angle of the insolation from standard reporting conditions (STC),

- the deviation of the real module parameters (especially efficiency) from the nominal parameters according to the data sheet,

- the mismatch losses of the generator,

- the DC-AC-inverter losses and all ohmic losses.

In Figure 2 the monthly Performance Ratios for the 12 measured systems are shown depending on the module type used in the systems. The Figure shows remarkable differencies between modules of different producers. These differencies indicate that a great part of the unsufficient energy production is caused by the modules. For a quantitative analysis deeper investigations are needed which are plannned for the next years.

3. Solar thermal application

The efforts in solar thermal application were focussed on two interconnected topics:

1. Realizing a pilot project to reduce CO_2-emission by integrating a solar domestic hot water system into a new district heating system,

2. Solar district heating - research on selected locations in Saxonia.

A solar domestic hot water system with integration into a newly finished district heating system is realized as a pilot project in cooperation with the town Freital near Dresden and the municipal energy supplier Technische Werke Freital.

This first project consists of planning and construction of a thermosolar facility (Figure 3) comprising 100 m^2 collectors on the roof of a school in Freital and its connection to the district heating station in the cellar of this school.

Additionally the project includes the scientific attendance of the thermosolar facility, comprising the measurement of temperatures, heat flows, computer-aided system simulation, economic evaluation and educational impact on environmental knowledge.

Innovative push is given through

- the combined use of the system for the hot water delivery to showers and to the school restaurant as well as feeding the solar surplus heat into the gasfuelled

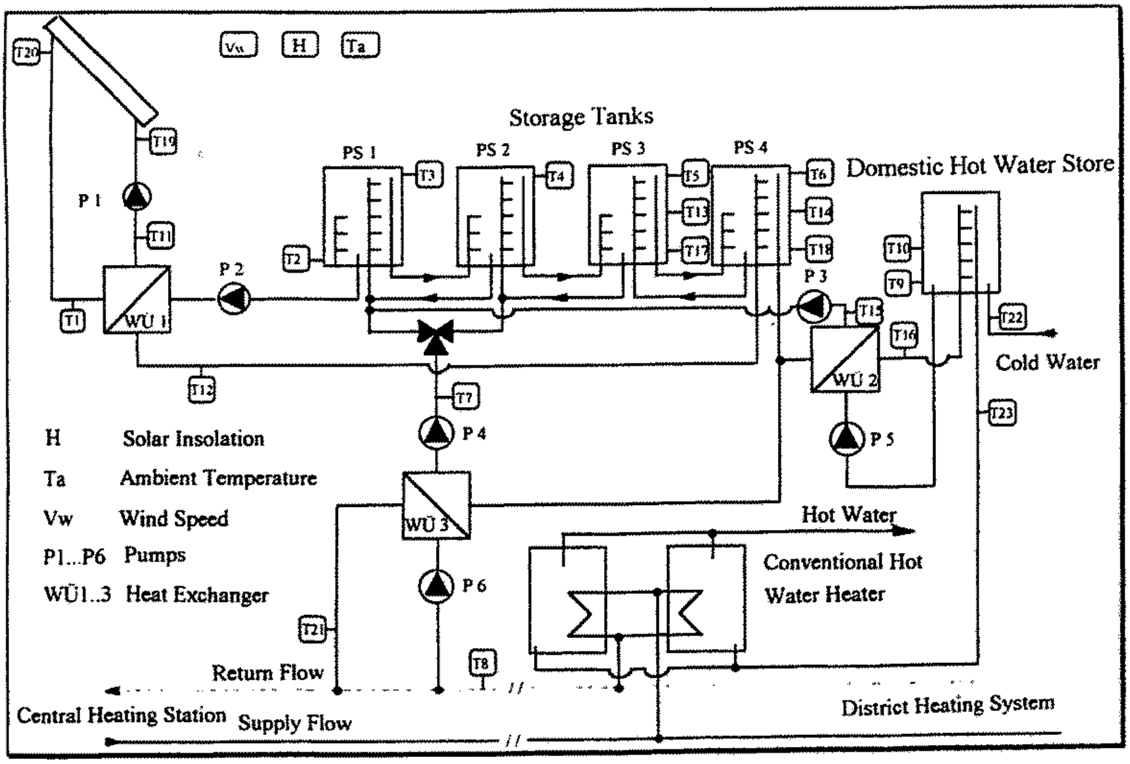

Fig. 3: Hydraulic scheme of the solar thermal system in Freital

district heating net, thereby raising its back line temperature, hence optimizing both uses,

- enhancing the efficiency of the system by specially layered loading of the heat store battery in conjunction with low flow principle in the collector area,
- long-term measurement and scientific research for transfering knowledge to Saxonian industries and trade and delivering the requisites for a solar district heating system around the school,
- advanced heat system reconstruction combined with the use of renewable energy in an official building in East Germany.

The project started on 1st Nov. 1993. The solar and the data gathering system will be set into operation in May 1994.

In the other project suitable locations for the installation of solar heating systems are searched for. It investigates, whether solar heat could be well feeded into a district heating network providing hot water and heating of the dwellings. It aims at promising projects of solar heat use with seasonal storage. This programme runs over two years starting on Oct. 1st.

Settlements are analyzed that are typical for the use of district heating in the east of the FRG:

1. blocks of flats built in the fifties at countryside suitable for reconstuction, and which are connected to a district heating system that should be retrofitted,

2. a new provincial settlement with small houses for one or two families and terraced houses that will be built with the support of a mayorship that is interested in ressource saving concepts,

3. expanding the solar concept to the residential building blocks that are located at the school of the project described above to merge different conventional and solar heat systems.

4. Wind energy estimation

Further the Renewable Energy Group contributes to the estimation of the wind energy potential in Saxony in the frame of the Saxony wind measuring programme (supported by the Saxonian State Ministry of Environment).

The landscape of Saxony is characterized by lowland regions in the northern, by gently undulating and hilly regions in the middles, and by strongly undulating and highland regions up to 1000 m in the southern areas.

Based on wind measuring data from Deutscher Wetterdienst and additional stations the wind climate was calculated by means of the Danish Wind Atlas Analysis and Aplication Program WASP. At the additional wind measuring stations the wind speed was measured at two heights between 10 m and 36 m a.g.l.; the direction only on the top. Ten-minutes-averaging-values of wind velocity and direction were recorded over a time of one year in minimum. The program WASP requires as input also the digitized orography, the roughness, and the obstacles in the surroundings of the measuring stations. The output of this program, the wind atlas library, represents the wind climate around the station.

By means of the WASP-resourcefile-option the average wind power density was calculated in several regions of Saxonia. An example in fig. 4 illustrates the calculation in a grid distance of 200 m over an area of 38 km x 23 km (region Oberlausitz). The result was converted into lines with constant average wind power density.

Furthermore, investigations were performed about representance regions of wind climate. Since WASP was developed mainly for coast and lowland regions far from mountains, special efforts were necessary to decide the region of representance in Saxony. It was shown, that in lowland regions the area of representance regions in some cases was comparable with WASP results from coast regions. Especially in the mountain region of the "Erzgebirge" the representance regions were found to be very small, the WASP technique is practically not applicable in this region.

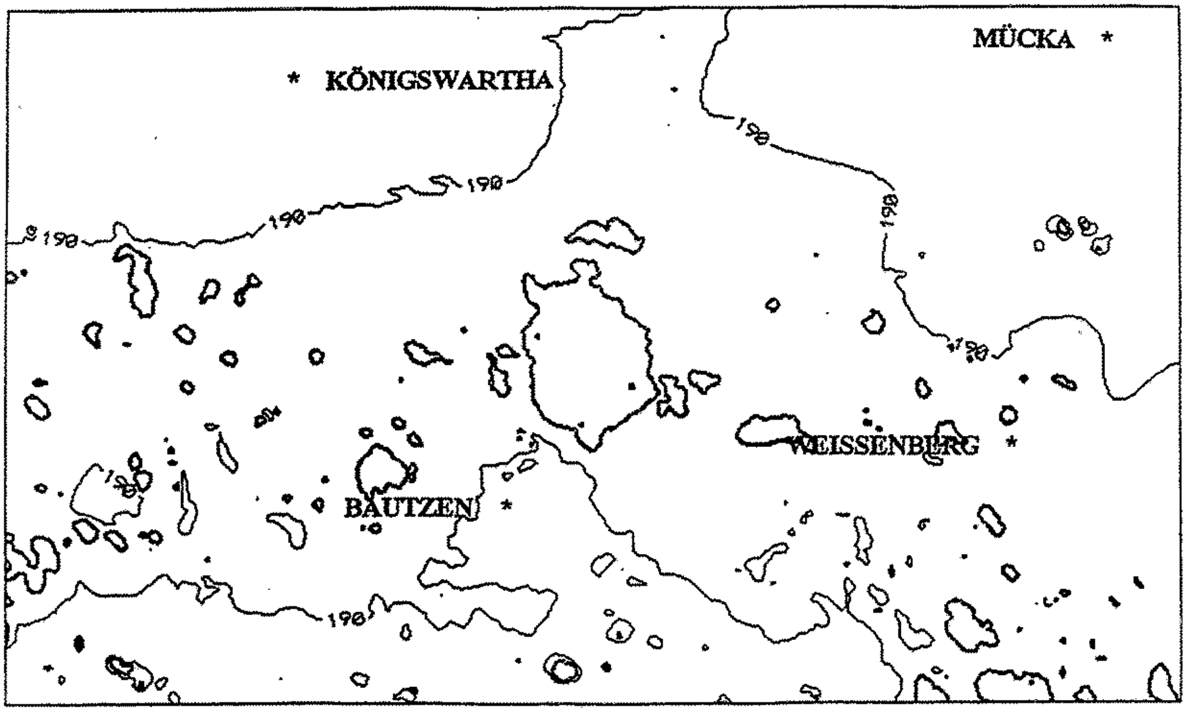

Fig. 4: Wind power density (W/m²) in the Saxonian Oberlausitz. A usable wind energy potential was estimated in the areas marked by thick lines.

Finally, an approximative calculation method was established to extend the one year wind measuring values of a measuring station to long time values by comparison with short time and long time wind data of another wind measuring station in the same representance region.

5. Outlook

The activities of the Renewable Energy Group will be focussed also in the next years on the discussed topics. The main aim of the group consists in the scientific preparation and monitoring of selected demonstration and pilot systems based on solar and wind energy. A close cooperation has been established with the Technical University Dresden and the University Leipzig.

Abstracts of Publications

Conference Contributions

Altstadt, E., F.-P. Weiß
Experimental and Numerical Investigation of Control Element Vibration During Abnormal Core Barrel Motion at a VVER-440 Type Reactor
International Simulators Conference (SIMULATORS X)
Arlington / Virginia, 29 March - 1 April 1993

In 1985 abnormal core barrel motion had occured at unit 2 of the Greifswald NPP indicated by extremly large neutron noise. Amplitudes of up to 4mm were estimated from the external neutron noise signals.
The coherence and phase relations between excore and incore neutron noise signals exhibited typical features from which it could be concluded that even the control elements were forced to vibrations by the moving core barrel.
To obtain principal understanding about these phenomena and to draw conclusions for the surveillance of the excore and incore neutron signals, experimental and numerical investigations were performed. An experimental set-up was constructed providing all necessary displacement signals via HALL probes. This physical model, being a double pendulum with an annular channel surrounding the lower pendulum, can be operated in a linear mode (small excitation amplitudes) as well as in a non-linear mode (larger amplitudes which cause impacts between channel and lower pendulum).
The numerical simulation algorithm is based on a mechanical system consisting of linear elements (inertia, dampers, springs) and non-linear elements (gaps). In this way impacts between control element and neighbouring fuel cassettes which are strongly non-linear events can be modeled. After simulating the time series, which is possible for any detector position at the control element or at the set-up respectively, transfer functions, coherences, phase relations etc. can be computed.
It could be shown that the typical linear phase shifts between excore and incore neutron noise signals are due to impacts between the control elements and the neighbouring fuel cassettes. The obtained results can be used to establish a sensitive detection procedure for control element vibrations induced by abnormal core barrel motion.

Altstadt, E., F.-P. Weiß
Regelelementschwingungen bei anomaler Kernbehälterbewegung in einem Druckwasserreaktor vom Typ WWER-440
4. Tagung über Dynamische Probleme, Modellierung und Wirklichkeit,
Universität Hannover, 07. - 08. Okt. 1993

Während der anomalen Kernbehälterbewegung bei einem Reaktor vom Typ WWER-440 wurden signifikante Phasen- und Kohärenzbeziehungen zwischen dem Excore- und dem Incoreneutronenrauschen beobachtet. Für die Erklärung der Phänomene wurde ein numerischer Algorithmus entwickelt, der auf den nichtlinearen Bewegungsgleichungen eines Doppelpendels beruht. Zur qualitativen Verifizierung der numerischen Resultate wurden außerdem Experimente an einem kleinen physischen Modell der Regelelemente durchgeführt. Es konnte nachgewiesen werden, daß die am WWER-440 beobachteten typischen Signalmuster von mechanischen Anschlagvorgängen zwischen Regelelementen und benachbarten Brennstoffkassetten herrühren.

Altstadt, E., F.-P. Weiß
Vibration Modelling - Investigation of Mechanical Accident Sequences at a VVER-440 Type Reactor
International Conference on Fault Diagnosis
Toulouse / France, 05 - 07 April 1993

During abnormal core barrel motion of a VVER-440 type reactor significant phase relations and coherences between incore and excore neutron noise signals were observed. For the explanation of the phenomena a numerical algorithm based on the non-linear equations of motion of a double pendulum was developed. In order to confirm the numerical results qualitatively additional experiments at a small set-up modelling the control elements were performed. The typical signal patterns observed at the VVER-440 could be shown to originate from mechanical impacts between the control elements and the neighbouring fuel cassettes.

Barz, H.-U.
Adjustment and Application of Monte Carlo Neutron Calculation with Respect to Embrittlement Problems
Common Workshop of the EURATOM Working Group for Reactor Dosimetry and the Working Group for Reactor Dosimetry of VVER-Reactors on Pressure Vessel Surveillance Programmes and Their Applications
Rez / Czech Republic, March 1993

Problems of the calculation of neutron fluences for reactor pressure vessel embrittlement determination were discussed. For the example of the calculation of neutron fluences of specimens irradiated within the Rheinsberg reactor (time period 1984-1988) it was shown, for which parts of the problem Monte Carlo methods can be very well applied.
Some special measures were discussed which are implemented in the Rossendorf Monte Carlo codes (system TRAMO), especially the improved "Weight Window Method" and an exact calculation method for the needed weights. Further the preparation of all needed data to take into account the history of each irradiation period was described and the influence of different neutron group data and the different handling of anisotropy of elastic scattering was considered.

Barz, H.-U.
Experiences in Monte-Carlo-Calculations for VVER-Pressure Vessel Fluence Monitoring
Multilaterales Symposium zur Sicherheitsforschung für WWER-Reaktoren
Köln, 28.09. - 30.09.1993

Information was given about the Rossendorf system of Monte Carlo codes including measures for variance reduction with respect to the calculation of fluences at irradiation points within the Rheinsberg reactor. It was shown that by the used methods it was possible to obtain results with low statistical errors and therefore Monte Carlo methods are well suited for the determination of neutron fluences if applied to that part of the problem, where transport calculations are needed. The sensitivity of the obtained results against the used group sets of neutron data was considerably reduced by improving the calculation of scattering at hydrogen isotope, which is very important for this kind of calculation.

Barz, H.-U.
Neutronentransportberechnungen mit der Monte Carlo Methode - Möglichkeiten und Probleme
Seminarvortrag, Technische Universität Dresden, Abteilung Physik
Dresden, 18. November 1993

A general survey was given about the problems and growing possibilities of the Monte-Carlo method applied to particle transport.
In particular the following items were considered:
- the mathematical foundations of Monte Carlo methods
- analog games
- nonanalog games and the possibility to obtain zero variance
- equation for the variance in the analog and nonanalog case, meaning of importance function
- danger of miscalculation connected with nonanalog games
- "Weight Window Method" and analytical investigations to improve this method
- alternative methods to decrease the statistical errors
- possibilities to calculate optimum weights

Böhmer, B.
Comments on Spectrum Adjustment for Reactor Pressure Vessel Dosimetry
Common Workshop of the EURATOM Working Group for Reactor Dosimetry and the Working Group for Reactor Dosimetry of VVER-Reactors on Pressure Vessel Surveillance Programmes and Their Applications
Rez / Czech Republic, March 1993

After a short review about the state of art of spectrum adjustment for reactor pressure vessel dosimetry and their realization in Rossendorf plans for future developments are described. The most important outstanding problem is the calculation of covariances of the theoretical input spectra.
As example for an advanced spectrum adjustment some preliminary results of a reevaluation of 1984/85 irradiation experiments in Rheinsberg were presented.
Suggestions are made for common projects in the frame of the WGRD, VVER and EWGRD, especially the development and maintenance of a common reactordosimetric database for VVER type reactors and the organization of benchmark exercises for calculations of detector cross sections and spectrum covariances.

Böhmert, J., F. Bergner, M. Große, H.-W. Viehrig
Influence of the Depth Position on the Neutron Embrittlement of the VVER Reactor Pressure Vessel Steel 15Cr2MoV(A) - Consequences for the Assessment of Reactor Safety
Jahrestagung Kerntechnik 1993
Köln, 25. - 27. Mai 1993

The dependence of the mechanical properties on the depth position in unirra- diated state and after irradiation up to neutron fluences of approximately. 5×10^{18}

and 70 x 10^{18} cm^{-2} (E > 0.5 MeV) is tested on a forging made of VVER 440 reactor pressure vessel steel 15CrMoV. Specimens taken from a sub-surface region shows a higher strength and a lower transition temperature than ones from 1/4 - 3/4 of the wall thickness. Increased irradiation reduces these differences. The testing of specimes from the 1/4 depth position within the surveillance programme, as normally demanded by monitoring rules for nuclear power plants, results in a conservative safety assessment against brittle fracture even in the case of EOL fluence. By taking into account fluence attenuation, the flux effect etc., the toughness increases over the wall thickness from the inside to the outside after a longer operating time of the RPV.

Böhmert, J., H.-W. Viehrig
Results of Material Investigations Based on the Rheinsberg - Irradiation Programme
Multilateral Symposium on Safety Research for VVER-Reactors
Cologne, September 1993

Neutron embrittlement of reactor pressure vessel is a critical safety-related problem for VVER type reactors. For a better knowledge of this problem an irradiation programme was carried out in the VVER-2 reactor in Rheinsberg from 1984 - 89. With the programme the procedure and methods for the calculation of the transition temperature shift should be examined, the irradiation-induced change of fracture toughness should be determined and the influence of postirradiation annealing had to be investigated. 33 heats of both basic and weld material from low alloyed Cr-Mo-V and Cr-Mo-Ni steels were tested. The neutron fluence amounted to (1.5-79) x 10^{18} n/cm^2 (E>1MeV). In the unirradiated state the VVER material shows satisfying properties of strength and toughness and is comparable with the performance of ASTM type steels. The shift of the transition temperature is not always correctly predicted by means of the normally applied trend curves.

Eckert, S.; G. Gerbeth, J.P. Thibault, G. Mihalache
Some Aspects of LMMHD Two-Phase Flow: MHD Generator Configuration
7th. Int. Beer-Sheva Seminar on MHD Flows and Turbulence
Jerusalem, February 1993

The influence of an external magnetic field on LMMHD two-phase flows in vertical rectangular ducts has been examined. The goal of the work is the construction of models being able to predict the average behaviour of the flow as well as being relatively easy to survey and to handle. Results regarding the slip ratio obtained from a bubbly flow model are compared with experimental data got from measurements at the mercury-air facility. In the case of an applied magnetic field discrepancies between model and experiment are obtained giving an indication of the imperfection of the present state of the model. The crucial point is the validation of the semiempirical closure laws involved in the LMMHD tow-phase flow models. In the present state of the experiments the influence of the void fraction on the apparent electrical conductivity of the two-phase flow has been investigated. The results obtained from the mercury-air facility of LEGI-IMG are located between the relations given by Maxwell and Petric & Lee, respectively.

Eckert, W., U. Knopf, U. Rindelhardt, G. Teichmann
1000-Roof-Programme in Saxony and Thuringia: Actual Situation, System Technique and Results
8. Nationales Symposium Photovoltaische Solarenergie
Staffelstein, 17. 03. - 19.03.1993

The paper dealt with the first results of the 1000-Roof-Photovoltaic Programme in the German Federal States of Saxony and Thuringia. Experiences in designing and mounting the pv-plants are discussed. Up to the end of 1992 totally 70 small pv-plants were coupled to the grid in both states. From the first results a mean energy production of about 700 kWh per installed power of 1 kW_p can be extrapolated. The most technical difficulties resulted from the used DC-AC-inverters. Additional problems were caused by the grid itself, which was still integrated in the East European Network.

Ferse, W.
Evaluation of Environmental Problems Using Decision-Analysis Methods and Knowledge-Based Systems
Workshop of the German PIN-Project Group (Processess of International Negotiation), Rossendorf, March 1993

A knowlegde-based strategy for the evaluation of risks produced by contaminated sites is presented, which also gives a ranking for the temporal sequence of remediation. This strategy supports the responsible government offices. It is based on the Saxonian evaluation method for contaminated sites and is implemented in the computer programs XUMA and GEFA.

Ferse, W.
Possibilities for Decision-Analysis in Planing Energy Distribution Systems
Workshop "Strategic Energy Planning", ESAG Dresden, October 1993

A concept for the use of decision-analysis in planning local energy distribution systems is introduced. The concept is based on the coupling of multiple independent modules, what enables the finding of a solution optimum in cost and environmental compatibility by variation of boundary conditions and input parameters. The first modul is presented.

Ferse, W.
The Application of the Expert System XUMA in Saxony
WINRE'93, 4th Workshop of Information Management in Nuclear Safety, Radiation Protection and Environmental Protection
Köln, November 1993

A computer system is presented which will be an effective support for the Saxonian government offices responsible for the evaluation of contaminated sites and the decision concernig the kind of remediation. This system XUMA (German synonym for expert system on environmental hazards of contaminated sites) includes a knowledge base with the principal methods for handling contaminated sites. The main features of XUMA are:

- Evaluation of contaminated sites,
- Creation of analysis plans,
- Assessment of contaminated sites,
- Knowledge acquisition tool and
- Explanation capability.

Furthermore XUMA's embedding into environmental IT-systems in Saxony is described.

Ferse, W.
The Possibilities of the Evaluation of Radioactive Contaminated Sites Using the Knowledge-Based System XUMA
Karlshorster Workshop, Bundesamt für Strahlenschutz, Berlin, November 1993

The possibilities to evaluate radioactive contaminated sites with knowledge-based methods are discussed on the basis of a knowledge-based evaluation system for non-radioactive sites. The discussion treats methodical and programming aspects.

Gerbeth, G., S. Eckert, H. Langenbrunner
Dispersion of Gas Bubbles in a Two-Dimensional MHD Turbulence
7th Beer-Sheva International Seminar on MHD Flows and Turbulence
Jerusalem, 14. - 18. Febr. 1993

The dispersion of small gas bubbles in a vertical upwards liquid metal two phase flow is investigated theoretically as well as experimentally. Local void fraction measurements are presented for a vertical sodium-argon flow with and without external magnetic field. The dispersion of an initially narrow void distribution shows this behaviour clearly: There is an overall focussing effect of the magnetic field on the void distribution, but the dispersion of gas bubbles is much more suppressed parallel to the field than perpendicular to it.
The bubble transport is modelled by a simple diffusion equation. The model takes into account that bubbles represent no passive tracer of the flow field but have an own dynamics due to their relative velocity to the liquid phase. The experimental results will be analyzed in terms of the corresponding diffusion coefficients.

Große, M., G. Schuster et. al.
Neutron and X-Ray Investigations of the Oxygen Bonding in $YBa_2Cu_{30}O_{(7-x)}$ Combined with Physico-Chemical Methods
7. Tagung Festkörperanalytik, Chemnitz, 19. - 23. Juni 1993

The occupancy of the different oxygen lattice places at different annealing conditions in $YBa_2Cu_{30}O_{(7-x)}$ was determined by Rietveld Refinement with neutron and X-ray diffraction data. The occupation density for the oxygen positions O1 to O4 was ascertained. The values of the oxygen content of the samples accounted by this method were compared with those measured by thermoanalysis and solid electrolyte coulometry. It could be shown, that the atoms of oxygen exchangeable by thermal treatment are O4, that is the oxygen in the O-Cu-O chains and O1, the oxygen atoms connecting the planes. The oxygen in the planes is fixed and cannot be removed up to 935 °C. The strength binding O1 in the lattice is stronger than those of O4 atoms, what is demonstrated by higher temperature of dissoziation of the O1 atoms. At 935 °C less than 10 % of the O1 positions are vacant. The amount of the received oxygen is not exactly equal to the really installed oxygen at the lattice places. Especially in the temperature region below 400 °C adsorption and chemisorption processes are ascertained.

Grundmann, U., U. Rohde
3-D Simulation of Reactivity Transients in Cores of VVER-Reactors
SCS Simulation Multi-Conference
Arlington / Virginia / USA, 29 March - 01 April 1993

Reactivity initiated accidents (RIA) have to be analyzed for safety assessment of nuclear reactors. The presented 3-dimensional core simulator DYN3D/M2 describes the space dependent effects of reactivity perturbations caused by control rod motions or local changes of coolant temperature and boron concentration. The safety margin can be determined more precisely by use of 3-D models than with simpler methods as point model or one-dimensional kinetics. A nodal expansion method (NEM) for hexagonal geometry of VVER fuel elements was developed to reduce the numerical effort of 3-dimensional neutron kinetics. The changes of thermohydraulic parameters as fuel and coolant temperatures, coolant density and poisoning are determined with the help of the thermo-hydraulic model FLOCAL included in the code. Feedback results from the influence of the thermohydraulic parameters on the neutron physical constants. Applying DYN3D to safety calculations of reactivity transients, the code was validated by comparing its essential parts with benchmarks, other codes and experiments. An accident caused by the ejection of a single control rod in a VVER-440 reactor was analyzed. The results show a very high power peak in the neighbourhood of the ejected rod. Runs with time step control indicate that the computer time can be reduced in comparison to fixed time step. Simulations with a smaller number of coolant channels were investigated for coupling the core model with codes simulating the whole coolant system of a nuclear power plant.

Grundmann, U.; U. Rohde
Definition of the Second Benchmark of AER
3rd Symposium of AER, Pieštany (Slovakia)
27. Sept. - 1. Okt. 1993

The first kinetic benchmark of AER was defined for comparison of different 3-dimensional kinetic codes developed for the hexagonal geometry of fuel assemblies in a VVER-reactor. The transient was assumed to be caused by ejection of nonsymetric control rod in a VVER-440 reactor. Feedback effects were neglected. The positive reactivity insertion not leading to prompt criticality results in a slower power increase and was compensated by insertion of shutdown rods.
The benchmark problem No. 2 discussed on the meeting of working group D in Budapest 1993 consists also of a control rod ejection accident in a VVER-440. The initial configuration is similar to benchmark No. 1. A nonsymetric control rod with a worth of 2 β_{eff} is ejected at hot zero power (HZP). The Doppler effect being the main feedback effect for this type of transients is the only feedback and is taken into account by an adiabatic model of fuel temperature. Therefore it is possible to calculate this type of transient with codes which do not contain a complete

thermohydraulic model.
As in problem No. 1, the nuclear data are given to exclude at this step of comparison the effects caused by different nuclear data. A sharp and high power peak connected with large deformations of flux shape is expected to give a serious test for codes and methods of calculation.
The problem, the input data and the expected results which will be used for comparisons are specified.

Grundmann, U.; U. Rohde
Assessment of the Influence of a Mixing Model on a Boron Dilution Transient in the VVER-440 Core by Help of the Code DYN3D/M2
3rd Symposium of AER, Piešťany (Slovakia)
27. Sept. - 1. Okt. 1993

A reactivity initiated transient caused by entering a water plug with diluted boron concentration into the core during incorrect loop startup in a VVER-440/W-213 reactor is analyzed with the help of the code DYN3D/M2. The water with diluted boron concentration from the one loop is mixed with the water of the other loops before the core inlet. The results for the transient are influenced by three different mixing models that were investigated:

- ideal mixing: the boron concentration at all inlets of fuel assemblies is uniformly distributed,
- no mixing: the boron perturbation occurs only in the fuel elements of the sector belonging to the considered loop,
- mixing model: estimation of boron dilution at the core inlet by superposition of reference distributions, defined experimentally or pre-calculated by a simplified analytical model.

The results of DYN3D/M2 for these three cases presented in the paper show significant differences of the safety parameters, i. e. nuclear power, maximum fuel temperature or critical power ratio.
The asymmetric boron perturbation and the short length of the plug requires a more-dimensional core model for the treatment of this transient. The code DYN3D/M2 is capable of describing the space-dependent effects of the diluted boron in the core for all three cases. The power excursion is connected with strong deformations of the neutron flux distribution and power shape as a result of the space-dependent boron perturbation. Therefore the feedback effects are also influenced by the space effects.
The different boron mixing models lead to different boron distributions in the core, which influence the power excursion and the results for the safety parameters. By using the mixing model, more severe consequences of the transient are obtained than by assuming ideal mixing. Assuming no mixing, the perturbation results in a severe accident with partial core damage. The results indicate the importance of the applied mixing model for the investigations of this type of transient.

Grunwald, G., E. Altstadt
Analytical and Experimental Investigations for Modelling the Fluid-Structure Interaction in Annular Gaps
IMORN-24 (Informal Meeting on Reactor Noise)
Oybin / Germany, 23 - 25 June 1993

Modelling the mechanical vibrations of pressurized water reactor internals the fluid-structure-interaction is to be taken into account. Especially at VVER-440 reactors there is a strong influence of the fluid due to the specific geometry. The intention of the presentation is to provide a solution of the continuity and the Navier-Stokes equations for the special case of a narrow annular gap geometry considering the fluid friction.
To obtain an analytical solution for these coupled 3D partial differential equations further assumptions and simplifications must be made:
- the width of the annular gap is small compared with the diameter,
- displacements of the mechanical structure are small compared with the gap width
- the fluid flow velocity components are independent on the radius.
Keeping these assumptions in mind one can reduce the dimension of the continuity equation from 3D to 2D by averaging over the gap width.
Two elementary types of motion of the cylinder are considered: parallel displacement and pendular motion. By superimposing these elementary types even more general motions can be described.
In practice the application could be meaningful for core barrel motion at LWRs in general and for flow induced vibrations of control elements at VVER-440 reactors. The analytical results are compared with experimental ones from a cylindrical pendulum setup. The criteria of comparison are the eigenfrequency and the damping of the pendulum in the static and flowing fluid. There is a good agreement between analytical and experimental results. Especially the strong influence of the chosen boundary condition upon the pressure equations can be shown.

Hessel, G., W. Schmitt, F.-P. Weiß
A Method for Acoustic Leak Detection at Complicated Geometrical Structures
IMORN-24 (Informal Meeting on Reactor Noise)
Oybin / Germany, 23 - 25 June 1993

A method for detecting and localizing leaks at complicated three-dimensional topologies by measuring the leak induced structure-borne and airborne sound and by applying pattern recognition procedures is being developed. The sound patterns necessary to train fuzzy logic classifiers and neural networks are generated with simulated leaks at the original structure. As features for characterizing the occurrence and the location of a leak, coherence values between high-frequency microphone signals and RMS-values of acoustic emission sensors are used. The method is even applicable when localization based on propagation time differences or sound attenuation differences fail.

Kereszturi, A., M. Telbisz, U. Grundmann, J. Krell
Results of a Threedimensional Hexagonal Kinetic Benchmark Problem
ENS Regional Meeting, Energy in Central Europe: Present and Perspectives
Portoroz / Slowenia, June 1993

The recent safety analysis investigations of the VVER type reactors require the use of three-dimensional hexagonal kinetic codes. For this purpose the codes KIKO3D and DYN3D were developed in the Atomic Research Institute Budapest and in the Research Center Rossendorf, respectively. The kinetic codes have to be validated before being used for safety assessments. A benchmark problem is defined, as the

first step of the validation procedure of hexagonal kinetic programs.
The problem describes a rod ejection transient in a VVER-type geometry, where the worth of the ejected rod is just below the prompt critical value. The initial power is near to zero and the power rise is not too large. Therefore, the transient can be treated without feedback based on the given time-dependence of the cross sections and geometry.
KIKO3D results are presented, i.e the solution of time dependent nodal equations by the Improved Quasistatic (IQS) Method. The time dependence of the integrated power and the reactivity are compared with the adiabatic results. These results are also compared with the results of two different DYN3D calculations carried out in Rossendorf and in Berlin.

Krepper, E.
ISP-33 Pre- and Posttest Calculations in the FZR Rossendorf
2nd Workshop ISP 33
Lappeenranta / Finnland, 17 - 19 Mai 1993
ISP-33 Comparison Report, OECD/NEA in preparation

Calculations relating to the OECD/NEA/CSNI International Standard Problem No. 33 were carried out with the GRS code ATHLET.This problem was a natural circulation experiment with primary coolant inventory reduced stepwise. The experiment was conducted in the PACTEL facility in Lappeenranta (Finland), which is a 1/305 volumetrically scaled, full height three loop simulator of the Russian VVER-440 type reactor. The main events of the experiment could be shown and explained by the ATHLET calculations:

- After the second draining the mass flow in the loops stagnates. Simultaneously, the primary pressure increases and the pressurizer is partly refilled.
- In the periods after the third drain step the mass flow through the three loops is nonequally distributed, which could be reproduced by the ATHLET calculations at least qualitatively.

Kumpf, H., K. Noack
Neutronic Problems of a Compact 14 MeV Plasma Neutron Source
International Conference on Open Plasma Confinement Systems for Fusion
Novosibirsk, 14 - 18 June 1993

Neutronic problems connected with the design of a compact 14MeV neutron source for fusion material research based on a plasma mirror are treated. In particular it has been demonstrated, that further construction efforts are necessary to comply with the established radiation limits for the magnetic system. Further it is not possible to raise the useful high energy flux by arranging reflectors. If one of the source areas of the machine is equipped with a moderator, a thermal neutron source with a flux of about $5 \cdot 10^{14}$ n cm^{-2} s^{-1} can be achieved.

Lucas, D.
Influence of the ATHLET Maximum Permissible Time Step Size on the Results
Second meeting of the ATHLET user group
Garching, 28. and 29. October 1993

The maximum permissible time step size is an input parameter of the ATHLET code. In the ATHLET input data description a value of 5 s is recommended for this parameter. For first tests of the coupling of the ATHLET code with the 3D neutron kinetic code DYN3D test calculations with a simplified VVER-440 data set were carried out. The results were compared with ATHLET calculations with point kinetics. The influence of the maximum permissible time step size on the results of these calculations with point kinetics is discussed for two test cases. In the first case the time points for opening and closing of safety valves are shifted for maximum permissible time steps greater than 0.5 s. In the second case there is an oscillation of power for maximum time steps of 2 s, which is removed by a maximum time step size of 0.5 s. These examples show, that the recommended value for the maximum permissible time step size is not suitable for all problems.

Maroti, L., H.-M. Prasser, P. Windberg
Investigation of Two-Phase Flow Phenomena at Integral Test Facilities Using Needle Shaped Conductivity Probes
8th International Conference on Thermal Engineering and Thermogrammetry THERMO, Budapest, June 2-4, 1993

The paper deals with the utilization of needle shaped conductivity probes developed in Rossendorf during a small break LOCA experiment at the Budapest PMK test facility. A 1-%-break at the down-comer inlet was simulated, the ECC tanks were switched off. The probes worked properly under primary circuit conditions (12.3 MPa, 300 °C), the data acquision system provided clearly readable data in spite of the high electrical disturbance level caused by the directly heated fuel rod simulators of PMK. The paper presents plots of the signals of the probes. The level drop in the upper plenum of the reactor, the hot leg loop-seal clearing and the emptying of the steam generator cold collector were indicated. Closely after the loop-seal clearing void fraction oscillations with a period of about 22-24 sec were observed at the reactor outlet and the steam generator inlet.

Noack, K.
Eine Plasmaneutronenquelle für die Fusionsmaterialforschung
Institut für Strahlenschutzphysik, TU Dresden
Dresden, 27.05.1993

The contents is largely covered by a the extended contribution to this annual report.

Rindelhardt, U., G. Teichmann
Project managing of the 1000-Roof-Photovoltaic-Programme
Photovoltaik/BMFT-Statusseminar
Bad Breisig, 27.04. - 29.04.1993

The report summarizes the present state of the 1000-Roof-Photovoltaic-Programme (sponsered by the BMFT and the Federal States) in the five new German Federal states. After some starting problems the programme is well accepted also in East Germany now, especially in Brandenburg, Saxony and Thuringia. Statistical data are given on the siutation in the single states.
Some operation results are discussed in more detail. A final yield of 2 kWh/kW$_p$·a

seems to be possible, at least in the region of Saxony. The share of the direct used *solar energy by the plant* owner strongly depends on the individual energy consumption and on the season. During the winter only a share of 10 % is realistic, but in summer the value can reach 50 % or more. The average performance ratio of several systems is estimated to 68 %.

Schumann, P.
Experimental Investigation of *Bias and Confidence of the Ordinary* Coherence Function
IMORN-24 (Informal Meeting on Reactor Noise)
Germany / Oybin, 23 - 25 June 1993

The ordinary coherence function $\gamma^2(\omega)$ defined by

$$\gamma^2(\omega) = \frac{|S_{xy}(\omega)|^2}{S_{xx}(\omega) * S_{yy}(\omega)} \tag{1}$$

is of squared type with a positive bias depending on the number N of accumulated estimations. If the analyzed signals x(t), y(t) as well as the correlated contribution inside x(t), y(t) are normally distributed the power *spectral densities* S_{xx}, S_{yy} *are* χ^2-distributed. Then the product as well as the quotient in equ. 1 are not of a classical distribution type and the determination of the concrete type becomes difficult. Therefore the bias and the corresponding standard deviation are investigated experimentally using uncorrelated normally distributed white noise. The result shows for estimation numbers N > 5, that the bias of γ^2 corresponds to the amount of 1/N. The belonging positive standard deviation

$$\sigma(\overline{\gamma^2}(f_i)) = \sqrt{\frac{\sum_{i=1}^{M} (\overline{\gamma^2}(f_i) - \overline{\gamma^2})^2}{M-1}} \tag{2}$$

for N > 5 t is in the same order of magnitude as the bias itself. That means: For the evaluation of coherences a confidence band of +(4...5) * σ should be used to select values of significant statistical accuracy. Only for these selected values one can be sure, that the phase values belonging the same frequency point are useful for system identification.

Viehrig, H.-W., J. Böhmert
Nachbestrahlungsuntersuchungen zum Bestrahlungsprogramm Rheinsberg
4. Seminar zur wissenschaftlich-technischen Zusammenarbeit zwischen der Russischen Föderation und der Bundesrepublik Deutschland zum Thema: "Komponentensicherheit und Qualitätssicherung (WWER)"
St. Petersburg, Mai 1993

The irradiation programme Rheinsberg serves to investigate the neutron embrittlement of VVER type reactor pressure vessel steel. Within this programme Charpy-V (partly with fatigue crack and side grooved), CT- and tensile specimes of 24 different heats from VVER 440 type and VVER 1000 type reactor pressure vessel steel (basic or weld material) were irradiated in the high flux channels of the VVER-2 Rheinsberg from 1984 - 88. The testing and evaluation of the irradiated specimen will be done within the framework of bilateral scientific-technical cooperation between Russia and Germany. The report gives a systematic review of all material data existing for the unirradiated initial state. Results of Charpy- V-impact tests and quasistatic 3-point-bending tests are discussed in detail.

Viehrig, H.-W., J. Böhmert, U. Bergmann
Material Investigations at Research Center Rossendorf Inc. related to CRP, Phase 3
Sixth Meeting of Participants in the Coordinated Research Programme "Optimizing of Reactor Pressure Vessel Surveillance Programmes and Their Analysis - Phase 3
Vienna, Nov. 1993

The paper gives results of the contribution of Research Center Rossendorf to the IAEA Coordinated Research Programme "Optimizing of Reactor Pressure Vessel Surveillance Programmes and Their Analysis - Phase 3". The report includes information about material and specimen fabrication, the irradiation conditions, and the test methods. For the unirradiated state impact energy-temperature curves, dynamic J integrals for cleavage fracture, quasistatic crack resistance curves, and crack initiation J integral values are given.

Publications in scientific and technical journals and in conference proceedings

Altstadt, E., F.-P. Weiß
Experimental and Numerical Investigation of Control Element Vibration During Abnormal Core Barrel Motion at a VVER-440 Type Reactor
Proc. International Simulators Conference (SIMULATORS X)
Arlington / Virginia, 29 March - 1 April 1993

In 1985 abnormal core barrel motion had occured at unit 2 of the Greifswald NPP indicated by extremly large neutron noise. Amplitudes of up to 4mm were estimated from the external neutron noise signals.
The coherence and phase relations between excore and incore neutron noise signals exhibited typical features from which it could be concluded that even the control elements were forced to vibrations by the moving core barrel.
To obtain principal understanding about these phenomena and to draw conclusions for the surveillance of the excore and incore neutron signals, experimental and numerical investigations were performed. An experimental set-up was constructed providing all necessary displacement signals via HALL probes. This physical model, being a double pendulum with an annular channel surrounding the lower pendulum, can be operated in a linear mode (small excitation amplitudes) as well as in a non-linear mode (larger amplitudes which cause impacts between channel and lower pendulum).
The numerical simulation algorithm is based on a mechanical system consisting of linear elements (inertia, dampers, springs) and non-linear elements (gaps). In this way impacts between control element and neighbouring fuel cassettes which are strongly non-linear events can be modeled. After simulating the time series, which is possible for any detector position at the control element or at the set-up respectively, transfer functions, coherences, phase relations etc. can be computed.
It could be shown that the typical linear phase shifts between excore and incore neutron noise signals are due to impacts between the control elements and the neighbouring fuel cassettes. The obtained results can be used to establish a sensitive detection procedure for control element vibrations induced by abnormal core barrel motion.

Altstadt, E., F.-P. Weiß
Vibration Modelling - Investigation of Mechanical Accident Sequences at a VVER-440 Type Reactor
Proc. International Conference on Fault Diagnosis
Toulouse / France, 05 - 07 April 1993

During abnormal core barrel motion of a VVER-440 type reactor significant phase relations and coherences between incore and excore neutron noise signals were observed. For the explanation of the phenomena a numerical algorithm based on the non-linear equations of motion of a double pendulum was developed. In order to confirm the numerical results qualitatively additional experiments at a small set-up modelling the control elements were performed. The typical signal patterns observed at the VVER-440 could be shown to originate from mechanical impacts between the control elements and the neighbouring fuel cassettes.

Altstadt, E., F.-P. Weiß
Regelelementschwingungen bei anomaler Kernbehälterbewegung in einem Druckwasserreaktor vom Typ WWER-440
Proc. 4. Tagung über Dynamische Probleme, Modellierung und Wirklichkeit, Universität Hannover, 07. - 08. Okt. 1993

Während der anomalen Kernbehälterbewegung bei einem Reaktor vom Typ WWER-440 wurden signifikante Phasen- und Kohärenzbeziehungen zwischen dem Excore- und dem Incoreneutronenrauschen beobachtet. Für die Erklärung der Phänomene wurde ein numerischer Algorithmus entwickelt, der auf den nichtlinearen Bewegungsgleichungen eines Doppelpendels beruht. Zur qualitativen Verifizierung der numerischen Resultate wurden außerdem Experimente an einem kleinen physischen Modell der Regelelemente durchgeführt. Es konnte nachgewiesen werden, daß die am WWER-440 beobachteten typischen Signalmuster von mechanischen Anschlagvorgängen zwischen Regelelementen und benachbarten Brennstoffkassetten herrühren.

Böhmert, J., F. Bergner, M. Große, H.-W. Viehrig
Influence of the Depth Position on the Neutron Embrittlement of the VVER Reactor Pressure Vessel Steel 15Cr2MoV(A) - Consequences for the Assessment of Reactor Safety
Proc. Jahrestagung Kerntechnik 1993
Köln, 25. - 27. Mai 1993

The dependence of the mechanical properties on the depth position in unirradiated state and after irradiation up to neutron fluences of approximetely. 5×10^{18} and 70×10^{18} cm^{-2} ($E > 0.5$ MeV) is tested on a forging made of VVER 440 reactor pressure vessel steel 15CrMoV. The surface-near position shows a higher strength and a lower transition temperature than the positions > 1/4 wall thickness. Increased irradiation reduces these differences. The testing of specimes from the 1/4 depth position within the surveillance programme, as normally demanded by monitoring rules for nuclear power plants, results in a conservative safety assessment against brittle fracture even in the case of EOL fluence. By taking into account fluence attenuation, the flux effect etc., the toughness increases over the wall thickness from the inside to the outside after a longer operating time of the RPV.

Böhmert, J. (FZR), M. Dietrich, J. Linek (KFA Jülich)
Comparative Studies on High-temperature Corrosion of ZrNb1 and Zircaloy-4
Nuclear Engineering and Design 147 (1993) S. 53-62

A comparative study of the oxidation behaviour of ZrNb1 and Zircaloy-4 was carried out in a steam atmosphere in the temperature range from 700-1100 °C. ZrNb1 and Zircaloy-4 are oxidizing approximately according to similar oxidation kinetics. The oxidation rate of ZrNb1 is somewhat lower. It can be described by the equation $\Delta m = 0.4873 \sqrt{t} \exp(-10261/T)$. However, remarkable differences are observed in respect to morphology of the oxide and the O-stabilized α-layer, hydrogen uptake, and both the fraction and distribution of the oxygen dissolved in the metal. Above all the rapid drop in ductility by exposure to steam is of significance under safety aspects. Differences in the thermodynamic conditions for equilibrium of the ternary systems Zr-O-Nb and Zr-O-Sn may provide an appropriate explanation of these differences.

Eckert, S.; G. Gerbeth, J.P. Thibault, G. Mihalache
Some Aspects of LMMHD Two-Phase Flow: MHD Generator Configuration
Proc. 7th. Int. Beer-Sheva Seminar on MHD Flows and Turbulence
Jerusalem, February 1993
to be published in: American Institute of Aeronautics ans Astronautics Washington

The influence of an external magnetic field on LMMHD two-phase flows in vertical rectangular ducts has been examined. The goal of the work is the construction of models being able to predict the average behaviour of the flow as well as being relatively easy to survey and to handle. Results regarding the slip ratio obtained from a bubbly flow model are compared with experimental data got from measurements at the mercury-air facility. In the case of an applied magnetic field discrepancies between model and experiment are obtained giving an indication of the imperfection of the present state of the model. The crucial point is the validation of the semiempirical closure laws involved in the LMMHD tow-phase flow models. In the present state of the experiments the influence of the void fraction on the apparent electrical conductivity of the two-phase flow has been investigated. The results obtained from the mercury-air facility of LEGI-IMG are located between the relations given by Maxwell and Petric & Lee, respectively.

Eckert, W., U. Knopf, U. Rindelhardt, G. Teichmann
1000-Roof-Programme in Saxony and Thuringia: Actual Situation, System Technique and Results
Proc. 8. Nationales Symposium Photovoltaische Solarenergie
Staffelstein, 17. 03. - 19.03.1993

The paper dealt with the first results of the 1000-Roof-Photovoltaic Programme in the German Federal States of Saxony and Thuringia. Experiences in designing and mounting the pv-plants are discussed. Up to the end of 1992 totally 70 small pv-plants were coupled to the grid in both states. From the first results a mean energy production of about 700 kWh per installed power of 1 kW_p can be extrapolated. The most technical difficulties resulted from the used DC-AC-inverters. Additional problems were caused by the grid itself, which was still integrated in the East European Network.

Enkelmann, W.
Promotion of Renewing of District Heating Systems in Saxonia
Energieanwendung und Energietechnik 42 (1993) 5, S. 276

In 1992 in the new Federal States of Germany the renewing of district heating plants was supported by the gouvernment. Plants for heat generation, and heat transport and distribution and customer installations were included in the renewing. In Saxonia an amount of approximately 80 million DM could be devided among the applicants. With regard to the enormous uncovered demand the gouvernment decided to continue the program from 1993 up to 1995. Based on the experiences with the 1992 promotion program some hints can be given to the user of the new program.

Galindo, V., G. Gerbeth
A Note on the Force on an Accelerating Spherical Drop at Low Reynolds-Number
Physics of Fluids A5, 12 (1993), S. 3290 - 3292, American Institute of Physics, New York

The time-dependent drag force on a spherical drop is analyzed for the linear limit of small Reynolds numbers. There is an error in the literature on the generalization of the known Basset memory kernel of a rigid sphere to the case of a drop. Correct results are presented here. A new overshooting effect is found if thermocapillarity is driving the drop motion rather than gravity.

Gerbeth, G., A. Alemany
Magnetohydrodynamic Flow Around a Circular Cylinder
In: Bluff Body Wakes Dynamics and Instabilities, p. 51 - 54
Berlin, Heidelberg, New York, Springer 1993, pp. 51-54

The flow around a circular cylinder is considered for the following particular configuration: The fluid is electrically conducting and the whole system is inside an external magnetic field. This magnetohydrodynamic (MHD) flow is of interest for various applications but also for basic fluiddynamic research.
As an introduction to typical MHD effects a simple model system is considered: Fluid flow parallel to the cylinder axis. It allows an analytical solution of the combined system of Navier-Stokes- and Maxwell-equations. The results clearly show the development of the typical shear-layers resulting from the electromagnetic and viscous forces: Boundary layer at the cylinder surface, tangential layers at the cylinder poles, deep core and outer core of the wake.
Analytical and experimental results will be summarized concerning the more interesting standard geometry of a flow perpendicular to the cylinder axis.
The experimental results include turbulence intensities and the induced magnetic field at different locations in the up- and downstream wakes, as well as the pressure at the cylinder surface.

Gerbeth, G., S. Eckert, H. Langenbrunner
Dispersion of Gas Bubbles in a Two-Dimensional MHD Turbulence
7th. Beer-Sheva International Seminar on MHD Flows and Turbulence
Jerusalem, February 1993

The dispersion of small gas bubbles in a vertical upwards liquid metal two phase flow is investigated theoretically as well as experimentally. Local void fraction measurements are presented for a vertical sodium-argon flow with and without external magnetic field. The dispersion of an initially narrow void distribution shows this behaviour clearly: There is an overall focussing effect of the magnetic field on the void distribution, but the dispersion of gas bubbles is much more suppressed parallel to the field than perpendicular to it.

The bubble transport will be modelled by a simple diffusion equation. The model takes into account that bubbles represent no passive tracer of the flow field but have an own dynamics due to their relative velocity to the liquid phase. The experimental results will be analyzed in terms of the corresponding diffusion coefficients.

Gerbeth, G.
New results on MHD drag coefficients
Progress in Astronautics and Aeronautics, Ed. H. Branover, Y. Unger
Washington 148 (1993), S. 551 - 565

Theoretical and experimental results of MHD drag coefficients are summarized. Special attention is paid to Stokes flow, where a typical error has been found in the literature. This situation is clarified here, and correct results are presented. Numerical calculations are performed for the MHD Stokes flow around a cylinder in a transverse magnetic field, yielding qualitative agreement for the drag with both measurement as well as a rough asymptotic analysis. The MHD drag coefficient of the cylinder in a transverse magnetic field increases proportionally to $M \cdot \ln M$ if $M >> 1$ (where M is the Hartmann number). Finally, the deflection of a rising bubble in a liquid metal is determined if the direction of the magnetic field is inclined relative to the vertical line.

Gerbeth, G., G. Uhlmann, D. Hamann
Survey of liquid metal MHD activities in Dresden
Progress in Astronautics and Aeronautics, Ed. H. Branover, Y. Unger
Washington 148 (1993), S. 470 - 475

This study briefly summarizes the activities of the Rossendorf group in the field of liquid metal MHD. It shows in which way the present investigations on basic problems in liquid metal MHD followed from the fast-breeder research. Special interest is focussed on liquid metal two-phase flow and MHD flow around obstacles, as well as the laminar-turbulent transition in two-dimensional MHD flows. Most of the investigations are theoretical, but partly connected to experiments performed in Riga, Latvia or Grenoble, France. Own experiments at a sodium loop are described. Finally, the most promising directions of future research are presented.

Große, M., G. Schuster et. al.
Neutron and X-Ray Investigations on the Oxygen Bonding in $YBa_2Cu_{30}O_{(7-x)}$ Combined with Physico-Chemical Methods
Proc. 7. Tagung Festkörperanalytik, Chemnitz, June 1993

The occupancy of the different oxygen lattice places at different annealing conditions in $YBa_2Cu_{30}O_{(7-x)}$ was determined by Rietveld Refinement with neutron and X-ray diffraction data. The occupation density for the oxygen positions O1 to O4 was ascertained. The values of the oxygen content of the samples accounted by this method were compared with those measured by thermoanalysis and solid electrolyte coulometry. It could be shown, that the atoms of oxygen exchangeable by thermal treatment are O4, that is the oxygen in the O-Cu-O chains and O1, the oxygen atoms connecting the planes. The oxygen in the planes is fixed and cannot be removed up to 935 °C. The strength binding O1 in the lattice is stronger than those of O4 atoms, what is demonstrated by higher temperature of dissoziation of the O1 atoms. At 935 °C less than 10 % of the O1 positions are vacant. The amount of the received oxygen is not exactly equal to the really installed oxygen at the lattice places. Especially in the temperature region below 400 °C adsorption and chemisorption processes ar ascertained.

Grundmann, U., U. Rohde
3-D-Simulation of Reactivity Transients in Cores of VVER-Reactors
Proc. SCS Simulation Multi-Conference
Arlington / Virginia / USA, 29 March - 01 April 1993

Reactivity initiated accidents (RIA) have to be analyzed for safety assessment of nuclear reactors. The presented 3-dimensional core simulator DYN3D/M2 describes the space dependent effects of reactivity perturbations caused by control rod motions or local changes of coolant temperature and boron concentration. The safety margin can be determined more precisely by use of 3-D models than with simpler methods as point model or one-dimensional kinetics. A nodal expansion method (NEM) for hexagonal geometry of VVER fuel elements was developed to reduce the numerical effort of 3-dimensional neutron kinetics. The changes of thermohydraulic parameters as fuel and coolant temperatures, coolant density and poisoning are determined with the help of the thermo-hydraulic model FLOCAL included in the code. Feedback results from the influence of the thermohydraulic parameters on the neutron physical constants. Applying DYN3D to safety calculations of reactivity transients, the code was validated by comparing its essential parts with benchmarks, other codes and experiments. An accident caused by the ejection of a single control rod in a VVER-440 reactor was analyzed. The results show a very high power peak in the neighbourhood of the ejected rod. Runs with time step control indicate that the computer time can be reduced in comparison to fixed time step. Simulations with a smaller number of coolant channels were investigated for coupling the core model with codes simulating the whole coolant system of a nuclear power plant.

Grundmann, U.; U. Rohde
Definition of the Second Benchmark of AER
3rd Symposium of AER, Pieštany (Slovakia)
27. September - 1. Oktober 1993, Proceedings p. 325

The first kinetic benchmark of AER was defined for comparison of different 3-dimensional kinetic codes developed for the hexagonal geometry of fuel assemblies in a VVER-reactor. The transient was assumed to be caused by ejection of nonsymetric control rod in a VVER-440 reactor. Feedback effects were neglected. The positive reactivity insertion not leading to prompt criticality results in a slower power increase and was compensated by insertion of shutdown rods.
The benchmark problem No. 2 discussed on the meeting of working group D in Budapest 1993 consists also of a control rod ejection accident in a VVER-440. The initial configuration is similar to benchmark No. 1. A nonsymetric control rod with a worth of 2 $ß_{eff}$ is ejected at hot zero power (HZP). The Doppler effect being the main feedback effect for this type of transients is the only feedback and is taken

into account by an adiabatic model of fuel temperature. Therefore it is possible to calculate this type of transient with codes which do not contain a complete thermohydraulic model.
As in problem No. 1, the nuclear data are given to exclude at this step of comparison the effects caused by different nuclear data. A sharp and high power peak connected with large deformations of flux shape is expected to give a serious test for codes and methods of calculation.
The problem, the input data and the expected results which will be used for comparisons are specified.

Grundmann, U.; U. Rohde
Assessment of the Influence of a Mixing Model on a Boron Dilution Transient in the VVER-440 Core by Help of the Code DYN3D/M2
3rd Symposium of AER, Piešťany (Slovakia)
27. September - 1. Oktober 1993, Proceedings p. 491

A reactivity initiated transient caused by entering a water plug with diluted boron concentration into the core during incorrect loop startup in a VVER-440/W-213 reactor is analyzed with the help of the code DYN3D/M2. The water with diluted boron concentration from the one loop is mixed with the water of the other loops before the core inlet. The results for the transient are influenced by three different mixing models that were investigated:
- ideal mixing: the boron concentration at all inlets of fuel assemblies is uniformly distributed,
- no mixing: the boron perturbation occurs only in the fuel elements of the sector belonging to the considered loop,
- mixing model: estimation of boron dilution at the core inlet by superposition of reference distributions, defined experimentally or pre-calculated by a simplified analytical model.

The results of DYN3D/M2 for these three cases presented in the paper show significant differences of the safety parameters, i. e. nuclear power, maximum fuel temperature or critical power ratio.
The asymmetric boron perturbation and the short length of the plug requires a more-dimensional core model for the treatment of this transient. The code DYN3D/M2 is capable of describing the space-dependent effects of the diluted boron in the core for all three cases. The power excursion is connected with strong deformations of the neutron flux distribution and power shape as a result of the space-dependent boron perturbation. Therefore the feedback effects are also influenced by the space effects.
The different boron mixing models lead to different boron distributions in the core, which influence the power excursion and the results for the safety parameters. By using the mixing model, more severe consequences of the transient are obtained than by assuming ideal mixing. Assuming no mixing, the perturbation results in a severe accident with partial core damage. The results indicate the importance of the applied mixing model for the investigations of this type of transient.

Haefele, W., U. Rindelhardt
Energy Problems of the United Germany
Perspectives in Energy 2 (1993) S. 369 - 375

After the reunification of Germany, the energy situation in Germany has changed and particularly so in eastern Germany. There the demand for electric energy has suddenly decreased owing to industrial closures and accordingly, for this and for environmental reasons, the production of lignite has decreased as well. All nuclear capacity was shut down. Instead, a number of very modern high-performance coal-fired plants are being installed that also allow a sharp reduction of air pollution. Naturally, a modernisation and integration of the electrical grid is under way.

Hamann, D., G. Gerbeth
Recent Developments of Liquid Metal MHD Thermoacoustic Engines
Progress in Astronautics and Aeronautics, Ed. H. Branover, Y. Unger
Washington 148 (1993), S. 441 - 455

A literature review on thermoacoustic engines (TAEs), with particular emphasis on liquid metal MHD TAEs is presented. The main aim of this paper is to draw the attention and the interest of the international MHD community to these new developments since it has only been discussed in the literature on acoustics.
TAEs provide a new way to convert heat to mechanical energy, or more strictly speaking, to acoustic power. They have an efficiency comparable to existing techniques but with the possibility of increasing reliability because there are no moving parts. TAEs utilize heat flow from a high-temperature source to a low-temperature sink to generate acoustic power in the form of high-amplitude sound waves in liquid sodium. Since acoustic power is inconvenient in most situations, a power transducer is required to convert acoustic power into an electric one. Though there are a number of converter mechanisms, the magnetohydrodynamic one is particularly suited for sound waves in liquid metals. A magnetic field perpendicular to the direction of sound propagation is applied to the center of the resonator, in which the sound has been generated. There are electrodes in the sodium that form an electric current path perpendicular to both magnetic field and sound velocity.

Josserand, J., Ph. Marty, A. Alemany, G. Gerbeth
MHD Flow Around a Cylinder in an Aligned Magnetic Field
Progress in Astronautics and Aeronautics, Ed. H. Branover, Y. Unger
Washington 148 (1993), S. 519 - 534

Recent results on the study of a liquid metal flow around an insulating cylinder with constant aligned magnetic field are presented. From the experimental point of view, a special type of differential pressure transducer using strain gauges is described. The results obtained with mercury as liquid metal are presented for an interaction parameter N ranging from O to approximately 8. The stabilizing effect of the magnetic field on the boundary layer separation is shown. Pressure distribution around the cylinder as well as the overall pressure drag coefficient C_D are given for different values of N. The last section presents analytical calculations of the flow distribution of an inviscid fluid when $N << 1$. The theoretical results are in good agreement with these experimental results.

Keresztùri, A., M. Telbisz, U. Grundmann, J. Krell
Results of a Threedimensional Hexagonal Kinetic Benchmark Problem
Proc. ENS Regional Meeting, Energy in Central Europe: Present and Perspectives
Portoroz / Slowenia, June 1993

The recent safety analysis investigations of the VVER type reactors require the use of three-dimensional hexagonal kinetic codes. For this purpose the codes KIKO3D and DYN3D were developed in the Atomic Research Institute Budapest and in the Research Center Rossendorf, respectively. The kinetic codes have to be validated before being used for safety assessments. A benchmark problem is defined, as the first step of the validation procedure of hexagonal kinetic programs.
The problem describes a rod ejection transient in a VVER-type geometry, where the worth of the ejected rod is just below the prompt critical value. The initial power is near to zero and the power rise is not too large. Therefore, the transient can be treated without feedback based on the given time-dependence of the cross sections and geometry.
KIKO3D results are presented, i.e the solution of time dependent nodal equations by the Improved Quasistatic (IQS) Method. The time dependence of the integrated power and the reactivity are compared with the adiabatic results. These results are also compared with the results of two different DYN3D calculations carried out in Rossendorf and in Berlin.

Kumpf, H., K. Noack
Neutronic Problems of a Compact 14 MeV Plasma Neutron Source
Proc. International Conference on Open Plasma Confinement Systems for Fusion
Novosibirsk, 14 - 18 June 1993

Neutronic problems connected with the design of a compact 14MeV neutron source for fusion material research based on a plasma mirror are treated. In particular it has been demonstrated, that further construction efforts are necessary to comply with the established radiation limits for the magnetic system. Further it is not possible to raise the useful high energy flux by arranging reflectors. If one of the source areas of the machine is equipped with a moderator, a thermal neutron source with a flux of about $5 \cdot 10^{14}$ n cm^{-2} s^{-1} can be achieved.

Maletti, R.
Remarks About the Thermal Use of Solar Energy in Saxonia
Energieanwendung/Energie- und Umwelttechnik 42 (1993) S. 578

By the installation of more than 400 modern solar thermal collector plants with a summarized collector area of about 3000 m^2 a remarkable entry in the thermal use of solar energy was reached in Saxonia in 1992. Simultaneously a network of little enterprises came into existence, which now work actively in the field of energy and environmental techniques. This development was essentially supported by the Saxonian promotion programme of rational use and application of renewable sources of energy.

Maroti, L., H.-M. Prasser, P. Windberg
Investigation of Two-Phase Flow Phenomena at Integral Test Facilities Using Needle Shaped Conductivity Probes
Proc. 8th International Thermal Conference
Budapest, 02 - 04 June 1993, p. 275 - 280

The paper deals with the utilization of needle shaped conductivity probes developed in Rossendorf during a small break LOCA experiment at the Budapest PMK test facility. A 1-%-break at the down-comer inlet was simulated, the ECC tanks were switched off. The probes worked properly under primary circuit conditions (12.3 MPa, 300 °C), the data acquision system provided clearly readable data in spite of the high electrical disturbance level caused by the directly heated fuel rod simulators of PMK. The paper presents plots of the signals of the probes. The level drop in the upper plenum of the reactor, the hot leg loop-seal clearing and the emptying of the steam generator cold collector were indicated. Close after the loop-seal clearing void fraction oscillations with a period of about 22-24 sec were observed at the reactor outlet and the steam generator inlet.

Popp, K., U. Bergmann, F. Bergner, E. Hampe, W.-D. Leonhardt, H.-P. Schützler, H.-W. Viehrig
Irradiation and Annealing Behaviour of 15Kh2MFA Reactor Pressure Vessel Steel in L.E. Steele (ed.): Radiation Embrittlement of Nuclear Reactor Pressure Vessel Steels: An International Review , ASTM-STP 1170
Philadelphia, 1993, pp. 344 - 368, Vol. 4

Usually the assessment of the irradiation sensitivity and annealing behavior of reactor pressure vessel (RPV) steels is performed by means of destructive test methods, mainly impact and tension tests. In this paper a new kind of search for an efficient temperature-time regime for postirradiation thermal heat treatment is presented using nondestructive test methods like positron annihilation (Doppler broadening parameter S) and hardness (Vickers hardness HV 10).
Samples of Cr-Mo-V RPV steels (Soviet type 15Kh2MFA) were irradiated to different fluence levels of fast neutrons at temperatures $T < 156$ °C in a test reactor (base metal) and $T = 265$ °C in a pressurized water reactor (base as well as weld metal). From isochronal and isothermal annealing curves of HV 10 and S, favorable temperature-time regimes for each type of irradiated material were estimated. The data obtained from tension and impact tests indicate that sufficiently large recoveries took place by application of these regimes.
The new approach presented is especially useful in such cases where only the smallest amounts of irradiated materials are available-a case often met for RPV surveillance specimens.

Prasser, H.-M.; L. Küppers, R. Mai
Conductivity Probes for Two-Phase Flow Pattern Determination During Emergency Core Cooling (EEC) Injection Experiments at the COCO Facility (PHDR)
Held on: OECD (NEA) CSNI SPECIALIST MEETING ON INSTRUMENTATION TO MANAGE SEVERE ACCIDENTS GRS, Cologne, Germany, 16th - 17th March 1992.
Proceedings of the 1. OECED (NEA) CSNI-Specialist Meeting on Instrumentation to Manage Severe Accidents
GRS-93, NEA(CSNI/R(92)11, p. 273 - 289

Within the frame of the PHDR reactor safety research programme a large series of emergency core cooling injection tests was performed. The tests aimed at the study of the flow structure in the main circulation pipe and the heat exchange between the injected subcooled water and the saturated steam originating from the reactor, a KONVOI type PWR. They were carried out at the COCO facility (<u>CO</u>ntact <u>CO</u>ndensation). The paper deals with the results from hot leg injection tests obtained by the needle shaped conductivity probes developed in Rossendorf. Eight probes were placed at different positions around the injection nozzle. In KONVOI PWRs a special feature is used for the injection, the so called "Hutze", which is a cylindrical half-shell welded to the bottom of the circulation pipe and directing the water towards the reactor vessel against the steam flow. The probes provided very clearly readable data about the flow structure in a high time resolution. The flow regime was characterized in the cases of stratified flow (counter-current and co-current), complete flow revers and intermittent flow revers with plug formation. Additionally, in several cases the flow velocity was measured by means of cross correlation techniques.

Rindelhardt, U.
Grid Coupled PV-Plants: State of Art and Actual Results
Energieanwendung/Energietechnik 42 (1993)6, p. 300

The state of art of grid coupled photovoltaic systems is described. Based on a summary of the technical design actual operation results of small (i. e. 1 to 5 kW_p power) photovoltaic systems are discussed. The results are mainly based on systems, which were built in the frame of the 1000-Roof-Programme in Saxony. It is shown that a 3,5-kW_p-pv-plant produces yearly the amount of electrical energy which is needed by an energy saving household. The role of the grid as "energy storage" is discussed in more detail. Future options are mentioned finally.

Thess, A., G. Gerbeth, Ph. Marty
Electromagnetically Induced Flow Around a Cylinder
Progress in Astronautics and Aeronautics, Ed. H. Branover, Y. Unger
Washington 148 (1993), S. 535 - 550

The unidirectional flow of an electrically conducting fluid around a cylinder of arbitrary electrical conductivity, which is driven by the interaction of a homogeneous electric current with a homogeneous magnetic field and the resulting force on the cylinder are calculated numerically without any approximation in a large range of parameters. Asymptotic solutions are derived for the case of very strong and very weak magnetic fields respectively. A comparison with experimental results on insulating and highly conducting cylinders leads to a partial agreement although inertial forces are not taken into account in the model. Finally, confinement effects are considered leading to a better agreement between theory and experiment.

Viehrig, H.-W.; K. Popp, R. Rintamaa
Measurement of Dynamic Elastic-Plastic Fracture Toughness Parameters Using Various Methods
Int. J. Pres. Ves. and Piping 5 (1993), p. 233-241

Two improved impact testing facilities are used for the dynamic fracture toughness evaluation of precracked Charpy V-notch specimens. The methods of single specimen acoustic emission and crack mouth opening displacement testing are assumed to indicate the initiation points of stable crack growth. Thus, the dynamic ductile initiation J integral J_{Id} can be derived. It was shown that the toughness J_{Id} of the heat-resistant steel 10CrMo9.10 cannot be approximated by the J value at the maximum of the load deflection curve.

FZR-Reports and other publications

Altstadt, E., F.-P. Weiß
Numerische Untersuchungen zum mechanischen Schwingungsverhalten einer nassen LVD-Lanze
FZR-Bericht (nicht öffentlich)
Rossendorf, September 1993

Beyer, M., H. Carl, L. Langer, P. Schumann, A. Seidel, J. Zschau (FZR)
K. Nowak, P. Tolksdorf (TÜV Rheinland)
Aufbau eines technischen Systems zur Verbesserung der betrieblichen Überwachung der KKW durch die staatliche Aufsichtsbehörde (Saporoshje)
Abschlußbericht im Rahmen eines BMU-Projektes in 3 Teilen:
Kurzfassung, Anlage A: Textteil, Anlage B: Materialsammlung
Rossendorf; Köln, Dezember 1993

In order to improve operational surveillance of a WWER-1000 unit of the Ukrainian nuclear power plant Saporoshje a technical monitoring system has been specified. The system shall enable the state regulatory and supervisory bodies to survey the unit operation independently of operators, to assess its safety status, and to impose appropriate conditions. By its up-to-date configuration the system provides early indication of any operational incident and emission of radioactive materials connected. Based on the system an immediate warning in emergency situations is possible as well as an effective emergency management. For this purpose 49 operational parameters of the unit, 18 radiological parameters of the unit and the plant site and 6 meteorological parameters are monitored. The costs of establishing the technical system in its minimal size are estimated to about 1.3 Million DM (without expenses for installation of the system and of the data networks). Additionally about 650 000 DM are required for most necessary backfitting of measuring channels. Including another unit into the monitoring system implies further costs of about 200 000 DM.

Beyer, M., H. Carl, L. Langer, P. Schumann, A. Seidel, J. Zschau
Vorläufige Meßstellenliste technologischer Parameter für das behördliche Überwachungssystem des GosAtomNadsor am KKW Saporoshje, Block 5
Fachbericht FWSF-19/93, Sept. 93

In order to improve operational surveillance of a WWER-1000 unit of the Ukrainian nuclear power plant Zaporozh'ye a technical monitoring system has been specified. The system shall enable the state regulatory and supervisory bodies to survey the unit operation independently of operators, to assess its safety status, and to impose appopriate conditions. Based on the definition of safety functions and control tasks 49 different technological parameters are investigated and selected for monitoring. Technical specifications of these parameters at NPP Zaporozh'ye and derived alerts by crossing operational threshold values of single parameters and/or parameter combinations are described in the report.

Grundmann, U., U.Rohde
DYN3D/M2 - a Code for Calculations of Reactivity Transients in Cores with Hexagonal Geometry
FZR-Bericht, FZR 93-01, Jan. 1993

The code DYN3D/M2 consists of a the 3-dimensional neutron kinetic model of the code HEXDYN3D and the thermohydraulic model of the code FLOCAL. The neutron kinetics of DYN3D/M2 is calculated by using a nodal expansion method (NEM) for hexagonal geometry. The developed method solves the neutron diffusion equation for two energy groups. Stationary state and transient behaviour can be calculated. By help of the code PREPAR-EC parameterizid neutron physical constants of given burnup distribution can be transferred from the MAGRU library to an input file of DYN3D/M2. The code FLOCAL consisting of a two-phase coolant flow model, a fuel rod model and a heat transfer regime map up to superheated steam is coupled with neutron kinetics by the neutron physical constants. One coolant channel per fuel assembly and additional hot channels are considered. The activities for code validation and the range of application are described.

Grunwald, G., E. Altstadt
Analytische und experimentelle Untersuchungen zur Modellierung der Fluid-Struktur-Wechselwirkung in einem 2D-Ringspalt
FZR-Bericht, FWSM - 1/93

Ausgehend von den Grundgleichungen der Strömungsmechanik wird eine Modellierung der Fluid-Struktur-Wechselwirkung im 2D-Ringspalt kreiszylindrischer Strukturen vorgenommen. Dazu wird das mit Hilfe der Kontinuitätsgleichung potentialtheoretisch ermittelte Geschwindigkeitsfeld, welches durch die Strukturbewegung erzeugt wird und mit einer Grundströmung überlagert werden kann, mittels eines Parameters so variiert, daß die Geschwindigkeits- und Druckverteilungen im Ringspalt den geforderten Randbedingungen näherungsweise genügen. Die Druckverteilung im Ringspalt folgt dabei durch Integration eines linearisierten 2D-Systems der Navier-Stokesschen Gleichungen mit einem einfachen Ansatz für die laminare bzw. turbulente Fluidreibung und dient der Bestimmung der Fluidkräfte für die Bewegungsgleichung der Struktur.
Meßergebnisse für die Frequenz und Dämpfung eines ausschwingenden Pendels im ruhenden und strömenden Fluid werden mit den theoretischen Resultaten verglichen. Dabei liegen trotz der einfachen Modellierung, die auch auf kompliziertere Strukturbewegungen erweitert werden kann, im Vergleich zum Experiment gute Ergebnisse vor.

Hessel, G., W. Schmitt, F.-P. Weiß
Acoustic Leak Detection at Complicated Geometrical Structures Using Fuzzy Logic and Neural Networks
FZR-Bericht, FZR 93-21, Rossendorf, October 1993

Methods of acoustic leak monitoring are of great practical interest for the safety of pressure vessels and pipe lines not only at the primary circuit of nuclear power plants. In this report some aspects of acoustic leak localization at complicated three-dimensional topologies for the case of leakage monitoring at the reactor vessel head of a VVER-440 are discussed.
An acoustic method based on pattern recognition is being developed. During the

learning phase, the localization classifier is trained with sound patterns that are generated with simulated leaks at all locations endangered by leak. After training unknown leak positions can be recognized through comparison with the training patterns.
The sound patterns of the simulated leaks are simultaneously detected with an AE-sensor array and with high frequency microphones measuring structureborne sound and airborne noise, respectively.
The initial results show the used classifiers principally to be capable of detecting and locating leaks, but they also show that further investigations are necessary to develop a reliable method.

Kumpf, H., K. Noack, V. G. Krasnoperov
Neutronic Problems of a Compact 14 MeV Plasma Neutron Source
FZR-Bericht, FZR 93-11, Rossendorf, April 1993

Neutronic problems connected with the design of a compact 14MeV neutron source for fusion material research based on a plasma mirror are treated. In particular it has been demonstrated, that further construction efforts are necessary to comply with the established radiation limits for the magnetic system. Further it is not possible to raise the useful high energy flux by arranging reflectors. If one of the source areas of the machine is equipped with a moderator, a thermal neutron source with a flux of about $5 \cdot 10^{14}$ n cm^{-2} s^{-1} can be achieved.

Weier, T.
Untersuchungen zum Zylindernachlauf im MHD-Fall
Diplomarbeit Universität Halle-Wittenberg, November 1993
(Betreuer: G. Gerbeth)

In der Arbeit wird experimentell und theoretisch die Frage behandelt, wie ein externes longitudinales Magnetfeld die Stabilität des Zylinder-Nachlaufs (Karmansche Wirbelstraße) beeinflußt. Die Messungen wurden am Quecksilber-Versuchsstand des IMG Grenoble durchgeführt. Die Unterdrückung der Wirbelstraße wurde vom theoretischen Modell vorhergesagt und im Experiment verifiziert. Überraschend wurde sowohl vom Modell als auch im Experiment die Tendenz zu langwelligen Störungen gefunden, die bei wachsendem Magnetfeld immer ausgeprägter werden.

Zschau, J.
Konzeption zur Ausgestaltung des technischen Systems für das BMU-Projekt "Spezifikation Datenfernübertragung Saporoshje"
Fachbericht FWSF-20/93, Juni 1993

In the report the boundary conditions and the resulting technical possibilities are described for the construction of a technical system for remote monitoring of the nuclear power plant Zaporosh'ye, unit 5, available for the supervision by the state regulatory body. The general structure of the system and especially different technical solutions for the remote data transfer are discussed in more detail.

Meetings and Workshops

1. IAEA Working Group Meeting on Neutronic Analysis
Rez/Prag, Czech Republic, Januar 1993
held by scientists from RCR
20 - 25 participants from Central and Eastern Europe

2. PIN-Seminar
Workshop der Deutschen Gruppe des PIN-Projekts
Processes of International Negotiation
Rossendorf/Dresden, 30.03.93
≈ 15 German participants

3. Spezifikation Fernüberwachung Saporoshje
1. Arbeitstreffen zum BMU-Vorhaben
Rossendorf, 29.03. - 02.04.93
15 - 20 participants from Germany and Ukraine

4. Spezifikation Fernüberwachung Saporoshje
2. Arbeitstreffen zum BMU-Vorhaben
Saporoshje - Kiew, 24.04. - 08.05.93
≈ participants from Germany and Ukraine

5. Informal Meeting on Reactor Noise 24 (IMORN-24)
Oybin/Zittau, 23 - 25 June 1993
70 participants from Japan, Europa, USA

6. IAEA Working Group Meeting on Neutronic Analysis
Rez/Prag, Czech Republik, September 1993
held by scientists from RCR
20 - 25 participants from Central and Eastern Europe

7. Spezifikation Fernüberwachung Saporoshje
3. Arbeitstreffen zum BMU-Vorhaben
Rossendorf, 11.10. - 15.10.93
15 - 20 participants from Germany and Ukraine

8. Fortgeschrittene Technologien in der Kerntechnik
Arbeitstreffen mit BMFT-Vertretern
Rossendorf, 18.11.93
≈ 15 participants

9. Workshop Nutzung Erneuerbarer Energien in Sachsen
Rossendorf/Dresden, Okt. 1993
≈ 30 German participants

Seminars

Institutsseminare

1. Biobrennstoffe
   Ref.: Dr. F. Naehring
   T.: 13.01.93
2. Brucherkennung mit magnetischer und elektrischer Emission
   Ref.: S. Winkler (Fhl Freiburg)
   T.: 11.06.93
3. Modellierung der Fluid-Struktur-Wechselwirkung bei zylindrischen Strukturen
   Ref.: Dr. Grunwald, Dr. Altstadt
   T.: 30.06.93
4. Die Weiterentwicklung von Störfallcodes für WWER
   Ref.: Dr. Rohde
   T.: 12.07.93
5. Flüssigmetallgekühlte Fusions-Blanket-Konzepte und zugehörige MHD-Untersuchungen im Kernforschungszentrum Karlsruhe
   Ref.: Dr. L. Barleon (KFK)
   T.: 14.07.93
6. Zweiphaseninstrumentierung mit Ultraschall und Nadelsonden
   Ref.: P. Schütz, F. Hensel, Dr. Prasser
   T.: 19.07.93
7. 1. Experimentelle Möglichkeiten des ENIS Elektrogorsk auf dem Gebiet der Sicherheitsforschung
   2. Der integrale Versuchsstand ISB - ein thermohydraulisches Modell des WWER-1000

   Ref.: Dr. V.A. Gaschenko, M.P. Gaschenko (Elektrogorsk Rußland)
   T.: 28.07.93
8. Kostenoptimale Wärmedämmung bei Wohnblocks der fünfziger Jahre
   Ref.: Dr. F. Naehring
   T.: 29.07.93
9. Experiences with application of WASP in orographically complex regions
   Ref.: Dr. E.L. Petersen (Roskilde Dänemark)
   T.: 20.09.93
10. Ansätze der Entscheidungstheorie und Expertensystemanwendung im Umweltaltlastenbereich
    Ref.: Dr. Ferse, Kruber
    T.: 29.09.93
11. Paralleles Rechnen mit PARSYTEC
    Prof. V. Friedrich, Prof. A. Meyer (Chemnitz-Zwickau)
    T.: 14.10.93
12. The New Russian Group Constant System ABBN-93/MULTIC and the CONSYST2 Data Code System for different Neutron and Gamma Applications
    Ref.: Dr. G.N. Manturov (FEI Obninsk, Rußland)
    T.: 23.11.93
13. Zusammenhänge zwischen Mikrostruktur, Stretchzonenbildung und bruchmechanischen Kenngrößen
    Ref.: J. Ude (TU Magdeburg)
    T.: 06.12.93

14. Recent progress in experiments on the existing model of a plasma neutron source
Ref.: Dr. A. Ivanov (Novosibirsk Rußland)
T.. 10.12.93
15. Methods of Uncertainty Estimations of Neutron Transport Calculations Based on Sensitivity Analysis and their Application in Reactor Physics
Ref.: Dr. G.N. Manturov (FEI Obninsk Rußland)
T.: 15.12.93
16. Modell zur Berechnung von Neutronenflußdichteschwankungen infolge stochastischer Schwingungen von Kompensationskassetten mit hexagonalem Querschnitt
Ref.: Dr. Hollstein (FZR)
T.: 17.12.93
17. Rückblick 1993, Perspektiven, Trends
Ref.: Dr. F.-P. Weiß
T.: 21.12.93

Institutskolloquium anläßlich des 60. Geburtstages von Herrn Dr. habil. Hansulrich Barz
T.: 13.12.93

- Eröffnung durch Dr. F.-P. Weiß
- Beitrag zur störungstheoretischen Berechnung von Reaktivitäten
Ref.: Dr. Chr. Reiche (VKTA)
- Berechnung der radiologischen Auswirkungen potentiell schwerer Unfälle auf dem Forschungsstandort Rossendorf mit dem Programm COSIMA
Ref.: Dr. E. Franke (VKTA)
- Monte-Carlo-Berechnungen kleiner Störungen
Ref.: Dr. E. Seifert (VKTA)
- Spektrumsjustierung auf der Basis detaillierter Monte-Carlo-Rechnungen
Ref.: B. Böhmer
- Charakterisierung des Versprödungsverhaltens von RDB-Stählen
Ref.: Dr. H.-W. Viehrig
- Erste Erfahrungen mit dem Gruppendatenerzeugungsprogramm NJOY
Ref.: Dr. Hermsdorf (TUD)

Zentrumskolloquien

1. Das PHEBUS-P.F.-Projekt
Ref.: Dr. P. van der Hardt
T.: 04.10.93
2. 14 MeV High Power Plasma Type Neutron Sources (Survey)
Ref.: Prof. Kruglyakov (Novosibirsk, Rußland)
T.: 25.11.93

Lectures

1. J. Böhmert: Material Engineering
Lecture held at Fachhochschule Dresden, Fachbereich Maschinenwesen

2. J. Böhmert: Heat Treatment of Materials
Lecture held at Fachhochschule Dresden, Fachbereich Maschinenbau

3. U. Rindelhardt: Renewable Energies
Lecture held at HTWS Zittau/Görlitz

4. U. Rindelhardt: Photovoltaic/Wind Energy
Lecture held at TU Dresden, Fakultät für Maschinenwesen

5. G. Grunwald: Heat and Mass Transfer
Lecture held at HTWS Zittau/Görlitz

6. U. Rindelhardt: Renewable Energies
Lecture held at Universität Leipzig,
Fakultät für Physik und Geowissenschaften

7. U. Grundmann; U. Rohde: DYN3D/M2 for RIA-Analysis
Lecture held at IAEA Working Group,Meeting on Neutronic Analysis
Řež, (ČZ)

8. F.-P. Weiß: Reliability and Safety of Technical Systems
Offer for a Lecture held at TU Dresden, Fakultät für Maschinenwesen

9. U. Rindelhardt; G. Teichmann: Photovoltaic
Practicum held for the TU Dresden, Fakultät für Maschinenwesen

10. Schmitt, W.; Hessel, G.; Weiß, F.-P.: Neutron Noise in Zero Power Reactors
Practicum held for the TU Dresden, Fakultät für Maschinenwesen

11. Schmitt, W.; Hessel, G.; Weiß, F.-P.:
Power Noise in Pressurized Water Reactors
Practicum held for the TU Dresden, Fakultät für Maschinenwesen

Departments of the Institute

Research Center Rossendorf, Inc.
Institute for Safety Research
01314 Dresden, PF 510119
Tel.: (0351) 591. 3480 Fax (0351) 591. 3440

Organigram

Directorate
Weiß, F.-P., Dr.

Dpt. Accident Analysis
Prasser, H., Dr. Tel.: .3460

Dpt. Neutron Embrittlement
Böhmert, J., Dr. Tel.: .3186

Dpt. Mechanical Integrity
Weiß, F.-P., Dr. Tel.: .3470

Grp. NPP Remote Monitoring
Carl, H., Dr. Tel.: .3466

Grp. Plasma Neutron Source
Kumpf, H., Dr. Tel.: .3467

Grp. Renewable Energies
Rindelhardt, U.,Dr. Tel.: .3663

Grp. Decision Analysis / Hazard Ranking
Ferse, W., Dr. Tel.: .2903

Personnel

Director: Prof. Dr. F.-P. Weiß

Scientific Staff:

Altstadt, Eberhard Dr.
Barz, Hansulrich Dr.
Bergmann, Uwe
Beyer, Matthias
Brünig, Dietlinde Dr.
Böhmer, Bertram
Böhmert, Jürgen Dr.
Carl, Helmar Dr.
Enkelmann, Wolfgang Dr.
Ferse, Wolfgang Dr.
Galindo, Vladimir Dr.
Gerbeth, Günther Dr.
Große, Mirco
Grundmann, Ulrich Dr.
Grunwald, Gerhard Dr.
Hirsch, Werner Dr.
Hollstein, Frank Dr.
Kolevzon, Vladimir
Konheiser, Jörg
Krahl, Steffen
Kumpf, Hermann Dr.
Langer, Lutz
Lischke, Rosemarie
Lucas, Dirk Dr.
Maletti, Rainer Dr.
Mittag, Siegfried Dr.
Mutschke, Gerd
Naehring, Friedrich Dr.
Noack, Klaus Dr.
Prasser, Horst-Michael Dr.
Rindelhardt, Udo Dr.
Rohde, Ulrich Dr.
Scheffler, Michael
Schmitt, Wilfried Dr.
Schröder, Frank
Schumann, Peter Dr.
Seidel, Andre
Teichmann, Günther
Viehrig, Hans-Werner Dr.
Werner, Matthias Dr.
Wittke, Willy
Zschau, Jochen Dr.
Zippe, Winfried Dr.

Post Doc:

Steinkamp, Helmut Dr.

PhD Students:

Bergmann, Ute
Eckert, Sven
Hensel, Frank
Nitschke, Kerstin
Richter, Holger
Schäfer, Frank

Technical Staff:

Baldauf, Dieter
Behrens, Sieglinde
Blumentritt, Thea
Borchardt, Steffen
Bretschneider, Heidrun
Eichhorn, Christine
Elert, Edith
Fischer, Manfred
Futterschneider, Hein
Gebel, Margitta
Heinze, Gerda
Hessel, Günter
John, Annett
Kaule, Christian
Keulicht, Anke
Krepper, Eckhard Dr.
Kunadt, Heiko
Lang, Dorothea
Leonhardt, Wolf-Dietrich
Leuner, Bernd
Leuschke, Grit
Losinski, Claudia
Lotzmann, Roland
Otto, Gerlind
Richter, Annett
Richter, Henry
Richter, Joachim
Richter, Karl-Heinz
Rott, Sonja
Russig, Heiko
Schmidt, Johannes
Seidler, Christa
Skorupa, Ulrich
Stephan, Ingrid Dr.
Tamme, Marko
Tamme, Günter
Webersinke, Wolfgang
Weichelt, Steffen
Weiß, Rainer
Willkomm, Heike
Zimmermann, Wilfried